

**OPTIMAL FRACTURE TREATMENT DESIGN FOR DRY GAS  
WELLS MAXIMIZES WELL PERFORMANCE IN THE PRESENCE  
OF NON-DARCY FLOW EFFECTS**

A Thesis

by

HENRY DE JESUS LOPEZ HERNANDEZ

Submitted to the Office of Graduate Studies of  
Texas A&M University  
in partial fulfillment of the requirements for the degree of

MASTER OF SCIENCE

August 2004

Major Subject: Petroleum Engineering

**OPTIMAL FRACTURE TREATMENT DESIGN FOR DRY GAS  
WELLS MAXIMIZES WELL PERFORMANCE IN THE PRESENCE  
OF NON-DARCY FLOW EFFECTS**

A Thesis

by

HENRY DE JESUS LOPEZ HERNANDEZ

Submitted to Texas A&M University  
in partial fulfillment of the requirements  
for the degree of

MASTER OF SCIENCE

Approved as to style and content by:

---

Peter P. Valko  
(Chair of Committee)

---

William D. McCain, Jr.  
(Member)

---

Guy L. Curry  
(Member)

---

Stephen A. Holditch  
(Head of Department)

August 2004

Major Subject: Petroleum Engineering

## ABSTRACT

Optimal Fracture Treatment Design for Dry Gas Wells Maximizes Well Performance in the Presence of Non-Darcy Flow Effects. (August 2004)

Henry De Jesus Lopez Hernandez,

B.S., Universidad de Los Andes, Venezuela

Chair of Advisory Committee: Dr. Peter P. Valko

This thesis presents a methodology based on Proppant Number approach for optimal fracture treatment design of natural gas wells considering non-Darcy flow effects in the design process. Closure stress is taken into account, by default, because it is the first factor decreasing propped pack permeability at in-situ conditions. Gel damage was also considered in order to evaluate the impact of incorporating more damaging factors on ultimate well performance and optimal geometry. Effective fracture permeability and optimal fracture geometry are calculated through an iterative process. This approach was implemented in a spreadsheet.

Non-Darcy flow is described by the  $\beta$  factor. All  $\beta$  factor correlations available in the literature were evaluated. It is recommended to use the correlation developed specifically for the given type of proppant and mesh size, if available. Otherwise, the Pursell *et al.* or the Martins *et al.* equations are recommended as across the board reliable correlations for predicting non-Darcy flow effects in the propped pack.

The proposed methodology was implemented in the design of 11 fracture treatments of 3 natural tight gas wells in South Texas. Results show that optimal fracture design might increase expected production in 9.64 MMscf with respect to design that assumes Darcy flow through the propped pack. The basic finding is that for a given amount of proppant shorter and wider fractures compensate the non-Darcy and/or gel damage effect.

Dynamic programming technique was implemented in design of multistage fractures for one of the wells under study for maximizing total gas production. Results show it is a

powerful and simple technique for this application. It is recommended to expand its use in multistage fracture designs.

## **DEDICATION**

To God, my Mother, Mama Elena, my Wife, Paola Sofia and Gary. Thanks you all for being an enduring source of light, learning, joy, inspiration, and unfailing support.

## ACKNOWLEDGEMENTS

I wish to express my deep sincere gratitude to my advisor, Dr. Peter Valko, for his constant valuable support, encouragement, guidance and patience offered during this study. It was a great experience working with you.

Thanks to the Technology Group of El Paso Production for providing me with invaluable information and support for this project.

Thanks to Dr. William D. McCain, Dr. Guy L. Curry and Dr. Sergyi Butenko for serving on my committee and for their support to accomplish this requirement.

Thanks to all professors and students in the Department of Petroleum Engineering at Texas A&M University who shared their knowledge and experience with me.

## TABLE OF CONTENTS

	Page
ABSTRACT.....	i
DEDICATION.....	v
ACKNOWLEDGEMENTS.....	vi
TABLE OF CONTENTS.....	vii
LIST OF TABLES.....	x
LIST OF FIGURES.....	xii
CHAPTER	
I INTRODUCTION.....	1
II LITERATURE REVIEW.....	4
2.1 Proppant Number ( $N_{prop}$ ).....	4
2.2 Effective permeability formulation for non-Darcy flow effects.....	6
2.3 $\beta$ Factor Equations.....	8
2.3.1 Equations developed from proppants tests.....	8
2.3.1.1 Cooke.....	8
2.3.1.2 Kutasov.....	9
2.3.1.3 Maloney, Gall and Raible.....	9
2.3.1.4 Martins, Milton-Tayler and Leung.....	9
2.3.1.5 Penny and Jin.....	10
2.3.1.6 Pursell, Holditch and Blakeley.....	11
2.3.2 Equations developed from other sources.....	11
2.3.2.1 Belhaj, Agha, Nouri, Butt and Islam.....	11
2.3.2.2 Coles and Hartman.....	12
2.3.2.3 Ergun.....	12
2.3.2.4 Frederick and Graves.....	12
2.3.2.5 Geertsma.....	13
2.3.2.6 Janicek and Katz.....	13
2.3.2.7 Jones.....	13
2.3.2.8 Li.....	13
2.3.2.9 Macdonald, El-Sayed, Mow and Dullen.....	14
2.3.2.10 Tek, Coats and Katz.....	14
2.3.2.11 Thauvin and Mohanty.....	14
2.3.3 General form of $\beta$ equation.....	15
2.4 Optimization.....	17

CHAPTER	Page
2.4.1 Optimization of hydraulic fracture treatment designs.....	18
2.4.2 Dynamic programming .....	19
2.4.2.1 DP elements .....	19
2.4.2.2 Advantages and disadvantages .....	20
2.4.2.3 Applications of dynamic programming (DP) in the petroleum industry .....	20
<b>III FRACTURE TREATMENT DESIGN SPREADSHEET .....</b>	<b>22</b>
3.1 Spreadsheet capabilities definition .....	22
3.2 Effects to be considered in the effective propped pack permeability calculation .....	23
3.2.1 Closure stress .....	23
3.2.2 Non-Darcy flow .....	26
3.2.3 Gel damage effects.....	26
3.3 Effective permeability calculation .....	28
3.4 Spreadsheet structure .....	29
3.4.1 Input data window.....	30
3.4.1.1 Proppant data .....	30
3.4.1.2 Gas Properties .....	33
3.4.1.3 Constraints .....	35
3.4.1.4 Frac Job Parameters .....	36
3.4.1.5 Reservoir .....	37
3.4.1.6 Well.....	38
3.4.2 Proppant permeability correction window.....	38
3.4.2.1 Non-Darcy Flow .....	38
3.4.2.2 Gel Damage .....	40
3.5 Calculated results .....	41
<b>IV FIELD CASES APPLICATION AND ANALYSIS .....</b>	<b>43</b>
4.1 Calculation of the effective propped pack permeability for non-Darcy flow and gel damage effects .....	45
4.2 Beta correlation evaluation .....	51
4.3 Optimal fracture geometry and bottomhole pressure sensitivity analysis .....	57
4.4 Comparison of optimal fracture designs results considering non-Darcy flow and gel damage effects .....	59
<b>V MULTISTAGE FRACTURING OPTIMIZATION .....</b>	<b>63</b>
5.1 Problem statement.....	64
5.1.1 Definition and calculation of number of stages .....	64
5.1.2 Gas production calculations .....	67



CHAPTER	Page
5.2 Problem formulation for DP optimization .....	69
5.3 Example application.....	71
VI SUMMARY AND CONCLUSIONS.....	76
6.1 Summary .....	76
6.2 Conclusions.....	77
NOMENCLATURE .....	78
REFERENCES .....	80
APPENDIX A - PROPPANT AND BETA EQUATION DATABASE .....	85
APPENDIX B - VB CODE FOR GAS VISCOSITY AND Z FACTOR ESTIMATION .....	92
APPENDIX C - $\beta$ CORRELATIONS EVALUATION AND EFFECTIVE PROPPANT PERMEABILITY.....	96
APPENDIX D - VB CODE FOR OPTIMAL MULTISTAGE HYDRAULIC FRACTURING DESIGN USING DYNAMIC PROGRAMMING...	103
VITA.....	111

## LIST OF TABLES

	Page
Table 2.1 Constants a and b of Cooke equation.....	8
Table 2.2 Constants a and b of Penny & Jin equations for 20/40 mesh .....	10
Table 2.3 Constants a and b in Pursell equation .....	11
Table 2.4 Parameters a, b and c of $\beta$ equations in original units for $\beta$ and $k_f$ .....	16
Table 2.5 Parameters a, b and c of $\beta$ equations for $\beta$ in 1/ft and $k_f$ in md .....	17
Table 3.1 Additional proppant properties required in the design process .....	26
Table 3.2 Coefficients of Piper, McCain and Corredor correlation for critical properties calculation .....	34
Table 3.3 $\beta$ equations that depend only on permeability .....	40
Table 4.1 Reservoir properties of stages proposed for fracture design.....	44
Table 4.2 Additional well data required for fracture design.....	44
Table 4.3 Gas specific gravity and contaminants content.....	44
Table 4.4 Gas expected production increases after implementing an optimal design for non-Darcy flow effects .....	61
Table 4.5 Gas expected production increases after implementing an optimal design for non-Darcy flow and gel damage effects .....	62
Table 5.1 Reservoir properties and initial propped pack permeability for stages 1 to 10.....	72
Table 5.2 Common data for stages 1 to 10 .....	72
Table 5.3 Recursive relation for stage 10 .....	74
Table 5.4 Recursive relation for stage 9 .....	74
Table 5.5 Recursive relation for stage 1 .....	74

	Page
Table 5.6 Optimal policy for multistage fracturing of PS #1 for one realization of Montecarlo simulation.....	75
Table C.1 Effects of closure stress, non-Darcy flow and gel damage upon propped pack effective permeability.....	102
Table D.1 Recursive relation for stage 8 .....	108
Table D.2 Recursive relation for stage 7 .....	108
Table D.3 Recursive relation for stage 6 .....	109
Table D.4 Recursive relation for stage 5 .....	109
Table D.5 Recursive relation for stage 4 .....	109
Table D.6 Recursive relation for stage 3 .....	110
Table D.7 Recursive relation for stage 2 .....	110

## LIST OF FIGURES

		Page
Fig. 2.1	Dimensionless Productivity Index as a function of proppant number less than 0.1 and dimensionless productivity index.....	5
Fig. 2.2	Dimensionless Productivity Index as a function of proppant number above 0.1 and dimensionless productivity index .....	5
Fig. 3.1	Orientation of created fracture respect to principal stresses.....	24
Fig. 3.2	Closure stress compact the propped pack reducing its initial permeability .....	24
Fig. 3.3	Effective permeability at different closure stress for proppants considered in this work.....	25
Fig. 3.4	Polymers within the fracture reduces cross sectional area .....	27
Fig. 3.5	Algorithm to be implemented in spreadsheet VBA code to calculate the effective fracture permeability .....	29
Fig. 3.6	Structure of the input windows for a traditional design .....	31
Fig. 3.7	Selection of the type of proppants available in Proppants Database.....	31
Fig. 3.8	Selection of the mesh size available for the type of proppant selected .....	32
Fig. 3.9	Warning message when a proppant is going to be used above the maximum limit of closure stress.....	32
Fig. 3.10	Selection of factors to be considered in the effective propped pack permeability calculations .....	39
Fig. 3.11	List of $\beta$ factor available for actual proppant and mesh size.....	39
Fig. 3.12	Output parameters reported in the Traditional design worksheet.....	42
Fig. 3.13	Output parameters reported in the TSO design worksheet.....	42
Fig. 4.1	Comparison of optimal design results in terms of gas rate production for 20/40 RCS proppant.....	53

	Page
Fig. 4.2 Comparison of optimal design results in terms of gas rate production for 20/40 LWC_LS proppant.....	54
Fig. 4.3 Comparison of optimal design results in terms of gas rate production for 20/40 SB proppant .....	55
Fig. 4.4 Comparison of optimal design results in terms of gas rate production for 20/40 LWC_HS proppant .....	56
Fig. 4.5 Optimal fracture geometry varies for PS #3_Stage 2 at different values of $p_{wf}$ .....	57
Fig. 4.6 Optimal fracture geometry varies for PS #1_Stage 3 at different values of $p_{wf}$ .....	58
Fig. 4.7 Optimal fracture geometry varies for PS #2_Stage 1 at different values of $p_{wf}$ .....	58
Fig. 4.8 Considering non-Darcy flow effects in the fracture design maximizes ultimate well deliverability .....	60
Fig. 4.9 Considering non-Darcy flow and gel damage effects in the fracture design maximizes ultimate well deliverability .....	60
Fig. 5.1 Multilayered reservoir .....	64
Fig. 5.2 Fracture height grow is limited and only connects some layers of all prospective layers.....	65
Fig. 5.3 More fractures are required to connect prospective layers with the wellbore.....	66
Fig. 5.4 Calculation of number of stages .....	67
Fig. 5.5 Triangular probabilistic distribution.....	68
Fig. A.1 Steps to input a new proppant in the database.....	86
Fig. A.2 Access to $\beta$ equations database from Proppant Permeability Correction window.....	88
Fig. A.3 Steps to input a new $\beta$ equation in the database .....	91

Fig. C.1	Comparison of optimal design results in terms of gas rate production for 20/40 LWC_LS proppant (PS #1_Stage3).....	96
Fig. C.2	Comparison of optimal design results in terms of gas rate production for 20/40 SB proppant (PS #1_Stage3).....	97
Fig. C.3	Comparison of optimal design results in terms of gas rate production for 20/40 LWC_HS proppant (PS #1_Stage3).....	98
Fig. C.4	Comparison of optimal design results in terms of gas rate production for 20/40 LWC_LS proppant (PS #2_Stage1).....	99
Fig. C.5	Comparison of optimal design results in terms of gas rate production for 20/40 SB proppant (PS #2_Stage1).....	100
Fig. C.6	Comparison of optimal design results in terms of gas rate production for 20/40 LWC_HS proppant (PS #2_Stage1).....	101

## CHAPTER I

### INTRODUCTION

Laboratory tests,<sup>1</sup> well modeling and simulation,<sup>2</sup> and post fracture well evaluations<sup>3</sup> have shown that propped fracture permeability of natural gas wells may be significantly reduced by production and reservoir conditions as well as fracturing fluid and other secondary effects. Several authors<sup>4-6</sup> agree that the most important variables affecting proppant pack permeability are:

- Non-Darcy Flow
- Time & Closure stress
- Multiphase Flow
- Gel Damage
- Embedment
- Proppant crushing
- Fines migration

The effects of single phase non-Darcy flow within propped fractures have been widely discussed and evaluated by a number of authors.<sup>7-11</sup> Holditch and Morse<sup>8</sup> mention that high pressure drop due to high flow velocities might be due to both turbulence and inertial resistance. They develop a numerical model to show the impact of non-Darcy flow in the deliverability of fractured wells. A single phase, two dimensional model, finite difference reservoir simulator was used. They conclude that non-Darcy effects should be considered in the design of hydraulic fracture treatments, otherwise the design might be far from optimal. Holditch and Moore also pointed out that effects of non-Darcy flow on gas well productivity index is a function of proppant type and not to consider it might result in a wrong analysis of well test interpretation.

---

This thesis follows the style of Journal of Petroleum of Technology

Guppy, Cinco-Ley, Ramey and Samaniego<sup>2</sup> presented a method to estimate effective fracture conductivity from drawdown data at two different flow rates. They developed a dimensionless model to describe the flow and pressure distribution in the fracture. This model was coupled to a 2D, single phase finite difference reservoir simulator to evaluate the behavior of non-Darcy flow through the fracture. They saw that non-Darcy flow causes the fracture conductivity to appear lower than its nominal value (what they called true conductivity).

Alvarez, Holditch and McVay<sup>4</sup> pointed out that simulation history matching is the most appropriate method to analyze buildup pressure tests of hydraulically fractured natural gas wells due to non-Darcy flow effects. They mention that not considering non-Darcy flow effects through the propped pack and/or using conventional methods of well test interpretation may result in wrong estimations of fracture half-length and fracture conductivity. They concluded that wrong estimates of fracture conductivity and permeability might result in overestimation of future gas production and incorrect actions to improve fracture performance in future wells.

Vincent, Pearson and Kullman<sup>6</sup> mention that engineers usually do not consider the effects of non-Darcy flow when designing fracture treatments because they assume it only happens in high rate wells. They showed that non-Darcy flow effects are significant even in wells considered low rate wells. Vincent, Pearson and Kullman estimate that the effects of not considering non-Darcy flow are not optimum fractures which causes lost revenues of \$2 million per fracture. They use Stim-Lab's SLFrac production model to perform their studies. Results show that the initially least attractive proppant due to cost could be the most appropriate considering the effective permeability in real conditions. Therefore, they conclude that ignoring multiphase and non-Darcy effects can lead to incorrect decisions regarding the required fracture width and proppant type.

In 2002 unified fracture design<sup>12</sup> was introduced. It is based in a new dimensionless number called proppant number which already determines the maximum possible productivity index achievable with the given amount of proppant. The concept can be also applied to situations, where non-darcy flow through the propped fracture is significant<sup>13</sup>.



All works presented above address very well the effects of non-Darcy flow in well test analysis, fracture design and well performance. However little work has been done regarding the reliability of the estimation of the  $\beta$  factor and its effect on the outcome. In the other hand, damaging effects on the fractured well are compensated injecting more proppant which increase gas production but also increase dramatically the treatment cost.

We propose in this work to develop a spreadsheet for optimal fracture designs considering non-Darcy flow, closure stress and gel damage effects in the design process. The goal is to maximize gas production for a given mass of proppant. This application will be based in proppant number approach and H2FD spreadsheet.  $\beta$  correlations available in the literature will be evaluated to determine which of them really apply for non-Darcy flow analysis trough propped packs. Four 20/40 type of proppants will be considered in this evaluation. Spreadsheet will be used in the design of 11 hydraulic fractures in three wells completed in South Texas tight gas reservoir. Finally, Dynamic Programming technique will be implemented in the design of the multistage fracture, of one of these wells, for maximizing total gas production having as a constraint the total mass proppant to be injected into the well.

## CHAPTER II

### LITERATURE REVIEW

#### 2.1 Proppant Number ( $N_{prop}$ )

The best performance indicator of a stimulated natural gas well is the pseudo-steady state productivity index ( $J$ )<sup>12</sup>

$$J = \frac{q_{g,sc}}{p_{res} - p_{wf}} = \frac{2\pi k_g h_p}{\alpha_1 B_g \mu_g} J_D \dots\dots\dots(2.1)$$

The actual effect of the propped fracture appears in the variable  $J_D$ . Dimensionless fracture conductivity ( $C_{fD}$ ) and penetration ratio ( $I_x = 2x_f/x_e$ ) are the two primary variables that control it. The dimensionless fracture conductivity,  $C_{fD}$  is a measure of the relative ease with which the produced fluids flow inside the fracture compared to the ability of the fracture to gather fluids from the formation:

$$C_{fD} = \frac{k_f w_{fp}}{k_g x_f} \dots\dots\dots(2.2)$$

The Proppant number is a combination of the two dimensionless variables:

$$N_{prop} = I_x^2 C_{fD} \dots\dots\dots(2.3)$$

Substituting the definition of penetration ratio and dimensionless fracture conductivity into Eq. 2.3 we obtain the final form:

$$N_{prop} = \frac{2k_f}{k} \frac{V_{p-2w}}{V_{res}} \dots\dots\dots(2.4)$$

showing that the Proppant number is the ratio of the propped volume (volume of proppant in the pay, in the two wings) to the reservoir volume, weighted by the permeability contrast. From one hand, the Proppant number is easy to use, because it is already determined by the selection of the type and amount of Proppant. On the other hand, its use is helpful, because it determines the maximum achievable dimensionless productivity index, as seen in **Figs. 2.1** and **2.2**. For a specific  $N_{prop}$  the maximum  $J_D$

occurs for a well defined value of  $C_{fD}$ . For example, optimum  $C_{fD}$  is 1.6 for  $N_{prop}$  below 0.1 (**Fig. 2.1**). However, for  $N_{prop}$  larger than 0.1 the optimal  $C_{fD}$  increases with proppant number (**Fig. 2.2**). It happens because the  $I_x$  cannot exceed unity.

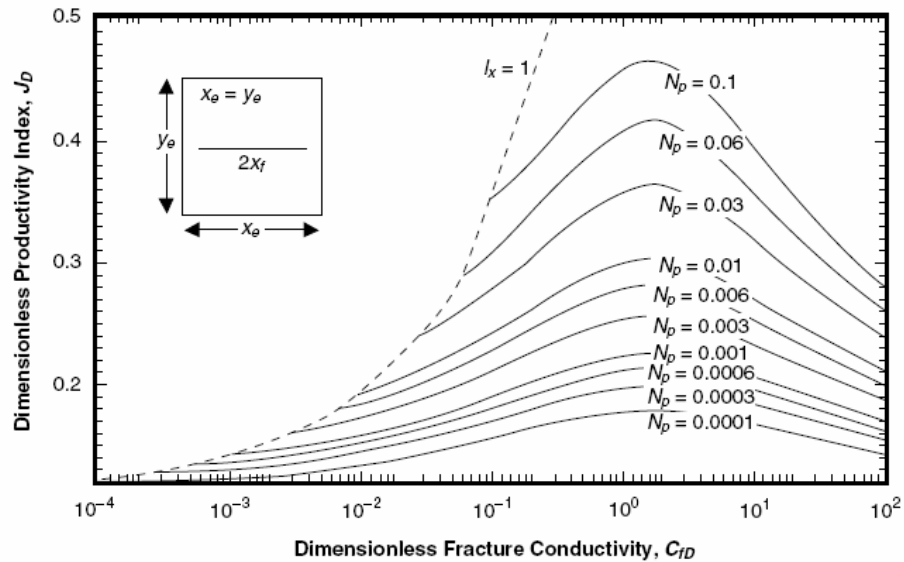


**Fig. 2.1** Dimensionless Productivity Index as a function of proppant number less than 0.1 and dimensionless productivity index (Economides, Oligney and Valko<sup>12</sup>)

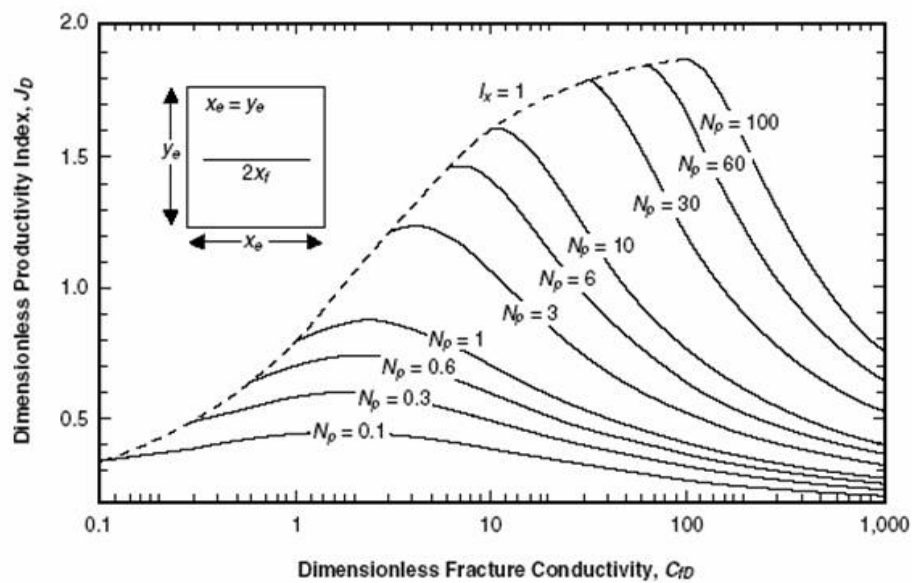


**Fig. 2.2** Dimensionless Productivity Index as a function of proppant number above 0.1 and dimensionless productivity index (Economides, Oligney and Valko<sup>12</sup>)

For all proppant numbers, the optimum fracture dimensions can be obtained from

$$w_{fp} = \left( \frac{C_{fDopt} k_g V_{p-1w}}{k_f h_p} \right)^{1/2} \dots\dots\dots(2.5)$$

$$x_f = \left( \frac{k_f V_{p-1w}}{C_{fDopt} k h_p} \right)^{1/2} \dots\dots\dots(2.6)$$

Once the spacing of the wells in the reservoir has been defined, the denominator of Eq. 2.4 is constant. Then, the proppant number will depend on propped fracture permeability ( $k_f$ ) and volume of proppant reaching the pay ( $V_{p-2w}$ ).

Though in the simple theory the treatment size already determines the maximum achievable dimensionless productivity index, this is not so in the case of non-Darcy flow in the fracture. The reason is that the effective Proppant permeability depends on the actual linear velocity of the gas in the fracture. Therefore, even if the treatment size is fixed, the effective Proppant number still varies with adjusting the width to length compromise. For gas wells, this effect is significant.

## 2.2 Effective permeability formulation for non-Darcy flow effects

Darcy's law describes laminar flow through porous media. In this case pressure gradient is directly proportional to flow velocity

$$\frac{\Delta P}{\Delta L} = \frac{\mu_g v}{k_f} \dots\dots\dots(2.7)$$

When flow velocity increases, Eq. 2.7 is not valid anymore due to the additional pressure drop caused by the frequent acceleration and deceleration of the particles of the moving fluid. These inertial effects<sup>8,14</sup> are well described by the equation developed by Forchheimer<sup>15</sup> :

$$\frac{\Delta P}{\Delta L} = \frac{\mu_g v}{k_f} + av^2 \dots\dots\dots(2.8)$$

Cornell and Kartz<sup>16</sup> rewrote the constant  $a$  as the product of the  $\beta$  factor (called also non-Darcy flow coefficient, inertial flow coefficient, turbulent factor) and the fluid density:

$$\frac{\Delta P}{\Delta L} = \frac{\mu_g v}{k_f} + \beta \rho_g v^2 \dots\dots\dots(2.9)$$

When velocities are low, the second term in Eq. 2.9 can be neglected. However, for higher velocities this term becomes more important, especially for low viscosity fluids.<sup>17</sup>

If we divide LHS and RHS of Eqs. 2.7 and 2.9 by  $\mu_g v$  we obtain

$$\frac{\Delta P}{\Delta L \mu_g v} = \frac{1}{k_f} \dots\dots\dots(2.10)$$

for Darcy flow and

$$\frac{\Delta P}{\Delta L \mu_g v} = \frac{1}{k_f} + \frac{\beta \rho_g v}{\mu_g} \dots\dots\dots(2.11)$$

for non-Darcy flow. Comparing Eq. 2.10 and 2.11 we see that the effective permeability (determining the actual pressure drop) is

$$k_{f-eff} = \frac{k_f}{1 + \frac{\beta k_f \rho_g v}{\mu_g}} \dots\dots\dots(2.12)$$

The Reynold number ( $N_{Re}$ ) in a porous media can be defined as

$$N_{Re} = \frac{\beta k_f \rho_g v}{\mu_g} \dots\dots\dots(2.13)$$

first suggested by Geertsma<sup>14</sup>. Substituting Eq. 2.13 into Eq. 2.12 we get the final expression of  $k_{f-eff}$  describing the non-Darcy flow effects.

$$k_{f-eff} = \frac{k_f}{1 + N_{Re}} \dots\dots\dots(2.14)$$

## 2.3 $\beta$ Factor Equations

$\beta$  factor is a property of the porous media.<sup>18,19</sup> Empirical equations have been developed to estimate this factor<sup>20</sup> based on lab data. For this work an extended search was done in various bibliographic databases to collect  $\beta$  factor equations developed so far. These databases are: SPE, Petroleum Abstracts, Transport in Porous Media and Science Citation Index. A detailed review of the references allowed identifying 24 equations. These can be divided into two groups: (1) Equations developed from proppant tests, (2) Equations developed from core, pack bead tests and analytical studies.

### 2.3.1 Equations developed from proppants tests

#### 2.3.1.1 Cooke

It was the first equation developed to estimate  $\beta$  factor of proppants.<sup>21</sup> Brady sand was used in the lab experiments. Based on the form of the Forchheimer equation presented in Eq. 2.9, Cooke plotted  $\Delta P/L\mu\gamma^b$  vs.  $\rho v/\mu\gamma$  (X) to get the  $\beta$  factor, which is the slope of the curve on this plot. Five sand sizes and various stress levels were considered. X values of all tests were below three. Fluids used were brine, gas and oil. Cooke observed no difference of the results among fluids evaluated. All curves followed Eq 2.15. Coefficients are shown in **Table 2.1**.

$$\beta = \frac{a}{k_f^b} \dots\dots\dots(2.15)$$

**Table 2.1** Constants a and b of Cooke equation

Sand Size (mesh)	a	b
8/12	3.32	1.24
10/20	2.63	1.34
20/40	2.65	1.54
40/60	1.10	1.60

### 2.3.1.2 Kutasov

A semitheoretical equation was proposed as a function of darcian permeability,  $k_f$  (Darcies), porosity,  $\phi_p$ , and irreducible water saturation,  $S_w$ .<sup>22</sup> From analyses of experimental and analytical investigations conducted by Evans and Evans, Fand, Ergun, Olovin and Bear, Kutasov he developed Eq. 2.16.

$$\beta = \frac{1.43E + 03}{k_f^{0.5} (\phi_p (1 - S_w))^{1.5}} \dots\dots\dots (2.16)$$

### 2.3.1.3 Maloney, Gall and Raible

Nitrogen was used to simulate gas production.<sup>17</sup> Pressure and temperature were maintained constant through the proppant pack to eliminate uncertainties in the variation of viscosity and density. Sandpack tests were performed at closure stresses from 1,000 to 10,000 psi using various type of proppants. Results show that relationship between  $\beta$  and  $k_f$  are independent of the sand concentration but is affected by proppant size distribution, grain shape and strength characteristics. They pointed out that if porosity is considered in  $\beta$  equation the dependence on proppant size distribution is less. Therefore, they proposed Eq. 2.17 for any type of proppant and mesh.

$$\beta = \frac{1.2E - 03}{k_f^{7.1} \phi_p^{0.5}} \dots\dots\dots (2.17)$$

### 2.3.1.4 Martins, Milton-Taylor and Leung

They pointed out that laboratory studies have been usually performed at X values below 10.<sup>23</sup> However, in field conditions X is normally higher than 10 so they performed tests for X up to 60 using dry nitrogen at ambient temperature, in order to identify different flow regimes. Tests were conducted for different type of proppants (i.e. intermediate strength proppant, sand) and mesh size (i.e. 16/20 and 20/40) at confining stresses of 2,000, 4,000 and 5,000. They observed that at high rates all results are very similar

irrespective of the type of sand and mesh, so they proposed Eq. 2.18 as general equation for proppants.

$$\beta = \frac{2.1E - 01}{k_f^{1.036}} \dots\dots\dots (2.18)$$

They found that several flow regimes may be present for the range of X evaluated. In general, two linear behaviors were observed, one for X above 10 and other one for 2<X<5. They conclude that the transition to the high rate flow regime occurs for 3<X<7 independently of particle size. These authors also concluded that interpretation of results for X < 10 requires special attention. Therefore, they recommend performing lab tests for X > 10.

### 2.3.1.5 Penny and Jin

They plotted  $\beta$  factor vs. permeability for different type of 20/40 proppants (i.e. northern wide sand, precurred resin coated white sand, intermediate strength ceramic products and bauxite).<sup>1</sup> Final equation developed by them has the same form as Cooke's equation (Eq. 2.15) where the coefficients *a* and *b* depends on type of sand. These coefficients are shown in **Table 2.2**. The correlation provides the so called dry  $\beta$  factor because the authors propose to correct it for multiphase flow (when water or condensate is also flowing). Tests were conducted for values of X up to 20. They considered only one equation for the entire range of X.

**Table 2.2** Constants a and b of Penny & Jin equations for 20/40 mesh

<b>Type of proppant</b>	<b>a</b>	<b>b</b>
Jordan Sand	0.75	1.45
Precurred Resin-Coated Sand	1	1.35
Light Weight Ceramic	0.7	1.25
Bauxite	0.1	0.98



### 2.3.1.6 Pursell, Holditch and Blakeley

Three type of proppant were evaluated (i.e. Brady sand, Interprop and Carbolite) injecting nitrogen at constant closure stress and pore pressure, at different flow rates.<sup>18</sup> They concluded that the relationship between permeability and  $\beta$  factor is only a function of mesh size and proppant permeability, and is independent of proppant type. They also concluded that  $\beta$  should be calculated in the region of high flow rate. However, X values in the tests were up to 6. Pursell, Holditch and Blakeley developed two equations, with the same form of Cooke's equation for 12/20 and 20/40 mesh size. Their coefficients a and b are shown in **Table 2.3**.

**Table 2.3** Constants a and b in Pursell equation

<b>Mesh</b>	<b>a</b>	<b>b</b>
12/20	1.144	0.635
20/40	1.123	0.326

### 2.3.2 Equations developed from other sources

#### 2.3.2.1 Belhaj, Agha, Nouri, Butt and Islam

A numerical model was developed to describe non-Darcy behavior in porous media.<sup>24</sup> This model was verified and tested with experimental data. A triaxial system was built to test artificial sandstone sample at in situ reservoir conditions. All tests were performed flowing water trough the core. Permeability and  $\beta$  factor were determined from experiment results and used as input data in the numerical model. In general, they found a good match between numerical and experimental predictions. They proposed Eq. 2.19 to estimate  $\beta$  factor.

$$\beta = \frac{1.15E + 07}{k_f \phi_p} \dots\dots\dots (2.19)$$

### 2.3.2.2 Coles and Hartman

They developed Eq. 2.20 to estimate  $\beta$  factor as a function of effective permeability and porosity.<sup>25</sup> They passed gas through dry and saturated limestone and sandstones core samples to estimate  $\beta$  factor, so it is valid for both dry and saturated cases where  $k_g$  is the effective permeability to gas. Core permeabilities ranged from 0.01 to 1000 md. They emphasized that relationship was obtained from plots with less scatter than data used to develop previous relationships.

$$\beta = \frac{2.49E + 11\phi_p^{0.537}}{k_f^{1.79}} \dots\dots\dots (2.20)$$

### 2.3.2.3 Ergun

He developed Eq. 2.21 from experiments of gas flow through packed spheres. Dependence on flow rate, properties of the fluids, porosity, orientation, size, shape, and surface of the granular solids were also analyzed.<sup>26</sup>

$$\beta = \frac{4.24E + 04}{k_f^{0.5} \phi_p^{1.5}} \dots\dots\dots (2.21)$$

### 2.3.2.4 Frederick and Graves

$\beta$  factor equation was developed from tests performed on 24 cores with confining stress from 1,000 to 5,000 psi and permeabilities ranged from 0.00197 to 1,230 md.<sup>27</sup> In the plot used to get the correlation they included data from Cornell and Katz<sup>16</sup>, Geertsma<sup>14</sup> and Evans et al<sup>28</sup> experiments so it can be considered valid for permeabilities up to 350,000 md. Tests were performed flowing gas in dry and brine saturated cores. Eq. 2.22 is a direct correlation between permeability and  $\beta$ .

$$\beta = \frac{1.98E + 11}{k_f^{1.64}} \dots\dots\dots (2.22)$$

### 2.3.2.5 Geertsma

He proposed Eq. 2.23 to estimate  $\beta$  factor as a function of permeability and porosity.<sup>14</sup> Experiments were conducted with both liquid and gas flow through unconsolidated sandstones, and gas flow through consolidated sandstones. This equation was validated for limestone using Gewers and Nichol data.

$$\beta = \frac{5E-02}{k_f^{0.5} \phi_p^{5.5}} \dots\dots\dots (2.23)$$

### 2.3.2.6 Janicek and Katz

They developed the first equation for  $\beta$  factor (Eq. 2.24) from laboratory experiments in sandstone, limestone and dolomite as function of permeability and porosity of porous media.<sup>29</sup>

$$\beta = \frac{1.82E+08}{k_f^{1.25} \phi_p^{0.75}} \dots\dots\dots (2.24)$$

### 2.3.2.7 Jones

355 sandstones and 29 limestones cores plugs from reservoirs around the world were used in his studies.<sup>30</sup> Confining stress between 800 psi and 6,000 psi was applied to all cores. Sandstones and limestones permeability ranged from 0.01 to 2,500 md and from 0.01 to 400 md respectively. Only Helium was used in all measurements. Finally Jones presented Eq. 2.25 like the equation that fits the best all data collected in the experiments.

$$\beta = \frac{6.15E+10}{k_f^{1.55}} \dots\dots\dots (2.25)$$

### 2.3.2.8 Li

A semitheoretical equation (Eq. 2.26) was developed for  $\beta$  which was verified comparing pressure drops predicted from simulations with results from experiments conducted by

him.<sup>31</sup> Nitrogen was injected in several directions through a wafer-shaped Berea sandstone core sample. Performance of Eq. 2.26 and other equations found in the literature was evaluated using lab data of Firoozabadi et al experiments. Eq. 2.26 had the lowest average error so Li conclude it is the best to predict  $\beta$  factor in berea sandstone.

$$\beta = \frac{1.39E + 07}{k_f^{0.85} \phi_p^{1.15}} \dots\dots\dots (2.26)$$

### 2.3.2.9 Macdonald, El-Sayed, Mow and Dullen

They modified equation proposed by Ergun<sup>26</sup> and use experiment results of Gupte, Kyan, Dudgeon, Fancher and, Lewis and Pahl all consisting of gas and liquid flow through packed sphere beds of uniform size or known distribution.<sup>32</sup> They got new values for the coefficients of modified Ergun equation

$$\beta = \frac{4.52E + 04}{k_f^{0.5} \phi_p^{1.5}} \dots\dots\dots (2.27)$$

### 2.3.2.10 Tek, Coats and Katz

A partial differential equation was derived to represent flow of fluids at all rates.<sup>33</sup> They presented an equation from Janice and Katz<sup>29</sup> data (Eq. 2.28) also as function of porosity and permeability.

$$\beta = \frac{5.5E + 09}{k_f^{1.25} \phi_p^{0.75}} \dots\dots\dots (2.28)$$

### 2.3.2.11 Thauvin and Mohanty

They developed a pore-level network model where inputs are pore sizes distribution and network coordination number and outputs are permeability,  $\beta$  factor, tortuosity and porosity.<sup>34</sup> They found that correspondence between  $\beta$  factor and permeability, porosity and tortuosity depend on the morphological parameters being changed. From all data

collected, a general correlation was derived to match all the morphological changes. However, correlation considered in our work is Eq. 2.29 that not considers tortuosity. Thauvin and Mohanty pointed out that there is no perfect correlation valid for all kind of porous media.

$$\beta = \frac{2.5E + 05}{k_f} \dots\dots\dots (2.29)$$

### 2.3.3 General form of $\beta$ equation

All  $\beta$  factor equations presented so far are function of  $k_f$  and/or  $\phi_p$ . Therefore all these equations can be summarized in a general expression (Eq. 2.30) where a, b and c parameters are the difference for each case. Parameter c is 0 for equations that depends only on permeability.

**Table 2.4** Parameters a, b and c of  $\beta$  equations in original units for  $\beta$  and  $k_f$ 

EQUATION	a	b	c	$\beta$	k
Belhaj <i>et al</i>	1.15E+07	1.00	1.00	1/m	md
Cole and Hartman	2.49E+11	1.79	-0.54	1/ft	md
Cooke_Sand 8/12	3.32E+00	1.24	0.00	atm-sec <sup>2</sup> /g	D
Cooke_Sand 10/20	2.63E+00	1.34	0.00	atm-sec <sup>2</sup> /g	D
Cooke_Sand 20/40	2.65E+00	1.54	0.00	atm-sec <sup>2</sup> /g	D
Cooke_Sand 40/60	1.10E+00	1.60	0.00	atm-sec <sup>2</sup> /g	D
Ergun	4.24E+04	0.50	1.50	1/m	md
Frederick and Graves	1.98E+11	1.64	0.00	1/ft	md
Geertsma	5.00E-02	0.50	5.50	1/cm	cm <sup>2</sup>
Janice and Katz	1.82E+08	1.25	0.75	1/m	md
Jones	6.15E+10	1.55	0.00	1/ft	md
Kutasov	1.43E+03	0.50	1.50	1/cm	D
Li et al	1.39E+07	0.85	1.15	1/cm	md
Mac Donal <i>et al</i>	4.52E+04	0.50	1.50	1/m	md
Maloney <i>et al</i>	1.20E-03	0.50	7.10	1/cm	cm <sup>2</sup>
Martins <i>et al</i>	2.10E-01	1.04	0.00	atm-sec <sup>2</sup> /g	D
Penny and Jin_Bauxite 20/40	1.00E-01	0.98	0.00	atm-sec <sup>2</sup> /g	D
Penny and Jin_LWC 20/40	7.00E-01	1.25	0.00	atm-sec <sup>2</sup> /g	D
Penny and Jin_RCS 20/40	1.00E+00	1.35	0.00	atm-sec <sup>2</sup> /g	D
Penny and Jin_Sand 20/40	7.50E-01	1.45	0.00	atm-sec <sup>2</sup> /g	D
Pursell et al_12/20	6.35E-01	1.14	0.00	atm-sec <sup>2</sup> /g	D
Pursell et al_20/40	3.26E-01	1.12	0.00	atm-sec <sup>2</sup> /g	D
Tek <i>et al</i>	5.50E+09	1.25	0.75	1/m	md
Thauvin and Mohanty	2.50E+05	1.00	0.00	1/cm	D

Most of these  $\beta$  equations were developed in different units. **Table 2.4** shows a summary of original units and a, b, and c values. In this work parameter  $a$  was recalculated (where necessary) in order to have  $\beta$  in 1/ft and  $k_f$  in md. Results are presented in **Table 2.5** where we already can see important differences among correlations based on values of  $a$ ,  $b$  and  $c$  parameters.

$$\beta = \frac{a}{k_f^b \phi_p^c} \dots \dots \dots (2.30)$$

**Table 2.5** Parameters a, b and c of  $\beta$  equations for  $\beta$  in 1/ft and  $k_f$  in md

<b>EQUATION</b>	<b>a</b>	<b>b</b>	<b>c</b>
Belhaj et al	3.51E+06	1.00	1.00
Cole and Hartman	2.49E+11	1.79	-0.54
Cooke_Sand 8/12	5.38E+11	1.24	0.00
Cooke_Sand 10/20	8.51E+11	1.34	0.00
Cooke_Sand 20/40	3.41E+12	1.54	0.00
Cooke_Sand 40/60	2.14E+12	1.60	0.00
Ergun	1.29E+04	0.50	1.50
Frederick and Graves	1.98E+11	1.64	0.00
Geertsma	4.85E+05	0.50	5.50
Janice and Katz	5.55E+07	1.25	0.75
Jones	6.15E+10	1.55	0.00
Kutasov	1.38E+06	0.50	1.50
Li et al	4.22E+08	0.85	1.15
Mac Donal et al	1.38E+04	0.50	1.50
Maloney et al	1.16E+04	0.50	7.10
Martins et al	8.32E+09	1.04	0.00
Penny and Jin_Bauxite 20/40	2.69E+09	0.98	0.00
Penny and Jin_LWC 20/40	1.22E+11	1.25	0.00
Penny and Jin_RCS 20/40	3.47E+11	1.35	0.00
Penny and Jin_Sand 20/40	5.19E+11	1.45	0.00
Pursell et al_12/20	5.30E+10	1.14	0.00
Pursell et al_20/40	2.35E+10	1.12	0.00
Tek et al	1.68E+09	1.25	0.75
Thauvin and Mohanty	7.62E+09	1.00	0.00

## 2.4 Optimization

One of the most important goals of any major or independent oil and gas company is to maximize the recovery of hydrocarbons for maximum profits. It demands the technical-economical optimization of operations performed in the field during the life of the asset. In fields where massive hydraulic fractures (MHF) are executed, to increase the productivity of the wells and consequently the field (i.g. tight gas reservoirs), optimal

fracture treatment designs are a key to maximize the economic return of the reservoir exploitation.

#### **2.4.1 Optimization of hydraulic fracture treatment designs**

Hydraulic fracturing is a multivariate process. It is because final results or objective function depends on more than one variable. In this work variables that can not be modified will be identified as system parameters.<sup>35</sup> For example, net pay, reservoir permeability, and closure stress. Variables that can be changed to affect final results (i.e. objective function) are denominated decision variables. In this case type of proppant, mesh size, mass of proppant, proppant concentration, pump rates, frac fluid, proppant schedule are decision variables of the hydraulic fracturing process. Objective function can be Net Present Value (NPV) of the job, dimensionless productivity index or gas rate.

Several approaches have been developed so far to optimize fracture treatment design in all type of reservoirs. The most important currents are:

- Multivariate optimization applying non-linear optimization techniques.<sup>35,36</sup>
- Parametric optimization using 2D and 3D fracture and production models .<sup>4,37-40</sup>
- Implementation of Virtual Intelligence tools to optimize future fracture jobs in a specific field based on results obtained in previous frac jobs performed in the same or similar fields.<sup>41-43</sup>

All these applications were developed for fracture design of one stage only. However, in multilayered reservoirs more than one fracture (i.e. stage) is usually required to connect all productive zones with the wellbore. In this case the goal is to maximize the overall performance of the well (i.e. total gas production) having the total mass of proppant available for the well as the main constraint.

There are several methods available to solve an optimization problem. Candidate methods depend on the nature of the problem. In this work we selected dynamic programming (DP) as the method to use because its simplicity and effectiveness to optimize multistage processes.



## 2.4.2 Dynamic programming

DP was developed by Richard Bellman in the mid 1950's.<sup>44</sup> DP is primarily applied to multistage decision processes. It is where a sequence of decisions has to be made at various stages of the evolution of the process. Since its creation DP has been used to solve resource allocation problems, production planning, problems with multiple constraints among other applications.<sup>44</sup>

### 2.4.2.1 DP elements

The following elements integrate the formulation of a problem to be solved using DP.<sup>45</sup>

Stages. Because this method was developed for multistage decision process, it is assumed that the problem can be subdivided in N number of stages. Stages can be in units of time or space.

State. This is a set of variables ( $s_0$ ,  $s_1$ , and so on) that can be used to describe the system at any stage. States can be deterministic or stochastic.

Decisions. They are made at each stage of the process. Decision affects how well we achieve our objective. A sequence of N decisions causes the state  $s$  to change from initial value  $s_0$  to final one  $s_N$ . They are usually constrained.

State equations. Define rules how a decision change the state of the process in one stage to another state in next stage. State equations can be: time invariant or time variant; and continuous or discrete.<sup>46</sup>

Objective function. Decisions are made to maximize or minimize the objective function. Ultimate value of the objective function depends on the policy (set of decisions made and constraints) and initial state  $s_0$ .

Optimality. The principle of optimality in DP is equivalent to the statement that certain derivatives are zero.<sup>45</sup> It considers that decision at each state does not depend on previous decisions or states. There is a recursive relationship representing the optimal decision for each state at stage  $i$  in terms of previously computed optimal decisions for states at subsequent stages  $i+1$ ,  $i+2$ , etc. Final result is an optimal policy that maximizes or minimizes the objective function.

### 2.4.2.2 Advantages and disadvantages

#### Advantages

1. The problem is reduced to N stages
2. The method gives a global maxima or minima
3. Provide a program for sequential computation when classical functional solutions (i.e. Linear Programming, Non-Linear Programming, etc) are difficult to solve
4. It does not require calculation of first or second derivative and is not subject to stability problems
5. It can be applied in the maximization or minimization of functions where continuity prevents differentiation
6. The same problem can be solved using different definitions of stages, states, decisions and recursions.

#### Disadvantages

1. The higher the dimensionality of the states is the higher computational requirement is.
2. There exist some problems that can be treated more simply and efficiently by other methods than using DP.
3. It considers many paths compared to other methods. However, it is an advantage in stochastic processes where we need to know what to do for any state of each stage.

### 2.4.2.3 Applications of dynamic programming (DP) in the petroleum industry

In 1969 Bentsen and Donohue<sup>47</sup> use DP to optimize the number and size of steam treatments in a thermal recovery process to maximize the profits over the entire life of the project. They mention that it is multistage decision problem because decision must be made each interval of time (i.g. a day).

In 1971 Shamir<sup>48</sup> implemented DP to define the optimal route of a pipeline transporting oil and gas for minimizing costs. Later in 1972 Martch and Norman<sup>49</sup> developed an application (TRANSOPT) based on DP to minimize the annual cost of owning and

operating the facilities required to transport gas through the system (i.e. arrangement of pipeline and compressor stations connected in some arbitrary manner).

Huppler<sup>50</sup> used DP to find the best investment schedule for well drilling and compression in the exploitation of a gas reservoir for maximum net present value. In 1983 Lang and Horne<sup>51</sup> found that DP was the most efficient technique to optimal production schedules (i.e. injection rates or downhole flowing pressure) that maximize oil production. They proposed to use this approach in enhanced oil recovery projects.

Jegier<sup>52</sup> developed an application based on DP for casing string design. The goal was to minimize the cost of a given casing size selecting the steel grade and weight that met strength requirements at each interval depth. It is the only DP application of all applications presented where stages are interval of space instead of unit of time. After extensive literature review, we noticed the opportunity to use DP for the first time in the design of hydraulic fracturing treatments specifically multistage fractures.

## CHAPTER III

### FRACTURE TREATMENT DESIGN SPREADSHEET

#### 3.1 Spreadsheet capabilities definition

Estimation of the effective propped fracture permeability at in situ conditions (i.e. assessment of damage mechanism that might affect final permeability) is a key in an optimal fracture treatment design. Proppant selection should be part of this process as well. Flowers, Hupp and Ryan<sup>19</sup> pointed out that the trend of the petroleum industry is to use less expensive proppant which usually have lower permeabilities for a specific closure stress. It reduces costs but affects dramatically overall job economics and ultimate productivity of the well.

Several production and fracture simulators for oil and gas wells have been developed so far. These simulators include remarks stated in previous paragraph and are commercial available. Some of them include the latest proppant permeability and  $\beta$  factors data as well as non-Darcy and multiphase flow effects.<sup>5,19</sup> For example, the Predict K simulator (developed by Stimlab) combines reservoir transient production forecasting with a damaged hydraulic fracture. Moreover, closure stress, embedment, filter cake deposition and erosion, bulk gel damage, multiphase flow, and non-Darcy flow are accounted for. Each simulator follows a different approach to get an optimal design but none of them are based on proppant number approach.

First fracture design application based on proppant number approach was developed by Economides, Oligney and Valko.<sup>12</sup> HF2D is a fast 2D design package for traditional (moderate permeability and hard rock) and frac & pack (higher permeability and soft rock) with the PKN model. The design starts from the available mass of proppant; then optimum fracture dimensions are determined; finally, a treatment schedule is proposed, based on the PKN model, to achieve optimum placement of the proppant. Proppant properties must be input by user (i.e proppant permeability, porosity and specific gravity) as well as fluid properties (i.e. gas viscosity and formation volume factor). It requires that user estimate proppant permeability after closure stress, non-Darcy flow and other effects for a specific proppant type and mesh size. Estimation of effective permeability after non-

Darcy flow effects is an iterative process and requires additional input variables other than those included in HF2D (i.g. Flowing bottomhole pressure, beta factor equation, etc). Based on these limitations the development of a new fracture design spreadsheet for natural gas wells is required.

The new application should satisfy the following requirements to have a versatile spreadsheet:

1. Include a proppant database with the option of including new proppants
2. Calculate effective permeability after closure pressure effects
3. Consider the effects of non-Darcy flow on effective proppant permeability
4. Include  $\beta$  factor equation database where new equations can be incorporated
5. Calculate gas properties (i.e. viscosity and Z factor) at specific conditions of temperature and pressure
6. Consider additional variables affecting effective fracture permeability such as gel damage for a more realistic assessment of actual fracture permeability

## **3.2 Effects to be considered in the effective propped pack permeability calculation**

### **3.2.1 Closure stress**

A hydraulic fracture grows normal to the plane of minimum principal in situ stress (**Fig. 3.1**). In a homogeneous formation the minimum principal stress is equal to closure stress. However, lithology typically varies with depth. Therefore, minimum principal stress varies in magnitude and direction over the gross pay interval. In this case, closure stress represents the stress at which created fracture globally close (i.e. global average for the interval). Techniques commonly used to determine closure stress are the step rate test, shut-in decline and flowback analysis.<sup>53</sup>

Fracturing fluid (i.e. pad and slurry) is injected at high pressures into the formation to overcome closure stresses and, create and propagate a hydraulic fracture. When fluid injection ceases stresses acts to close the fracture and confine proppant. The effective stress acting on the proppant is

$$\sigma_{eff} = P_c - P_{fracture} \dots\dots\dots (3.1)$$

Effective stress ( $\sigma_{eff}$ ) results in compaction and consequently some reduction in proppant permeability, which is then magnified by crushing of the grains (**Fig. 3.2**). Reservoir pressure depletion decreases the net closure stress ( $P_c$ ).<sup>54</sup> On the other hand, flowing pressure within the fracture ( $P_{fracture}$ ) typically decreases with time, increasing the net closure stress. In general, the most critical condition is when pressure within the fracture is 0 psi. It is the case assumed in this work .

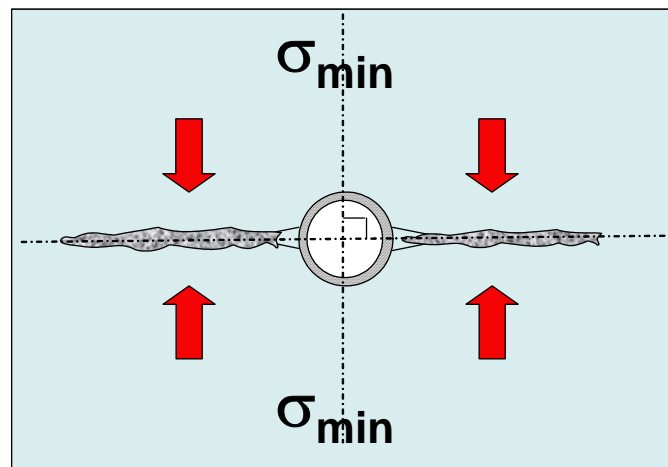


**Fig. 3.1** Orientation of created fracture respect to principal stresses

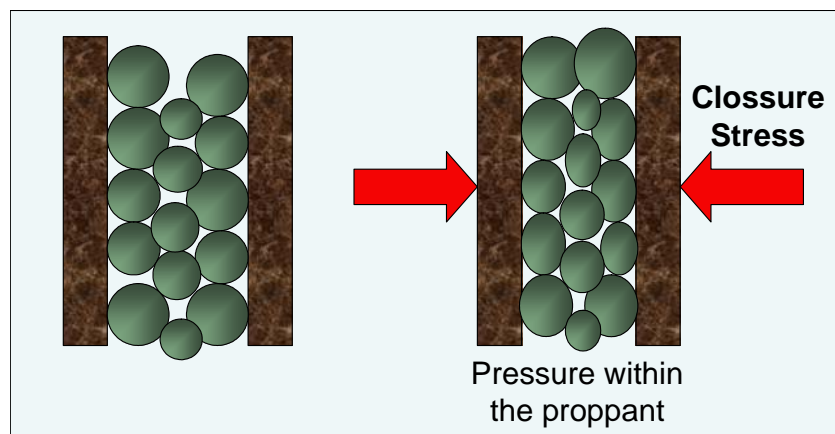


**Fig. 3.2** Closure stress compact the propped pack reducing its initial permeability

Four commonly used 20/40 mesh proppants will be initially included in the proppant database. These proppants are resin coated sand (RCS), low weight ceramic low strength (LWC\_LS), low weight ceramic high strength (LWC\_HS) and sintered bauxite (SB). Data on variation of proppant permeability with stress are usually provided by the proppant manufacturer. **Fig. 3.3** shows this information for all four proppants. The overall behavior is the result of proppant strength, grain size and grain size distribution, quantities of fines and impurities, roundness and sphericity, and proppant density.<sup>53</sup> The magnitude of the closure stress is the startpoint for selecting the proppants to be consider in the treatment design. Therefore, proppants which maximum stress reported in **Fig. 3.3** are below actual closure stress should not be considered in the design. **Table 3.1** shows the specific gravity and porosity for each proppant. This data will be used in the design process.

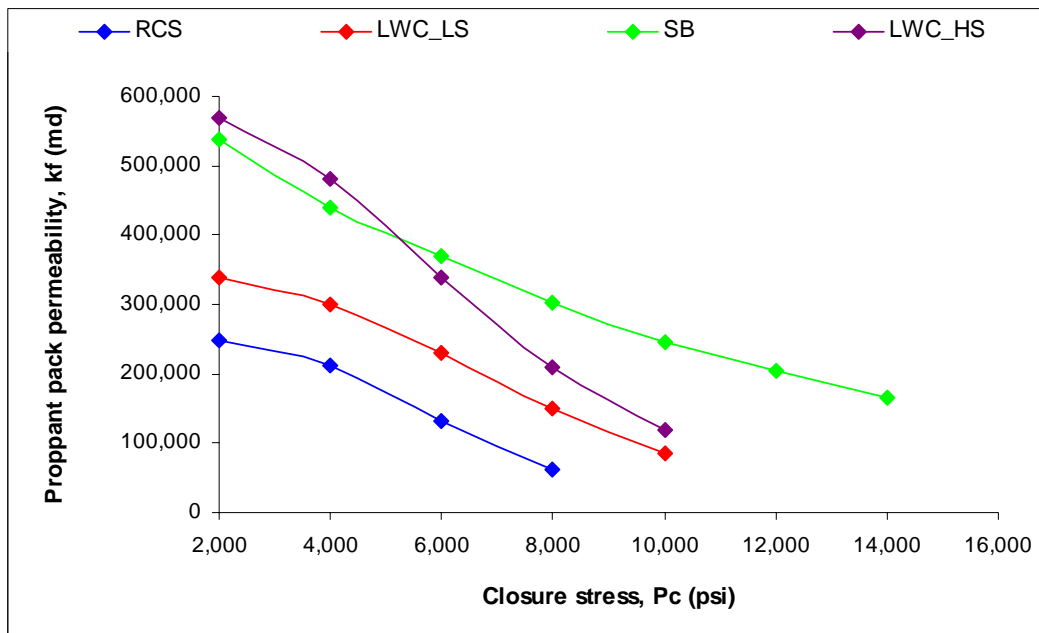


**Fig. 3.3** Effective permeability at different closure stress for proppants considered in this work

**Table 3.1** Additional proppant properties required in the design process

<b>Type of Proppant</b>	$SG_p$	$\phi_p$
RCS	2.62	0.40
LWC LS	2.70	0.42
SB	3.56	0.45
LWC HS	2.71	0.42

### 3.2.2 Non-Darcy flow

The main objective of this work is to consider the effects of non-Darcy flow in the design. In Chapter I, we mentioned that not considering this effect might result in wrong designs and proppant selection which impacts severely the ultimate economic performance of the job. All  $\beta$  equations presented in Chapter I will be included in this application to evaluate how equation selected affects optimum fracture geometry and well performance. The algorithm used to calculate the effective propped pack permeability due to non-Darcy flow effects is presented in Chapter IV through an application example.

### 3.2.3 Gel damage effects

Fracturing fluids are one the most important components of a successful fracture treatment. The main functions of these fluids are to transmit the hydraulic pressure from the pumps to the formation and transport proppant along the created fracture.<sup>12,53</sup>

Water based systems are the most widely used fracturing fluids. In this case, polymers are added to proportionate viscosity to the fluid. Guar gum and it derivatives such as hydroxypropil guar (HPG) and carboxymethyl-hydroxypropyl guar (CMHPG) are the polymers typically used as gelling agents.

During the treatment polymer deposits a filter cake on the fracture wall due to the leakoff of the fracturing fluid into the formation.<sup>55</sup> Gel concentration within the fracture increases with time as an effect of the fluid leakoff as well. Deposited cake is subject to erosion and part of the polymer within the fracture comes out in the flowback. However, most of



the polymer remains in the fracture (**Fig. 3.4**). Final effect is a reduction of the cross sectional area of flow which decreases permeability.

We considered two ways to account the effects of gel damage upon proppant permeability. The first one is as a percentage of retained permeability.<sup>56</sup> Flowers, Hupp and Ryan<sup>19</sup> mention that usually engineer designing hydraulic fractures include a damage of 50% or more to proppant permeability as a consequence of damage by polymers. In this case effective permeability is

$$k_{f-eff} = k_f \cdot \%damage \dots\dots\dots (3.2)$$

Second approach was presented by Pen and Jin.<sup>1</sup> They proposed to quantify the effects of gel damage upon  $\beta$  factor. This correlation was obtained from plot of measured percent of damage and  $\beta$  factor, for various frac fluids and proppants. Finally, gel damage effect is quantified with the following equation

$$F = 10^{\frac{\%damage}{100}} \dots\dots\dots (3.3)$$

where the beta factor after damage is

$$\beta' = F \times \beta \dots\dots\dots (3.4)$$

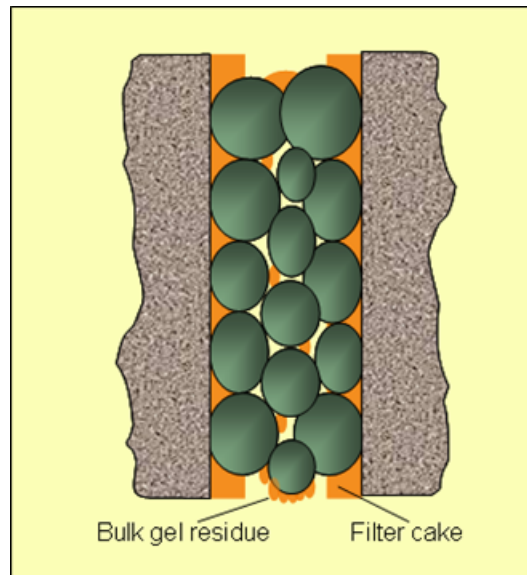


**Fig. 3.4** Polymers within the fracture reduces cross sectional area

### 3.3 Effective permeability calculation

Calculation of the effective permeability of the propped fracture considering the effects of closure stress, non-Darcy flow and gel damage should be performed in a sequential way. This sequence depends on factors finally to be considered, and the method selected to calculate the effective permeability due to these factors (i.e. for gel damage effect). In the development of this application, we consider that at least the effects of the closure stress upon permeability should be considered. Therefore, the user has the option of including or not the non-Darcy and/or gel damage effects.

The algorithm proposed to calculate the effective permeability is presented in **Fig. 3.5**. Effective permeability after closure stress effects are calculated from tables or figures provided by manufacturer. The proppant database included in the spreadsheet has the table of proppant permeability vs. closure stress for each mesh available of proppants considered. Porosity and specific gravity is also included. Structure of the database is presented in Appendix A. For closure stress magnitudes other than those provided in the table, the permeability will be calculated by interpolation. An important restriction to be implemented in this application is not allow the user select a proppant when actual closure stress is above the maximum closure stress reported in proppant database.

Once effective permeability for closure stress is calculated code check if user want to include gel damage effects (**Fig. 3.5**). If so and permeability correction is upon proppant permeability, code calculates new effective permeability from Eq. 3.2. Otherwise code will check if user wants to consider non-Darcy flow effects. If so, the code will execute algorithm presented in Chapter IV for calculating effective permeability due to non-Darcy flow effects. Otherwise, ultimate effective permeability will be nominal permeability after closure stress or permeability corrected with Eq. 3.2, if it applies.

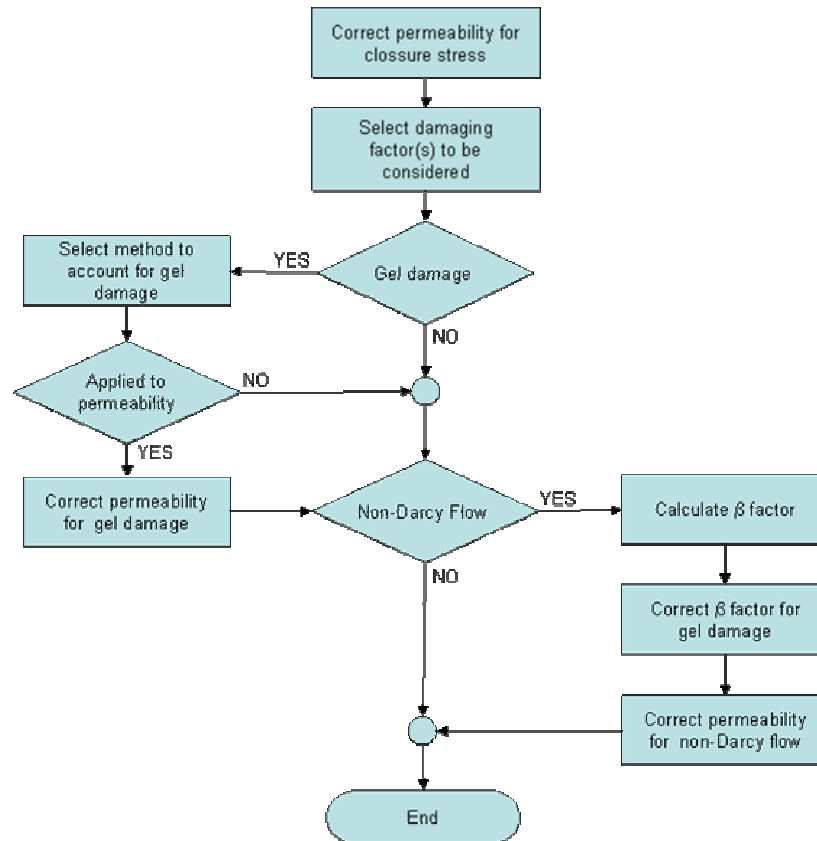


**Fig. 3.5** Algorithm to be implemented in spreadsheet VBA code to calculate the effective fracture permeability

### 3.4 Spreadsheet structure

Spreadsheet developed in this work is based on H2FD spreadsheet that comes with Unified Fracture Design book.<sup>12</sup> As stated in Chapter 3.1, H2FD was developed for fracture treatment design in low, medium and high permeability oil and gas wells. It is based on proppant number approach and includes PKN model to calculate fracture growth with time.

Proposed spreadsheet is an adaptation of HF2D spreadsheet for fracture treatment designs in natural gas wells. Main feature of this application is the calculation of effective proppant permeability considering closure stress, non-Darcy flow and gel damage effects. New application consists on four worksheets:

- Traditional design for low and medium permeability (“Traditional”)
- Tip screen out design (“TSO”) for high permeability
- Proppant database
- $\beta$  factor equations database

Traditional and TSO worksheets have the same data structure. It is considering that in both cases input and output variables are similar.

### 3.4.1 Input data window

It was structured by sections to facilitate the user the collection and input of data required. **Fig. 3.6** shows the INPUT window interface for Traditional design. The same input variables are required for TSO design except in the “CONSTRAINTS” section where one more variable is required for TSO design.

#### 3.4.1.1 Proppant data

- **Mass for two wings.** It is the total mass of proppant in lbm to be injected into the formation. It is the single most important decision variable of the design procedure.
- **Proppant selection.** Type of proppant to be used in the design can be picked up from corresponding list (**Fig. 3.7**). Only proppants included in proppant database will be displayed in this list. However, user can input new proppants as needed (Appendix A).
- **Size (Mesh).** The available sizes change automatically when a type of proppant is selected. Sizes displayed are the ones included in the proppants database for the proppant selected (**Fig. 3.8**).
- **Specific Gravity.** It depends only on the type of proppant selected and is independent of the mesh size and closure stress because is a property of the material which proppant is made. It is automatically updated when User select a new type of proppant. However, actual value be changed by the user based on his/her experience and

type of proppant to be finally used. The default value comes from the specific gravity specified in the Proppant database.

Section	Parameter	Value	Unit
PROPPANT	Mass for two wings	50,000	lbm
	Proppant Selection	SAND	
	Size (Mesh)	8/16	
	Specific Gravity	2.65	
	Pack permeability (nominal)	2,370,800	mD
GAS PROPERTIES	Gas Specific Gravity	0.60	
	Viscosity	0.5	cP
	Z-factor	1	
CONSTRAINTS	Max possible added proppant concentration	10.00	ppga
	Multiply opt length by factor	1.00	
	Multiply Nolte pad by factor	1.00	
FRAC JOB PARAMETERS	Fracture height	36.0	ft
	Slurry injection rate (two wings, liq+ prop)	12.50	bpm
	Rheology, K'	0.04	lb/ft <sup>2</sup>
	Rheology, n'	0.65	
	Leakoff coefficient in permeable layer	0.004	ft/min <sup>0.5</sup>
	Spurt loss coefficient	0.00	gal/ft <sup>2</sup>
RESERVOIR	Average reservoir pressure	5,720	psia
	Reservoir temperature	738	R
	Formation permeability	1.40	md
	Permeable (leakoff) thickness	36.0	ft
	Pre-treatment skin factor	12.0	
	Plane strain modulus, E'	3.65E+06	psi
WELL	Bottomhole pressure	1,500	psia
	Well drainage radius	1,053	ft
	Well radius	0.35	ft

Fig. 3.6 Structure of the input windows for a traditional design

Parameter	Value	Unit
Mass for two wings	50,000	lbm
Proppant Selection	SAND	
Size (Mesh)		
Specific Gravity		
Porosity of pack		
Pack permeability (nominal)	2,370,800	mD

Fig. 3.7 Selection of the type of proppants available in Proppants Database

**PROPPANT**

Mass for two wings 50,000 *lbm*

Proppant Selection SAND

Size (Mesh) 8/16

Specific Gravity 12/20

Porosity of pack 16/30

Pack permeability (nominal) 20/40 *mD*

**Fig. 3.8** Selection of the mesh size available for the type of proppant selected

- **Porosity of Pack.** It depends on type of proppant, mesh and closure pressure. This value is automatically updated when User changes one of the variables mentioned previously. However, User can input a new value directly in the cell if proppant to be used in the design is quite different to the proppant specified in database and data is not available.
- **Pack permeability.** It corresponds to the nominal permeability of the type of proppant and mesh selected at in situ conditions of closure stress. This value automatically changes when type of proppant, mesh or closure stress is changed. It comes from the permeability table specified for each proppant and mesh size as a function of the closure stress. If closure stress does not correspond to exact values specified in the table, the application interpolates to get the permeability at the actual closure stress. This application does not allow User to select a specific proppant above the maximum closure stress specified in the database. When it occurs a warning message box is displayed (see **Fig. 3.9**).

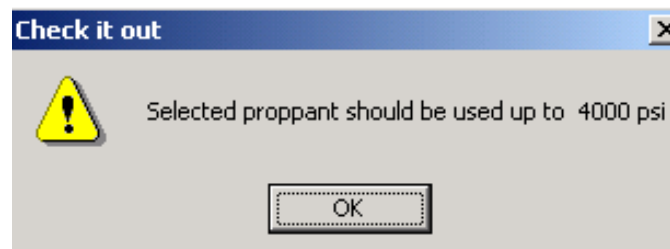


**Fig. 3.9** Warning message when a proppant is going to be used above the maximum limit of closure stress

### 3.4.1.2 Gas Properties

- **Gas Specific Gravity.** It is the measured or estimated specific gravity ( $SG_g$ ) of the gas to be produced.
- **Calculate Z and Viscosity.** Select this option when no lab measurements are available. Correlations used to calculate z-factor and viscosity were selected based on numerous evaluations performed by McCain<sup>57</sup> to establish what the best correlations are to estimate gas, oil and water properties at any condition of pressure and temperature.

Z Factor McCain recommends<sup>58</sup> to use the Dranchunk Abou-Kassem equation (Eq. 3.5)<sup>59</sup> that duplicates Standing Katz z-factor chart with an average absolute error of 0.6<sup>60</sup>. He mentions that accuracy of the equation decrease when pressure and temperature increase. For example, when pseudo reduce pressure and temperature are 30 and 2.8 respectively error is three percent.

$$z = 1 + \left( A_1 + \frac{A_2}{T_{pr}} + \frac{A_3}{T_{pr}^3} + \frac{A_4}{T_{pr}^4} + \frac{A_5}{T_{pr}^5} \right) \rho_{pr} + \left( A_6 + \frac{A_7}{T_{pr}} + \frac{A_8}{T_{pr}^2} \right) \rho_{pr}^2 - A_9 \left( \frac{A_7}{T_{pr}} + \frac{A_8}{T_{pr}^2} \right) \rho_{pr}^5 + A_{10} \left( 1 + A_{11} \rho_{pr}^2 \right) \left( \frac{\rho_{pr}}{T_{pr}} \right)^2 \exp(-A_{11} \rho_{pr}^2) \dots \dots \dots (3.5)$$

where,

$$A_1 = 0.3265, A_2 = -1.0700, A_3 = -0.5339, A_4 = 0.01569, A_5 = -0.05165, A_6 = 0.5475, A_7 = -0.7361, A_8 = 0.1844, A_9 = 0.1056, A_{10} = 0.6134, A_{11} = 0.7210.$$

$$\rho_{pr} = \frac{0.27 p_{pr}}{z T_{pr}} \dots \dots \dots (3.6)$$

$$T_{pr} = \frac{T}{T_{pc}} \dots \dots \dots (3.7)$$

$$P_{pr} = \frac{P}{P_{pr}} \dots \dots \dots (3.8)$$

McCain showed in further studies that the best estimation of z-factor is when critical pressure and temperature of the mixture is calculated with Piper, McCain and Corredor correlation (Eqs. 3.9 and 3.10).<sup>61</sup> This correlation was developed using a set of 1,482

data points, ranging in composition from lean sweet to rich acid, and fitted the data base with an average absolute error of 1.3 percent. Piper, McCain and Corredor correlation directly account for the effects of hydrogen sulfide, carbon dioxide (maximum 50%) and nitrogen (maximum 10%).

$$T_{pc} = \frac{K^2}{J} \dots\dots\dots (3.9)$$

$$P_{pc} = \frac{T_{pc}}{J} \dots\dots\dots (3.10)$$

where,

$$J = \alpha_0 + \sum_{i=1}^3 \alpha_i y_i \left( \frac{T_{pc}}{P_{pc}} \right)_i + \alpha_4 SG_g + \alpha_5 SG_g^2 \dots\dots\dots (3.11)$$

$$K = \beta_0 + \sum_{i=1}^3 \beta_i y_i \left( \frac{T_{pc}}{\sqrt{P_{pc}}} \right)_i + \beta_4 SG_g + \beta_5 SG_g^2 \dots\dots\dots (3.12)$$

$$y_i \in \{y_{H_2S}, y_{CO_2}, y_{N_2}\} \dots\dots\dots (3.13)$$

$\alpha_i$  and  $\beta_i$  are shown in **Table 3.2**

**Table 3.2** Coefficients of Piper, McCain and Corredor correlation for critical properties calculation

i	$\alpha_i$	$\beta_i$
0	0.11582	3.8216
1	-0.45820	-0.06534
2	-0.90348	-0.42113
3	-0.66026	-0.91249
4	0.70729	17.438
5	-0.099397	-3.2191



Gas viscosity McCain suggests<sup>57</sup> using Lee, Gonzalez and Eakin correlation<sup>62</sup> to estimate this variable. The accuracy of this correlation (Eq. 3.14) is 2% at low pressure and to within 4% at high pressure when the specific gravity of the gas is < 1.0.

$$\mu_g = A \exp(B\rho_g^C)(10^{-4}) \dots\dots\dots (3.14)$$

where,

$$A = \frac{(9.379 + 0.01607M_g)T^{1.5}}{209.2 + 19.26M_g + T} \dots\dots\dots (3.15)$$

$$B = 3.448 + \left(\frac{986.4}{T}\right) + 0.01009M_g \dots\dots\dots (3.16)$$

$$C = 2.447 - 0.2224B \dots\dots\dots (3.17)$$

VBA code was developed to calculate z-factor and gas viscosity from correlations presented above (Appendix B).

- **Input Z and Viscosity.** Select this option if lab measurements of z-factor and gas viscosity are available for temperature and pressure of interest. Then enter the magnitude of the variables in the corresponding text box. It is usually recommended to use measured values instead of calculated ones when they are available.

### 3.4.1.3 Constraints

- **Max possible added proppant concentration.** The most important equipment constraint. Some current mixers can provide more than 15 ppga. Often it is not necessary to ramp up to the maximum possible concentration.
- **Multiply opt length by factor.** This design parameter can be used to force a sub-optimal design. If the optimum length is considered too small (fracture width too large), a value greater than one is used. If the optimum length is too large (fracture width too small), a fractional value may be used. This possibility of user intervention is handy or investigating the pros and cons of departing from the technical optimum. The default value is 1.

- **Multiply Nolte pad by factor.** In accordance with Nolte's suggestion, the exponent of the proppant concentration schedule and the pad fraction (relative to total injected volume) are initially taken to be equal. Inputting a value other than 1 has the effect of increasing or decreasing the pad fraction accordingly. The program adjusts the proppant schedule to ensure the required amount of proppant is injected.
- **TSO criterion Wdry/Wwet (Only available in TSO worksheet).** Specifies the ratio of dry with (when only dehydrated proppant is left in the fracture) to wet width (dynamically achieved during pumping), and is needed only for the TSO design. According to our assumption, screenout happens when ratio of dry-to-wet width reaches the user specified value. We suggest using a number between 0.5 and 0.75 initially, but this number should be refined locally based on evaluation of successful TSO treatments.

#### 3.4.1.4 Frac Job Parameters

- **Fracture height** is usually greater than the permeable height. It is one of the most design parameters. Derived from lithology information, or can be adjusted iteratively by the user to roughly match the fracture length. Based on our experience the ratio of total fracture length to fracture height (i.e. aspect ratio AR) is approximately 4. In other words

$$AR = \frac{2x_f}{h_f} \approx 4.0 \dots\dots\dots (3.18)$$

- **Slurry injection rate (two wings, liq+ prop).** The injection rate is considered constant along fracture treatment. It includes both the fracturing fluid and the proppant. Additional proppant simply reduces the calculated liquid injection rate.
- **Rheology, K'.** Power law consistency of the fracturing fluid (slurry, in fact)
- **Rheology, n'.** Power law flow behavior index.
- **Leakoff coefficient in permeable layer.** Leakoff outside the permeable layer is considered zero, so when the ratio of fracture height to permeable-layer thickness is high, the apparent leakoff coefficient calculated from this input is much lower than the input

itself. If leakoff is suspected outside of the net pay, this parameter may be adjusted along with fracture height.

- **Spurt loss coefficient.** Accounts for spurt loss in the permeable layer. Outside of the permeable layer, spurt loss is considered zero.

#### 3.4.1.5 Reservoir

- **Average reservoir pressure.** It is used to calculate gas flow rate with the pressure square form of Darcy flow equation.
- **Reservoir temperature.** It is usually measured in °F but is required in °R. It is used to calculate gas properties and gas flow rate.
- **Formation permeability.** Effective permeability to gas of the formation.
- **Permeable (leakoff) thickness.** This parameter is used in calculation if the Productivity Index (as net thickness) and the apparent leakoff coefficient-assuming no leakoff (or spurt loss).
- **Pre-treatment skin factor.** Can be set to zero as it does not influence the design. It is only used as a basis for calculating the “folds of increase” in productivity.
- **Closure stress.** It is required to calculate proppant pack permeability at in situ stress conditions.
- **Plane strain modulus, E'.** Defined as Young’s modulus divided by one minus the Poisson ratio squared

$$E' = \frac{E}{1 - \nu^2} \dots\dots\dots (3.19)$$

Is almost the same as Young’s modulus, and about twice the shear modulus (the effect of the Poisson ratio is small). For hard rock, it might be  $10^6$ , for soft rock  $10^5$  psi or less.

### 3.4.1.6 Well

- **Bottomhole pressure.** Required to estimate gas rate and gas properties ( $B_g$ ,  $\mu_g$ ,  $\rho_g$  and  $z$ -factor). It can be obtained from direct measurements or using flow correlations.
- **Well drainage radius.** Needed for optimum design. It can be obtained from build-up test, well spacing, etc.
- **Well radius.** Needed for pseudo-skin factor calculation. Dimension can be obtained from caliper. If a caliper log is not available it can be estimated from drill-bit diameter.

### 3.4.2 Proppant permeability correction window

As mentioned before, this application was developed to consider the impairments of non-Darcy and gel damage on the effective permeability. **Fig. 3.10** shows the window where these factors are considered during the frac job design. This window is accessed by clicking on “Click here” button at the end of the PROPPANT section of INPUT DATA window. This window is the same for Traditional and TSO designs. Each worksheet (i.e. TRAD and TSO) has its own window to keep the individuality of each type of design.

#### 3.4.2.1 Non-Darcy Flow

This effect is considered when checkbox next to this label (**Fig. 3.10**) is active (i.e. a check mark is displayed in this checkbox). When it occur the list of  $\beta$  factor equations becomes actives. Initially all 24  $\beta$  factor equations reported in Chapter I are included in the spreadsheet (i.e. they are in Beta Equations worksheet). However,  $\beta$  factor equations displayed in the list are ones that can be used for type of proppant and mesh size selected in INPUT window. It is because some  $\beta$  factor equations were developed for specific type of proppant and mesh size. For example, Pen and Jin equation was developed only for 20/40 sand, resin coated sand, low weight ceramic and bauxite. Therefore, if a type of proppant and/or mesh size other than these is selected, this equation will not appear in the list.

## TRADITIONAL DESIGN

**PROPPANT PERMEABILITY CORRECTION**

**Effects to be consider** **Back Home**

Non-Darcy Flow

Gel Damage

**Non-Darcy Flow**

$\beta$  Equation:  \* Equation for proppant

**Input a new equation**

**Gel Damage**

% of Damage:

Apply to:

Proppant Permeability

Beta Factor

**Fig. 3.10** Selection of factors to be considered in the effective propped pack permeability calculations

## TRADITIONAL DESIGN

**PROPPANT PERMEABILITY CORRECTION**

**Effects to be consider** **Back Home**

Non-Darcy Flow

Gel Damage

**Non-Darcy Flow**

$\beta$  Equation:  \* Equation for proppant

**Gel Damage**

% of Damage:

Apply to:

Proppant Permeability

Beta Factor

**Fig. 3.11** List of  $\beta$  factor available for actual proppant and mesh size

Equations developed from proppant tests are identified with a star (\*) next to the name of the equation (**Fig. 3.11**). If User considers proppant porosity to be used in the design has a high degree of uncertainty only  $\beta$  equations presented in **Table 3.3** should be initially considered. If there is a correlation developed specifically for proppant type and mesh size considered in the design, then, it should be the correlation to use. Otherwise, a systematic evaluation of equations should be performed to select finally what correlation to use.

**Table 3.3**  $\beta$  equations that depend only on permeability

Cooke* 8/12
Cooke* 10/20
Cooke* 20/40
Cooke* 40/60
Frederick <i>et al</i>
Jones
Martins <i>et al</i> *
Penny and Jin* Bauxite
Penny and Jin* LWC
Penny and Jin* RCS
Penny and Jin* Sand
Pursell et al* 12/20
Pursell et al* 20/40
Thauvin and Mohanty

\* Equations developed for proppants

### 3.4.2.2. Gel Damage

This effect is considered when a checkmark appears in the check box next to gel damage label. When it occurs all elements of gel damage section are active. Then user can select what approach to use for considering gel damage effects. It can be either on effective permeability or  $\beta$  factor. In both cases a percentage of gel damage must be specified. It is introduced in the % of Damage text box (see **Fig. 3.10**). This percentage can be modified

by hand directly on the text box or clicking the up or down arrows of the spin button next the text box. In this case % of Damage increase or decrease by one unit.

Note that if in “Effects to be considered” section (**Fig. 3.10**) Gel Damage is selected and Non-Darcy Flow is not, the option by default in “Gel Damage” section is to apply % of Damage to proppant pack permeability.

User can return to input window clicking on Back Home button. Once all input data have been validated and entered user can run the code clicking on “Run application” button. A message will let know him/her when calculations are completed.

### 3.5 Calculated results

Results comprise theoretical optimum (variables reported in the “Optimum placement without constraints” section) and actual placement (variables reported in the section with the same name). One may or may not be able to achieve the technical optimum fracture dimensions, depending on certain constraints. A boldface blue message appears in the spreadsheet to denote when optimum fracture dimensions cannot be achieved. Output variables are the same for both Traditional and TSO design in the placements section (**Fig. 3.12** and **Fig. 3.13** respectively). These variables are:

- Reynold number
- Effective proppant pack permeability
- Proppant number
- Dimensionless productivity index
- Optimal dimensionless fracture conductivity
- Optimal half length
- Optimal propped width
- Post treatment pseudo skin factor
- Folds of increase of PI
- Gas well rate





## CHAPTER IV

### FIELD CASES APPLICATION AND ANALYSIS

Spreadsheet for optimal fracture designs considering non-Darcy flow and gel damage effects was presented in chapter III. Correlations and methods in which this application is based were introduced in chapter II and III.

The purpose of this chapter is to show the impact of implementing an optimal design considering appropriately the non-Darcy flow and gel damage effects versus neglecting them. Moreover, the importance of selecting appropriately  $\beta$  equation will be demonstrated.

Design and analysis of 11 fracture treatments in three natural gas wells are presented as application examples. These wells are identified as PS #1, PS #2 and PS #3. They are located in a tight gas reservoir in South Texas. It is a very heterogeneous reservoir with six multilayered producing sands. Therefore, several fractures are typically performed in each new well (i.e. multistage fractures), as part of the completion, to connect prospective sands with the wellbore.

Previous studies performed in this field, to optimize future fracture treatments, indicate that 60,000 lbm per stage and maximum 5 stages should be considered for each new well. Based on these recommendations and well log analyses, selected stages for cases of study are presented in **Table 4.1**. As can be seen, reservoir pressure, net pay and gas effective permeability ranges from 4,000 to 8,000 psi, 8 to 51 ft and 0.05 to 0.2 md respectively. An important index to be considered in our studies is the  $k_g h_p$  product that varies from 0.40 to 10.20 md-ft. Closure stress was included because its effects on the effective fracture permeability. It varies from 5,968 to 9,000 psi. **Table 4.2** shows additional data required in the design process. Flowing bottomhole pressure ( $p_{wf}$ ) in new wells is typically 1,400 psi. This value will be used in this study. Well spacing and well radius are all the same for all wells in this field except the well radius in PS #3 is 0.281 ft.

**Table 4.1** Reservoir properties of stages proposed for fracture design

Well	Stage	$P_{res}$ (psi)	$T_{res}$ (psi)	$P_c$ (psi)	$k_g$ (md)	$h_p$ (ft)	$k_g h_p$ (md-ft)
PS #1	1	8,050	264	9,000	0.073	74.5	5.44
	2	7,848	257	8,800	0.200	51.0	10.20
	3	7,365	250	8,300	0.123	15.0	1.85
	4	6,256	250	7,400	0.063	15.0	0.95
	5	5,842	250	7,200	0.083	9.5	0.79
PS #2	1	7,093	225	8,160	0.050	8.0	0.40
	2	7,091	228	7,900	0.070	12.0	0.84
	3	6,956	228	7,664	0.054	14.0	0.76
	4	6,894	229	7,670	0.044	12.0	0.53
PS #3	1	4,284	220	5,968	0.200	8.0	1.60
	2	5,254	220	5,968	0.200	39.0	7.80

**Table 4.2** Additional well data required for fracture design

Well	$P_{wf}$ (psi)	$r_e$ (ft)	$r_w$ (ft)
PS #1	1,400	745	0.281
PS #2	1,400	745	0.327
PS #3	1,400	745	0.327

Gas specific gravity and non-hydrocarbon content is required to estimate gas properties such as viscosity, z-factor, density and formation volumetric factor to be used in well deliverability and effective propped pack permeability calculations. This data is presented in **Table 4.3**. It was assumed that gas composition is constant for all stages of the same well.

**Table 4.3** Gas specific gravity and contaminants content

Well	$SG_g$	$N_2$ (mole %)	$CO_2$ (mole %)	$H_2S$ (mole %)
PS #1	0.664	0.099	0.159	0
PS #2	0.640	0.090	0.190	0
PS #3	0.644	0.511	0.044	0

#### 4.1 Calculation of the effective propped pack permeability for non-Darcy flow and gel damage effects

The algorithm implemented in the spreadsheet to find the optimum dimensions while incorporating the non-Darcy flow and gel damage effects will be illustrated here on the example of stage 2 of PS #3 using RCS as the proppant of choice.

Initially,  $k_f$  corresponding to the closure stress is calculated. It is obtained from the proppant permeability vs. closure stress data for RCS proppant (chapter III) at closure stress for this stage (i.e. 5,968 psi). The obtained  $k_f$  by interpolation is 134,248 md. Gel damage will be taking into account on the initial  $\beta$  factor (i.e. Pen & Jin correlation). Percentage gel damage is assumed 50%.

To estimate the amount of Proppant in pay, we need fracture height. There is no evidence of fracture height containment in wells fractured in this field. Based on our experience an aspect ratio (AR) of four will be kept as a general rule throughout the design.

$$AR = \frac{2x_f}{h_f} = 4 \dots\dots\dots (4.1)$$

When fracture length changes during the optimization process, the assumed fracture height changes too. In the given example the fracture height,  $h_f$  is assumed to be 111 ft.

The iterative process starts with a Reynold number guess. A sensitivity analysis was performed to determine is speed of convergence and final results (i.e. new effective permeability) are affected by the magnitude of initial guess. It was varied from 0 to 100 (values typically found at field conditions). Results show that speed of convergence and final results are independent of initial guess. Therefore, this value was set to 10 in the code. In this example initial guess is close to the ultimate Reynold number based on spreadsheet results (i.e. 21.51). Then, a new Reynold number is calculated at the end of the process. Iteration stops when error calculated in step 8 is 0.01% or less.

1. Calculate effective permeability ( $k_{f-eff}$ )

$N_{Re} = 21.51$ , this can be initial guess or new Reynold number calculated in step 8.

$$k_{f-eff} = \frac{k_f}{1 + N_{Re}} \dots\dots\dots (4.2)$$

where  $k_f$  is in md and  $k_{f-eff}$  is obtained in md.

$$k_{f-eff} = \frac{134,248}{1 + 21.51} = 5,963 \text{ md}$$

2. Calculate proppant number

Reservoir volume ( $V_{res}$ )

$$V_{res} = \pi r_e^2 h_p \dots\dots\dots (4.3)$$

where  $r_e$  is in ft,  $h_p$  is in ft and  $V_{res}$  is obtained in  $ft^3$ . Then

$$V_{res} = \pi \cdot 745^2 \cdot 39 = 6.8E7 \text{ ft}^3$$

The volume of proppant injected ( $V_{i-2w}$ )

$$V_{i-2w} = \frac{0.016(M_{p-2w})}{(1 - \phi_p)SG_p} \dots\dots\dots (4.4)$$

where  $M_{p-2w}$  is in lbm and  $V_{i-2w}$  is obtained in  $ft^3$ . Then

$$V_{i-2w} = \frac{0.016 \cdot (60,000)}{(1 - 0.40) \cdot 2.62} = 610 \text{ ft}^3$$

Volume of proppant reaching the pay ( $V_{p-2w}$ ) is estimated from the ratio of pay to the fracture height:

$$V_{p-2w} = V_{i-2w} \frac{h_p}{h_f} \dots\dots\dots (4.5)$$

where  $V_{i-2w}$  is in  $ft^3$ ,  $h_p$  is in ft,  $h_f$  is in ft and  $V_{p-2w}$  is obtained in  $ft^3$ . Then

$$V_{p-2w} = 610 \cdot \frac{39}{111} = 214 \text{ ft}^3$$

The Proppant number ( $N_{prop}$ ) is obtained from

$$N_{prop} = \frac{2k_{f-eff} V_{p-2w}}{k_g V_{res}} \dots\dots\dots (4.6)$$

where  $k_{f-eff}$  is in md,  $k_g$  is in md,  $V_{p-2w}$  is in  $\text{ft}^3$  and  $V_{res}$  is in  $\text{ft}^3$ . Then

$$N_{prop} = \frac{2 \cdot 5,963}{0.2} \cdot \frac{214}{6.8E7} = 0.19$$

### 3. Calculate optimal dimensionless fracture conductivity ( $C_{fDopt}$ ) and optimal dimensionless productivity index ( $J_{Dopt}$ )

It is obtained from algorithm to calculate these two parameters for a given proppant number . In this case the results are

$$C_{fDopt} = 1.66 \quad \text{and} \quad J_{Dopt} = 0.55$$

### 4. Calculate optimal fracture dimensions

Optimal fracture length ( $x_f$ )

$$x_f = \left( \frac{k_{f-eff} V_{p-1w}}{C_{fDopt} k_g h_p} \right)^{1/2} \dots\dots\dots (4.7)$$

where  $k_{f-eff}$  is in md,  $V_{p-1w}$  (for 1 wing) is in  $\text{ft}^3$ ,  $k_g$  is in md,  $h_p$  is in ft and  $x_f$  is obtained in ft.

$$x_f = \left( \frac{5,963 \cdot 107}{1.66 \cdot 0.2 \cdot 39} \right)^{1/2} = 221 \text{ ft}$$

(fracture height estimate was close enough, but might be improved to  $2 \cdot 221 / 4 = 110.5$  for the next iteration.)

The optimal propped width ( $w_{fp}$ )

$$w_{fp} = \left( \frac{C_{fDopt} k_g V_{p-1w}}{k_{f-eff} h_p} \right)^{1/2} \dots\dots\dots (4.8)$$

where  $k_g$  is in md,  $V_{p-1w}$  (volume in the pay in 1 wing) is in  $ft^3$ ,  $k_{f-eff}$  is in md,  $h_p$  is in ft and  $w_{fp}$  is in ft. Then,

$$w_{fp} = \left( \frac{1.66 \cdot 0.2 \cdot 107}{5,963 \cdot 39} \right)^{1/2} = 0.012 \text{ ft}$$

### 5. Calculate gas production ( $q_{gsc}$ )

$$q_{gsc} = \frac{k_g h_p (p_{res}^2 - p_{wf}^2)}{1,424 \mu_g z T_{res}} J_{Dopt} \dots\dots\dots (4.9)$$

where  $k_g$  is in md,  $h_p$  is in ft,  $p_{res}$  and  $p_{wf}$  are in psi,  $\mu_g$  is in cp,  $T_{res}$  is in  $^{\circ}R$  and  $q_{gsc}$  is in Mscf/day.

$\mu_g$  and  $z$ -factor are calculated for average pressure  $(p_{res} + p_{wf})/2$  and  $T_{res}$  using correlations recommended in Chapter III and data presented in **Table 4.3** for PS #3 well. Results are

$\mu_g = 0.0205$ , and  $z = 0.944$  herein

$$q_{gsc} = \frac{0.2 \cdot 39 \cdot (5,254^2 - 1,400^2)}{1,424 \cdot 0.0205 \cdot 0.944 \cdot 680} \cdot 0.55 = 5,871 \text{ Mscf / day}$$

### 6. Calculate gas velocity within the fracture

Gas formation volumetric factor ( $B_g$ )

$$B_g = 0.0282 \frac{z T_{res}}{P_{wf}} \dots\dots\dots (4.10)$$

where  $T_{res}$  is in  $^{\circ}R$ ,  $p_{wf}$  is in psi and  $B_g$  is obtained in rcf/scf. Z-factor is calculated at bottomhole conditions (i.e.  $p_{wf}$  and  $T_{res}$ ) because non-Darcy flow within the propped pack is more critical at this point. Z is 0.934. In the example,

$$B_g = 0.0282 \cdot \frac{0.934 \cdot 680}{1,400} = 0.0128 \frac{rcf}{scf}$$

Gas velocity ( $v$ )

$$v = \frac{500 B_g q_{gsc}}{h_f w_{fp}} \dots\dots\dots (4.11)$$

where  $B_g$  is in rcf/scf,  $q_{gsc}$  is in Mscf/day,  $h_f$  is in ft,  $w_{fp}$  is in ft and  $v$  is obtained in ft/day. In our example,

$$v = \frac{500 \cdot 0.0128 \cdot 5,871}{111 \cdot 0.012} = 28,209 \text{ ft / day}$$

### 7. Calculate Reynold number

Molecular weight of the mixture ( $M_g$ )

$$M_g = M_{air} \cdot SG_g, \dots\dots\dots (4.12)$$

where  $M_{air}$  is in lb/lb mole

$$M_g = 29 \cdot 0.644 = 18.68 \text{ lb / lb\_mole}$$

Density of the gas ( $\rho_g$ )

$$\rho_g = \frac{p_{wf} M_g}{z R T_{res}} \dots\dots\dots (4.13)$$

where  $p_{wf}$  is in psi,  $M_g$  is in lb/lb mole,  $T_{res}$  is in  $^{\circ}R$  and  $\rho_g$  is in lbm/ft<sup>3</sup> and

$$R = 10.732 \frac{psia \cdot ft^3}{lb\_mole \cdot ^{\circ}R}$$

z-factor is at bottomhole conditions too

Therefore,

$$\rho_g = \frac{1,400 \cdot 18.68}{0.934 \cdot 10.732 \cdot 680} = 3.84 \text{ lbm} / \text{ft}^3$$

Beta factor ( $\beta$ )

$$\beta = \frac{a}{k_f^b \phi_p^c} \dots\dots\dots (4.14)$$

where  $k_f$  is in md and  $\beta$  is in 1/ft. For Penny and Jin Correlation RCS 20/40,  $a = 3.47E11$ ,  $b = 1.35$ ,  $c = 0.00$ , then

$$\beta = \frac{3.47E11}{134,248^{1.35} \cdot 0.40^0} = 41,462 \text{ 1/ft}$$

It has to be corrected for gel damage

$$F = 10^{\frac{\%damage}{100}} \dots\dots\dots (4.15)$$

$$F = 10^{\frac{50}{100}} = 3.16, \text{ and}$$

$$\beta' = F \times \beta \dots\dots\dots (4.16)$$

where  $\beta$  is in 1/ft. In this example

$$\beta' = 3.16 \cdot 41,462 = 131,020 \text{ 1/ft}$$

Reynold number ( $N_{Re}$ )

$$N_{Re} = 1.83 \times 10^{-16} \frac{\beta k_f \rho_g v}{\mu_g} \dots\dots\dots (4.17)$$

where  $\beta$  is in 1/ft,  $k_f$  is in md,  $\rho_g$  is in lbm/ft<sup>3</sup>,  $v$  is in ft/day and  $\mu_g$  is in cp. In the example,

$$N_{Re} = 1.83 \times 10^{-16} \cdot \frac{131,020 \cdot 134,248 \cdot 3.84 \cdot 28,209}{0.0156} = 22.35$$



## 8. Error of Re number

$$Error = \frac{|N_{Re_{new}} - N_{Re_{old}}|}{N_{Re_{old}}} \cdot 100 = \frac{|22.35 - 21.51|}{21.51} \cdot 100 = 3.9\%$$

The Reynold number calculated in step 7 is used in step 1 and the calculations are repeated until the error  $\leq 0.01$ .

### **4.2 Beta correlation evaluation**

Some  $\beta$  equations have been developed for a specific type of proppant and/or mesh size. It is the case of Pen & Jin<sup>1</sup> and Cooke<sup>21</sup> equation. There are also other correlations obtained from proppant tests which have been proposed by their authors as general correlations for proppants. It means that these correlations can be used in the analysis of non-Darcy flow effects through propped packs irrespective the type of proppant and mesh size.

In the example calculation Pen and Jin correlation was used because it was developed specifically for type of proppant considered in the example (i.e. RCS 20/40). However three questions may arise: 1) What if a proppant to be injected into the formation does not have a specific  $\beta$  equation ? 2) Are general  $\beta$  equations for proppant really general? 3) Can be a  $\beta$  equation developed from a source other than proppant tests be used in this case?

These questions will be answered comparing the frac design results in term of ultimate gas rate using each  $\beta$  equation. Comparisons were performed in PS #1\_Stage 3, PS #2\_Stage 1 and PS #3\_Stage 2. It is because these stages represent a high, medium and low value of  $k_g h_p$  product relative to 11 stages proposed. These values are 1.85, 0.40 and 7.80 md-ft for PS #1\_Stage 3, PS #2\_Stage 1 and PS #3\_Stage 2, respectively. The purpose of this is to check if  $k_g h_p$  product affects the results and consequently conclusions derived.

The equation of Pen & Jin will be used as a reference in **Fig. 4.1** because it was developed specifically for RCS 20/40. We can see there that results obtained with general

correlation for proppants (i.e. Pursell et al, Kutasov, Maloney et al and Martins et al) are relatively close to the Pen & Jin results. But definitively the best match is obtained with Pursell *et al.* and Martins *et al.* equations, despite the fact that RCS was not used in the development of these equations. In both cases the equations were obtained from tests where X was varied up to 60 at different closure stresses using Nitrogen (similar to Pen & Jin). Therefore, lab test conditions and analysis were similar to the Pen & Jin experiments. Maloney *et al.* used several proppant types to derive their  $\beta$  equation but they only ran their experiments for one value of X. It might affect the applicability of this equation at different flow conditions, specially in field applications where X is typically above 10.<sup>23</sup> Kutasov used lab data from experiments of four different authors. This equation includes proppant and packed bed experiments which might affect its applicability to proppants.

In the other hand, only three equations derived from other sources gave similar results to the Pen & Jin equation (i.e. Thauvin and Mohanty, Geerstma, and Li). The Thauvin and Mohanty correlation evaluated in this work comes from the simplest morphological structure (i.e. model, pore size distribution and network coordination number) studied by them. This morphology is typical of a propped pack. It is high porosities (0.40) and low tortuosity. Geertma used unconsolidated sands in his experiments. Although permeabilities are lower compare to typical proppant permeability, the nature of the porous media is similar. In general, we can say that the best matches are obtained for equations derived from experiment or analysis in porous media very similar to a proppant bed. The findings confirm that  $\beta$  is a property of the porous media<sup>18,19</sup> and is related to the nature of its morphological structure.<sup>34</sup>

We can see in **Figs. 4.1, 4.2 and 4.3** that relative results among all equation are the same as presented in **Fig. 4.4**. The equations due to Martins *et al.* and Pursell *et al.* are the best *across the board* correlations. The same results were obtained for evaluations performed in PS #1\_Stage 3 and PS #2\_Stage 1 (Appendix C). The results suggest that selection of the  $\beta$  correlation should be independent of the  $k_g h_p$  product of the well. Thauvin and Mohanty and Li. equations could be also used but equations developed from proppant tests should be considered first.

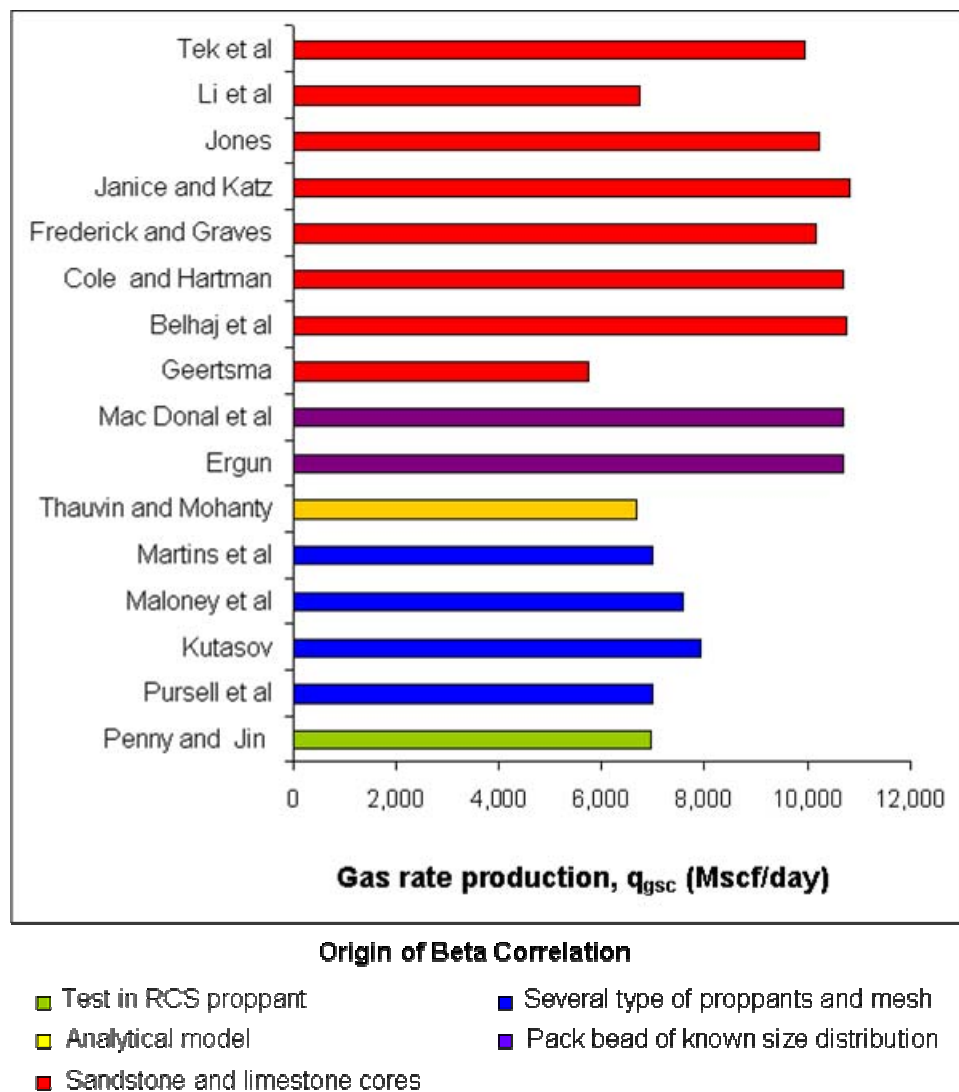


**Fig. 4.1** Comparison of optimal design results in terms of gas rate production for 20/40 RCS proppant

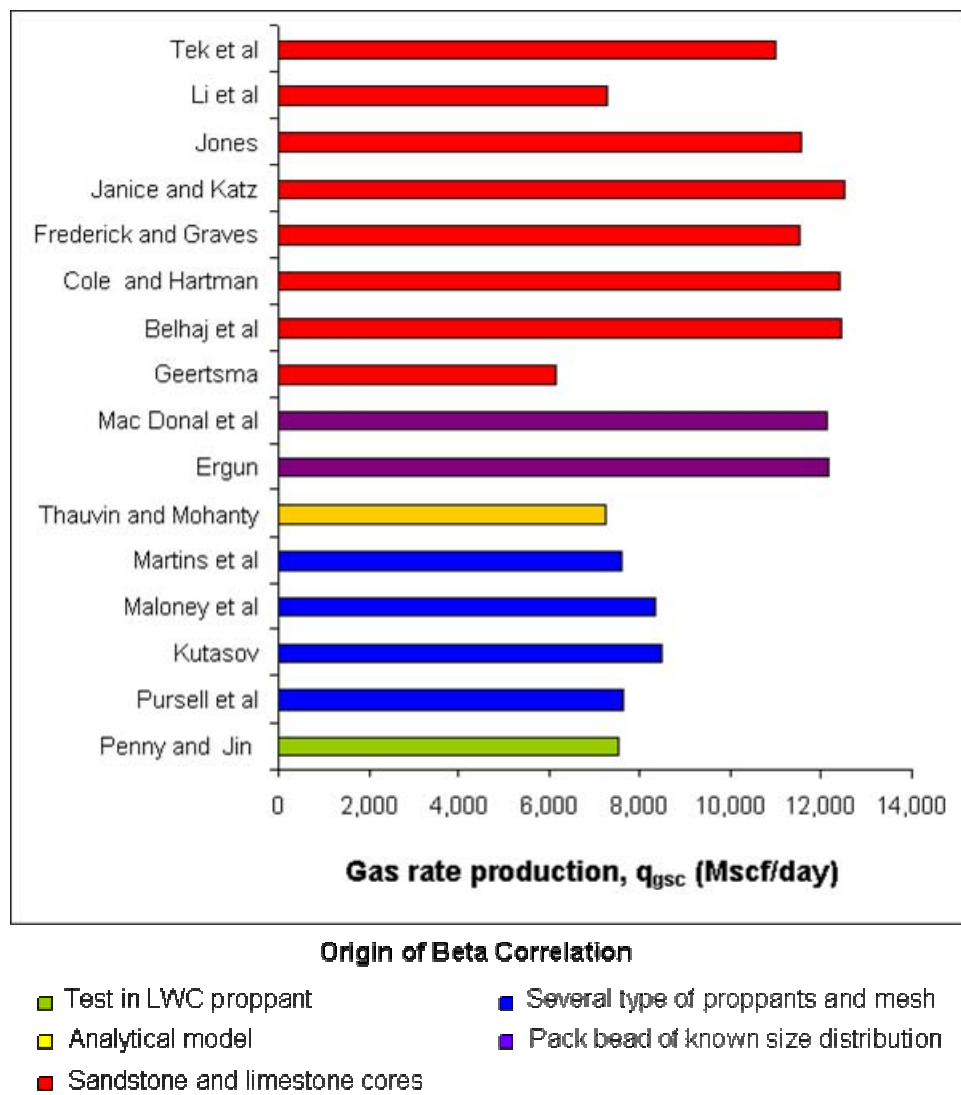


**Fig. 4.2** Comparison of optimal design results in terms of gas rate production for 20/40 LWC\_LS proppant

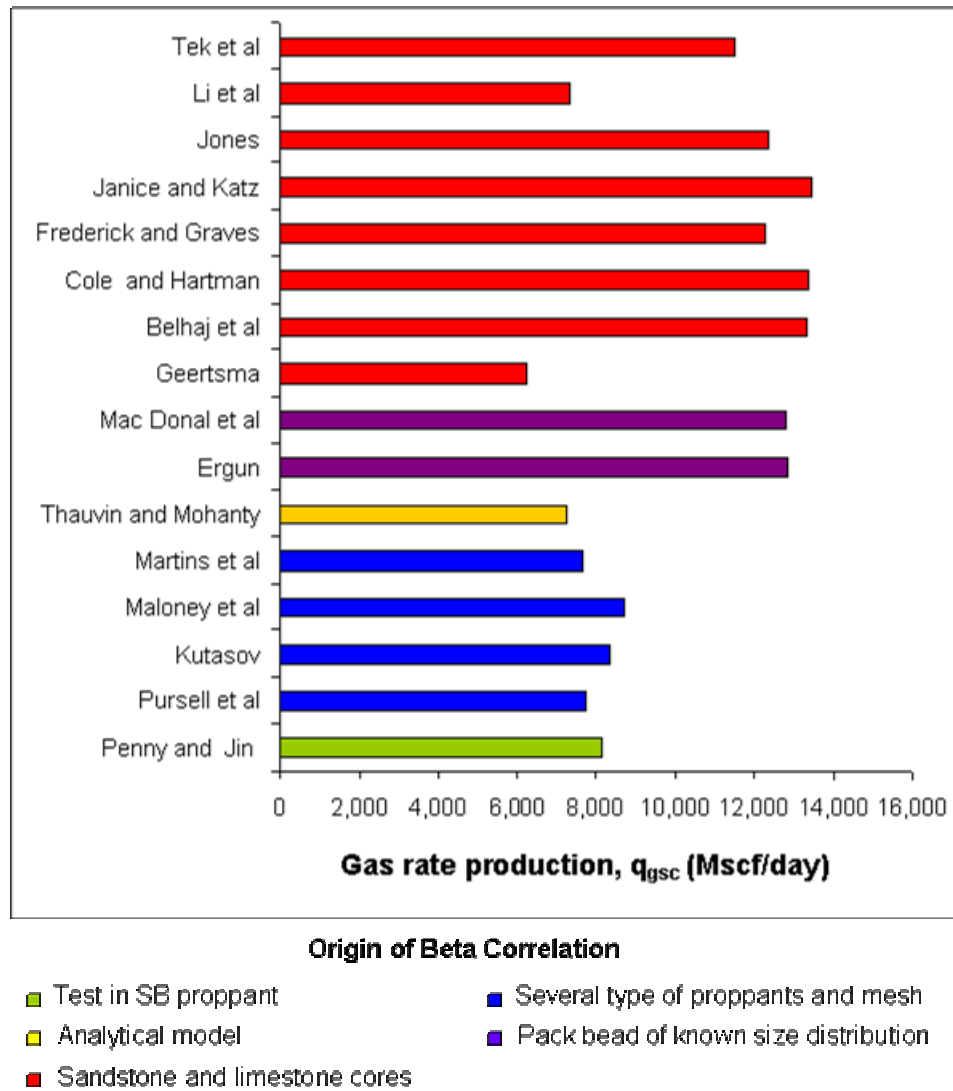


**Fig. 4.3** Comparison of optimal design results in terms of gas rate production for 20/40 SB proppant

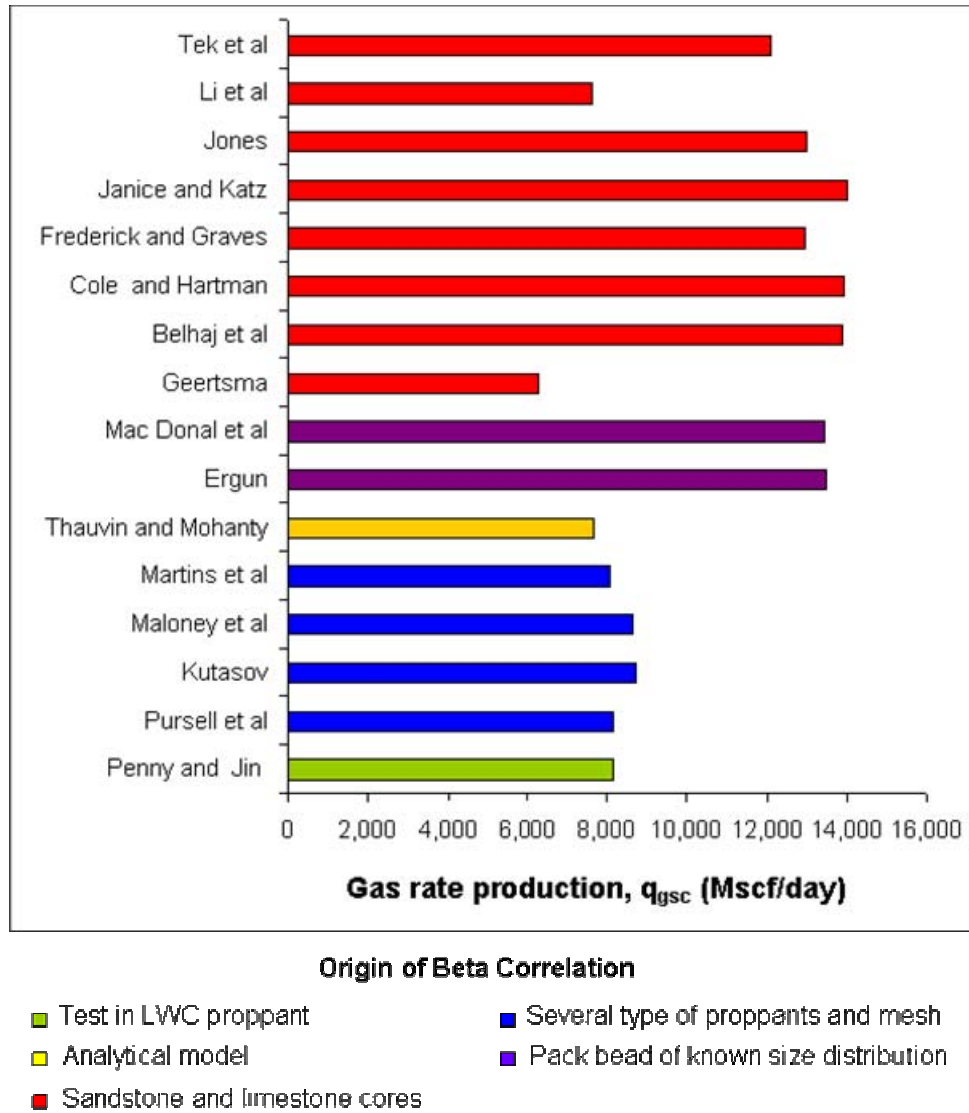


**Fig. 4.4** Comparison of optimal design results in terms of gas rate production for 20/40 LWC\_HS proppant

### 4.3 Optimal fracture geometry and bottomhole pressure sensitivity analysis

We can infer from application example presented in section 4.1 that  $k_{f\text{-eff}}$  and consequently fractured well performance and optimal fracture geometry depends on pressure drawdown ( $\Delta P$ ). It is determined by  $p_{wf}$ , in this case, which depends on operational conditions at the surface. PS #1\_Stage 3, PS #2\_Stage 1 and PS #3\_Stage 2 will be used in this analysis to show how variations in  $k_g h_p$  might also affect final results.

$P_{wf}$  was varied from 1,000 psi to 4,000 psi. We observe in **Figs. 4.5, 4.6** and **4.7** that the less  $p_{wf}$  is the wider and shorter fractures are required.

We also observe that the higher the  $k_g h_p$  product is variations of optimal lengths and widths are more substantial for the same increase in  $p_{wf}$ . For example, for PS #3\_Stage 2 optimal length varies from 321 to 396 ft for LWC\_LS when bottom pressure varies from 1,000 to 4,000 psi. It is an increase of 23.3 %; for PS #1\_Stage 3 optimal length varies from 375 to 420 ft (12 %); and for PS #2\_Stage 1 optimal lengths varies from 598 to 632 ft (5.7 %). The same relative variations can be observed regarding the optimum fracture width and proppant type. It suggests that the higher the  $k_g h_p$  product is, the more important is to incorporate the non-Darcy effect inside the optimization loop.

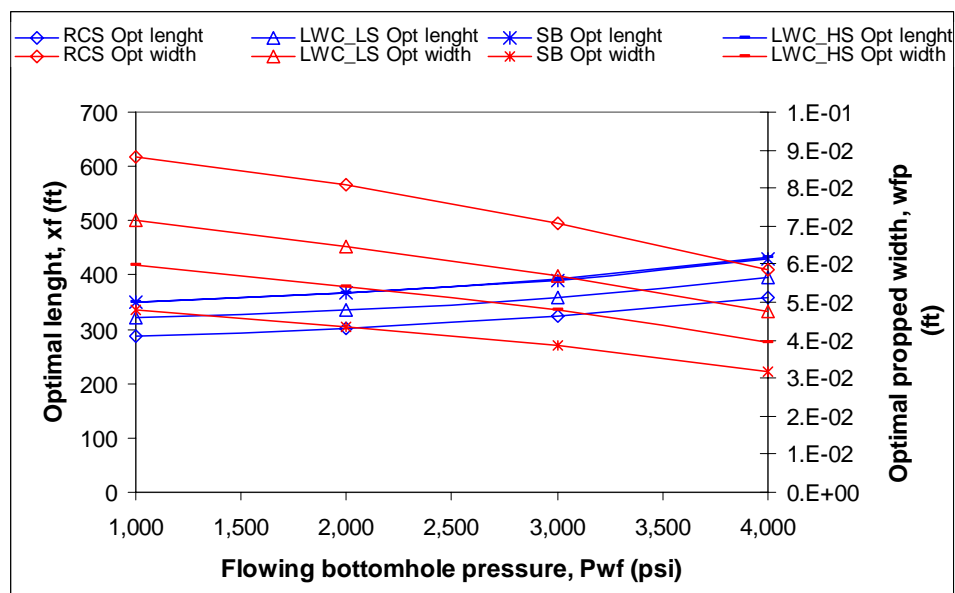


**Fig. 4.5** Optimal fracture geometry varies for PS #3\_Stage 2 at different values of  $p_{wf}$

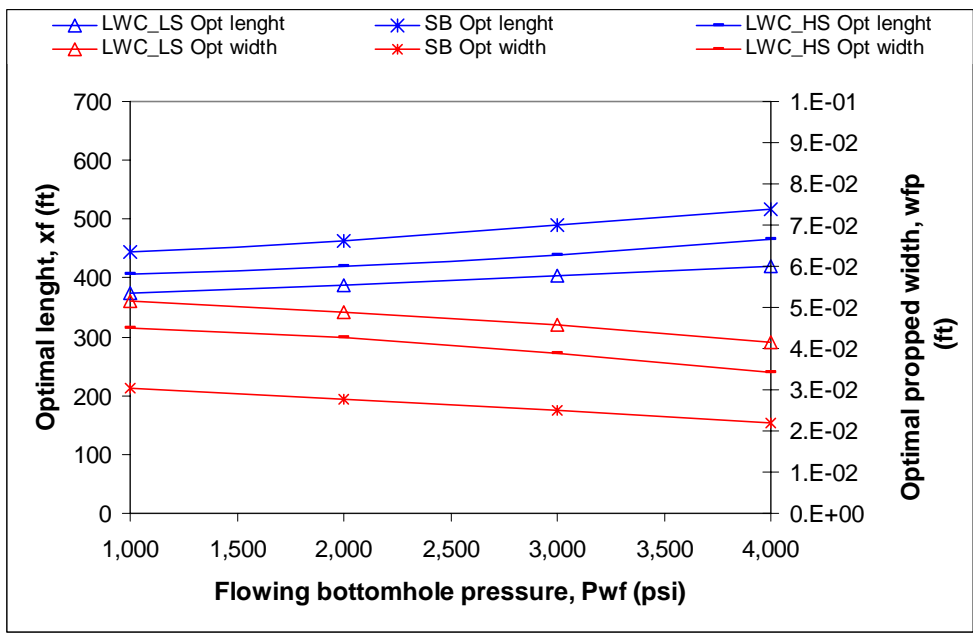


Fig. 4.6 Optimal fracture geometry varies for PS #1\_Stage 3 at different values of  $p_{wf}$

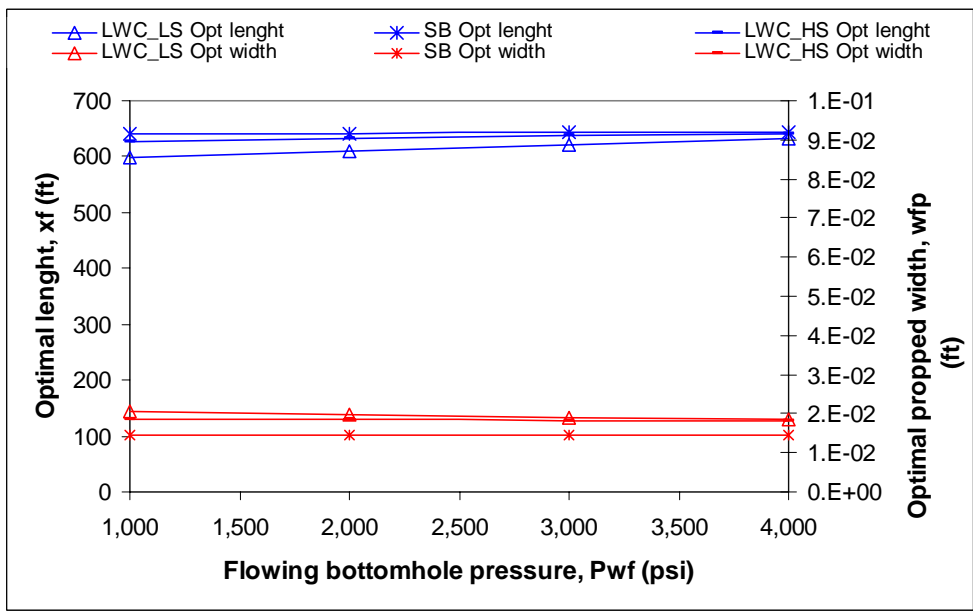


Fig. 4.7 Optimal fracture geometry varies for PS #2\_Stage 1 at different values of  $p_{wf}$



#### 4.4 Comparison of optimal fracture designs results considering non-Darcy flow and gel damage effects

We present in this section how neglecting non-Darcy flow and gel damage effects might result in poor fracture designs. Once the optimal mass of proppant to be injected into the formation has been established (i.e. 60,000 lbm in this work), the next step is to define how to place this amount of proppant into the formation (i.e. fracture geometry) for maximizing gas rate production and consequently return of the investment.

We can see from **Fig. 4.8** three different scenarios for Stage 2 of PS #3 using LWC\_LS 20/40 as the proppant of choice. First, Darcy flow is assumed during the fracture design process. Expected production is 12,619 Mscd/day from design resulting of this assumption. However, as we mention before, non-Darcy flow through the fracture is present. If we keep the first design, ultimate production will be in reality 5,591 Mscf/day. (Of course many authors have been pointed this out before us.) However, if we consider the non-Darcy flow effect during the optimization itself, applying the design methodology presented in this and previous chapters, a new optimal fracture geometry is obtained. It results in gas rate production of 7,545 Mscf/day which makes a difference of 1,954 Mscf/day with respect to the original design. We observe in **Fig. 4.8** that an optimal fracture design implies a shorter and wider fracture to compensate the effects of non-Darcy flow.

If gel damage effects are now considered similar results than **Fig 4.8** are obtained. We can see in **Fig. 4.9** that expected production is 4,822 Mscf/day when a Darcy design is implemented in the presence of non-Darcy flow and gel damage within the fracture. If this design is optimized, considering appropriately these factors, ultimate gas production will increase to 6,664 Mscf/day. Again, the effects of non-Darcy flow and gel damage are compensated in part with a shorter and wider fracture. From **Figs. 4.8 and 4.9** we can deduce that the more factors decreasing fracture permeability are considered (Appendix C), we will require wider and shorter fractures to compensate the new effects for a given amount of proppant.

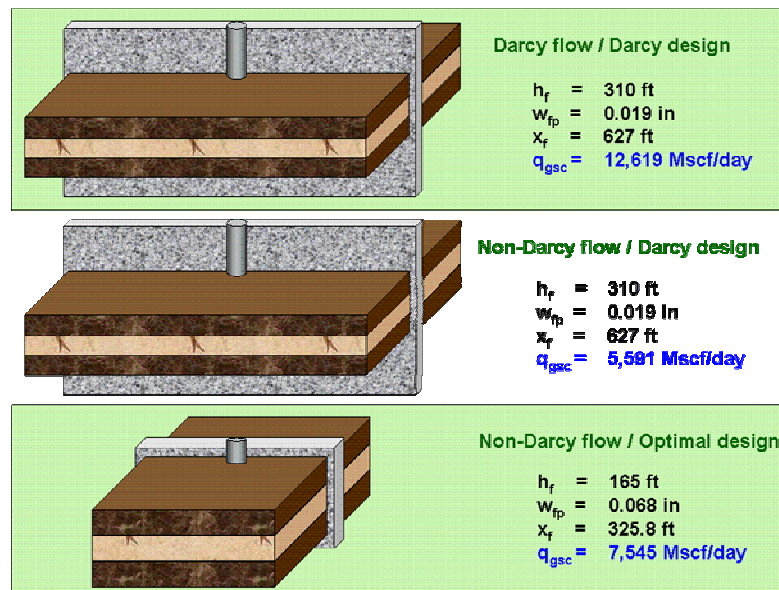


**Fig. 4.8** Considering non-Darcy flow effects in the fracture design maximizes ultimate well deliverability

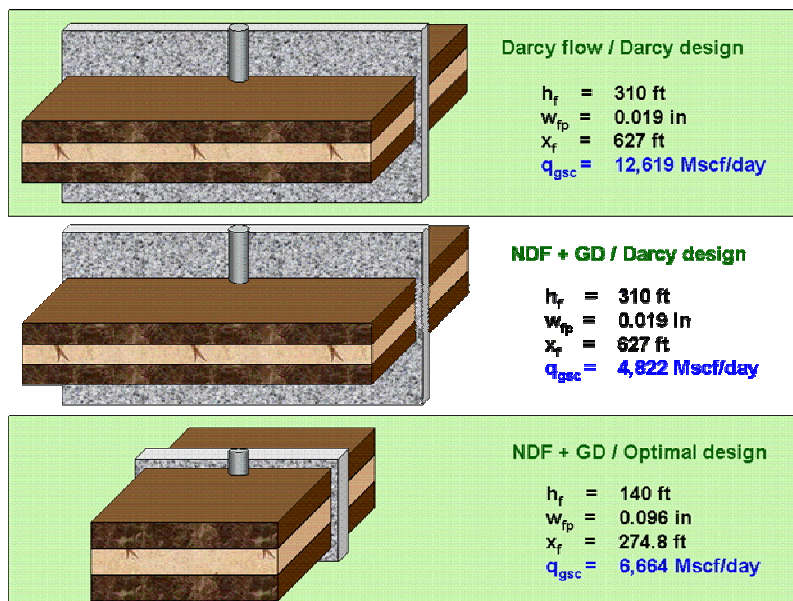


**Fig. 4.9** Considering non-Darcy flow and gel damage effects in the fracture design maximizes ultimate well deliverability

The result of implementing an optimal design in the multistage fractures of wells PS #1, PS #2 and PS #3 might result in an additional production of 9,600 Mscf/day with respect to the design where non-Darcy flow effects through the propped fracture are neglected (see **Table 4.4**). Moreover, if gel damage is present an optimal design for these stages might result in an additional production of 9,360 Mscf/day (see **Table 4.5**).

**Table 4.4** Gas expected production increases after implementing an optimal design for non-Darcy flow effects

Well	Stage	$q_{gsc}$ (Mscf/day) Darcy flow design	$q_{gsc}$ (Mscf/day) Optimal design	Difference (Mscf/day)
PS #1	1	6,869	9,578	2,709
	2	10,315	14,117	3,802
	3	2,554	3,256	702
	4	1,533	1,608	75
	5	1,155	1,202	47
PS #2	1	948	956	8
	2	1,623	1,744	121
	3	1,590	1,627	37
	4	1,237	1,230	-7
PS #3	1	1,166	1,364	198
	2	5,591	7,545	1,954
<b>TOTAL</b>				9,646

**Table 4.5** Gas expected production increases after implementing an optimal design for non-Darcy flow and gel damage effects

<b>Well</b>	<b>Stage</b>	<b>q<sub>gsc</sub> (Mscf/day) Darcy flow design</b>	<b>q<sub>gsc</sub> (Mscf/day) Optimal design</b>	<b>Difference (Mscf/day)</b>
<b>PS #1</b>	<b>1</b>	6,074	8,453	2,379
	<b>2</b>	8,949	12,740	3,791
	<b>3</b>	2,554	2,860	306
	<b>4</b>	1,245	1,459	214
	<b>5</b>	926	1,087	161
<b>PS #2</b>	<b>1</b>	961	832	-129
	<b>2</b>	1,300	1,591	291
	<b>3</b>	1,277	1,458	181
	<b>4</b>	1,003	1,062	59
<b>PS #3</b>	<b>1</b>	940	1,205	265
	<b>2</b>	4,822	6,664	1,842
<b>TOTAL</b>				<b>9,360</b>

## CHAPTER V

### MULTISTAGE FRACTURING OPTIMIZATION

Fracture designs and sensitivity analyses results presented in chapter IV were based on the premise that total mass of proppant to be injected in each well, selection of intervals (i.e. stages) to be fractured and amount of proppant to be placed into selected stages, and maximum number of stages to be fractured per well had been already determined by evaluations performed on datasets of fracture jobs executed in the field. These guidelines are:

- 60,000 lbm of proppant should be injected per stage
- Maximum 5 stages and 300,000 lbm per well
- The following sequence of depth intervals is suggested for selection of the 5 stages to be fractured :

1. 7,500'-7,750'
2. 7,000'-7,250'
3. 7,750'-8,000'
4. 7,250'-7,500'
5. 9,250'-9,500'
6. 9,000'-9,250'
7. 8,750'-9,000'
8. 9,750'-10,000'
9. 8,000'-8,250'
10. 8,250'-8,500'
11. 8,500'-8,750'

Based on these premises the optimum multistage fracture design is reduced to optimal single stage fracture designs (for each stage of each well). However, in multilayered tight gas reservoirs is not always the case. Engineers have to decide the total amount of proppant to inject per well, select what stages are going to be fractured and how much

proppant should be injected into each stage to maximize total gas rate of each new well. It does not have an obvious solution. In this chapter we propose a methodology based on Dynamic Programming to come up with an optimal solution for this case.

## 5.1 Problem statement

### 5.1.1 Definition and calculation of number of stages

A multilayered reservoir is composed of thin layers of rocks which properties varies based on depositional environment, composition of the rock, etc (see **Fig. 5.1**). Hydrocarbons can be produced from one these layers if the following requirements are satisfied: 1) Rock has porosity, 2) Gas or oil is found in the rock pores, 3) Pores are interconnected (i.e. has some permeability), 4) There is enough gas or oil to pay (at least) the investment made to drill, complete and produce the well. In tight gas reservoir (i.e. very low permeability gas reservoirs) wells are typically fractured to increase gas production.

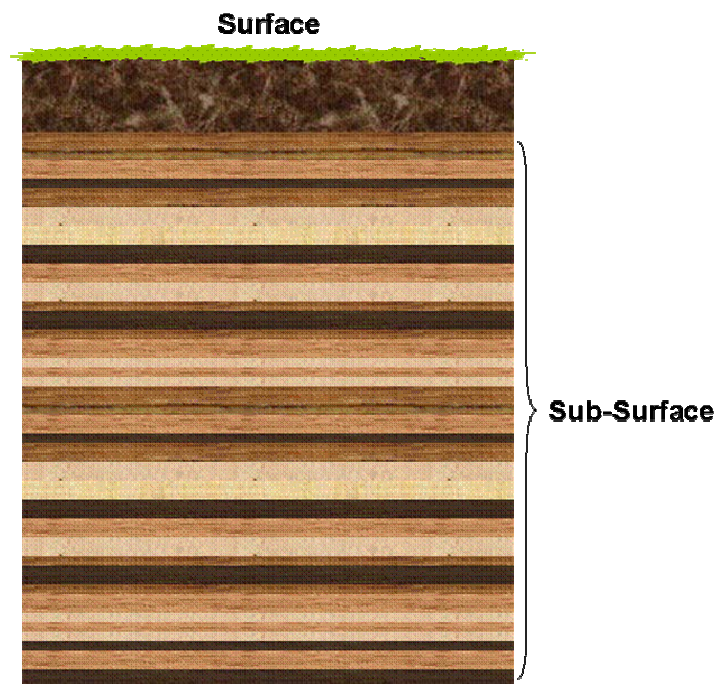


**Fig. 5.1** Multilayered reservoir

Because of restrictions imposed by mechanical properties of the rock, in situ stress, equipment used to inject the fracturing fluid at high pressures into the formation, etc. the final fracture height is limited (see **Fig. 5.2**). Then, only some layers are connected to the wellbore (through the fracture) which is considered one stage. Production coming from these layers might not be enough to make the project economically attractive. Therefore, more fractured interval or stages are required to connect more prospective producer layers to the wellbore (see **Fig.5.3**). It is called multistage hydraulic fracturing.

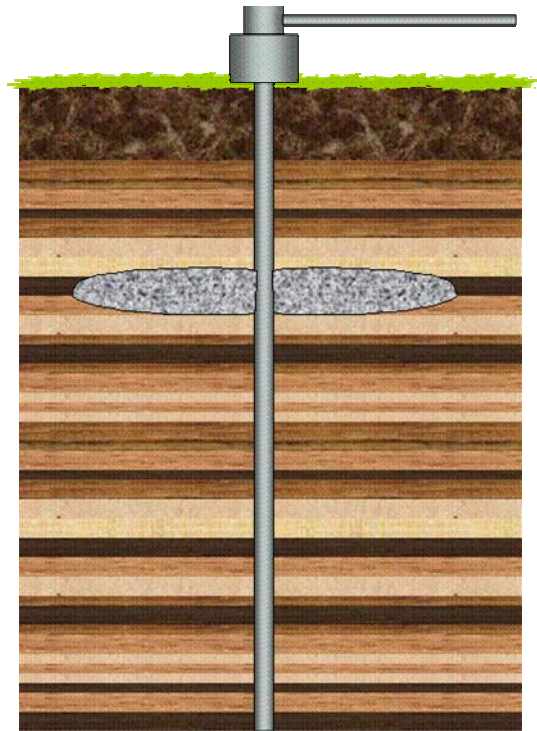


**Fig. 5.2** Fracture height grow is limited and only connects some layers of all prospective layers

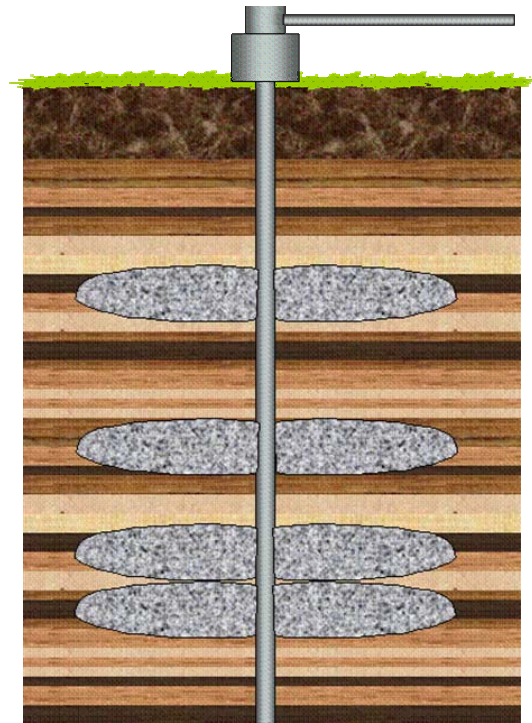


**Fig. 5.3** More fractures are required to connect prospective layers with the wellbore

The first step is to calculate the number of stages that will be considered in the optimization process applying DP. It is obtained as follow:

- 1) Select the top depth of prospective layers (i.g. 7,000 ft)
- 2) Select the bottom depth of prospective layers (i.g. 9,000 ft)
- 3) Divide total interval in sub-interval (i.e stages) of same length (i.g. 250 ft)
- 4) Number of stages are

$$N = \frac{|Top\_depth - Bottom\_depth|}{Stage\_length} \dots\dots\dots (5.1)$$

In the example,

$$N = \frac{|7,000\text{ft} - 9,000\text{ft}|}{250\text{ft}} = 8 \quad (\text{see Fig. 5.4})$$



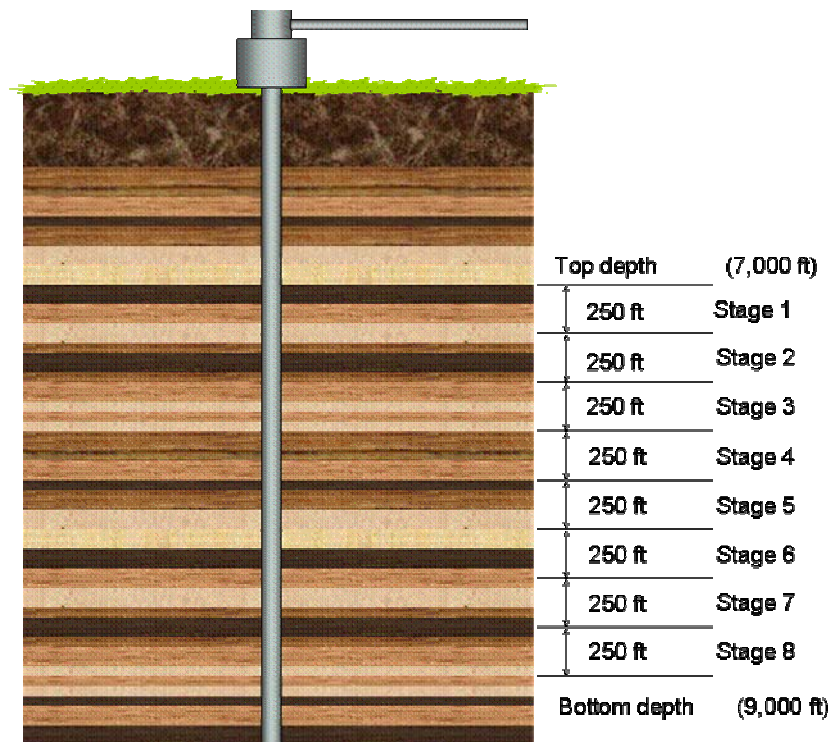


**Fig. 5.4** Calculation of number of stages

### 5.1.2 Gas production calculations

Once the number of stages ( $N$ ) has been calculated, the next step is to determine which of these stages should be fractured and how much proppant (i.e. mass of proppant) should be placed into each one to maximize total gas production (i.e. the sum of gas production coming from each fractured stage). In the optimization arena it is called an *Allocation Problem*. The star point of our methodology is that total mass of proppant ( $M_{\text{total}}$ ) to be injected into the well had been already dictated by economics. It is one and by far the most important restriction.

From chapters II, III and IV we can conclude that gas production coming from a fractured stage is a function of:

- Reservoir properties: Reservoir pressure, reservoir temperature, net pay, reservoir permeability to gas and drainage area

- Gas properties
- Proppant number: mass of proppant in the net pay, specific gravity, porosity and effective proppant permeability (considering non-Darcy flow effects and 50% of gel damage)
- Bottomhole pressure

We can see in **Fig. 5.4** that one stage comprise several layers. Therefore, reservoir properties are the average for the stage. In addition to this, we assume in chapter IV that reported  $h_p$  and  $k_g$  have deterministic values. However, previous studies performed in this field showed that there are uncertainties in the ultimate value of these parameters. We will assume that the average values of  $h_p$  and  $k_g$  for each stage follow a triangular probabilistic distribution (**Fig. 5.5**).

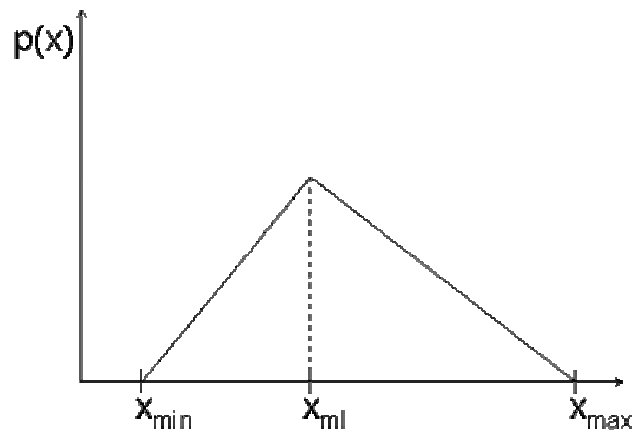


**Fig. 5.5** Triangular probabilistic distribution

$X$  in **Fig. 5.5** is the variable of interest (i.e. either  $k_g$  or  $h_p$ ), and  $p(x)$  is the probabilistic distribution function of  $X$ . Therefore for each stage  $X_{\min}$ ,  $X_{ml}$  and  $X_{\max}$  for  $h_p$  (i.e.  $\min_{h_p}$ ,  $ml_{h_p}$  and  $\max_{h_p}$ ) and  $k_g$  (i.e.  $\min_{k_g}$ ,  $ml_{k_g}$  and  $\max_{k_g}$ ) is part of the required data. Given

$U(X)$  (i.e. probability of occurrence of  $X$ ),  $X$  is calculated using inversion function of triangular distribution (Appendix D).

Although we mention previously that gas production is a function of several parameters, in next section we will consider it is only a function of mass of proppant because it is the only parameter that will be varied. Because of the stochastic nature of  $h_p$  and  $k_g$ , gas rate (for a specific mass of proppant at any stage) will be calculated using Monte Carlo simulation as follow:

1. Generate a random number between 0 and 1 (i.e.  $U(X)$ )
2. Calculate correspondent value of  $h_p$  using inversion function
3. Generate a second random number between 0 and 1 (i.e.  $U(X)$ )
4. Calculate correspondent value of  $k_g$  using inversion function
5. For the mass of proppant considered, and  $h_p$  and  $k_g$  calculated in step 2 and 4 respectively, calculate gas rate expected from an optimal fracture design (i.e. considering non-Darcy flow and 50% of gel damage)
6. Repeat 100 times steps 1 to 5. At this point we will have 100 values of gas rates for same mass of proppant in the same stage. Ultimate gas production is the arithmetic average of these 100 production rates.

This algorithm was implemented as an Excel function called  $q_{gas}$  (Appendix D).

## 5.2 Problem formulation for DP optimization

Basic elements of any optimization problem using DP are presented below adapted to multistage hydraulic fracturing case.

### Stages

It corresponds to the number of candidates stages ( $N$ ) for being fractured. Method to calculate  $N$  was introduced in section 5.1.1.

### Decisions

Decision to be made at each stage  $i$  is the mass of proppant ( $m_i$ ) to be placed in such stage for maximizing total gas rate production. Gas rate is a continuous function of mass of proppant. However, we will treat  $m_i$  as a discrete variable (i.e. positive integer series). For example, set of values of  $m_i$  for one stage could be 0, 20,000, 40,000 and 60,000 lbm.

### State

The variable of state at stage  $i$  is the mass of proppant remaining ( $s_i$ ) of total mass of proppant ( $M_{total}$ ) initially available for the well.

### Equation of state

It establish the relationship between state at stage  $i + 1$  ( $s_{i+1}$ ) and state ( $s_i$ ) and decision made ( $m_i$ ) at stage  $i$ .

$$s_{i+1} = s_i - m_i \dots\dots\dots (5.2)$$

where  $i = 1, 2, \dots, N$

### Objective function

It is to maximize total gas production coming from fractured stages having as constraint the total mass of proppant available for the well. In other words,

$$Max \sum_{i=1}^N q_i(m_i) \dots\dots\dots (5.3)$$

Subject to,

$$\sum_{i=1}^N m_i = M_{total} \dots\dots\dots (5.4)$$

where,

$$q_i(m_i) = 0, \quad \text{if } m_i = 0 \quad \text{and}$$

$q_i(m_i)$  is calculated following approach presented in section 5.1.2 ,  $\quad \text{if } m_i > 0$

### Recursive relation

It will allow establishing the *optimal policy* to maximize gas rate production. In this case, optimal policy is the amount of proppant to inject into each stage, even 0 lbm, to satisfy the objective function.

$$f_i(s_i) = \begin{cases} q_i(m_i), & \text{if } i = N \\ \max \{q_i(m_i) + f_{i+1}(s_i - m_i) : m_i \leq \{s_i\}\}, & \text{if } i = 1 \text{ to } N-1 \end{cases}$$

### **5.3 Example application**

Proposed optimization methodology will be implemented in the design of multistage fractures of PS #1 in order to show the potential of DP technique for this specific application. LWC\_LS 20/40 proppant will be the proppant to use in the design. Non-Darcy flow and 50% of gel damage will be considered.  $\beta$  factor will be calculated using Pen & Jin correlation. DP components specified in section 5.2 will be defined below for PS #1 application example.

#### Stages

After a detailed review of well logs of PS #1, the interval of interest for multistage fracturing is from 8,000' (i.e. top of the interval) to 10,000' depth (i.e. bottom of the interval). The stage length was set to 200' to avoid fracture overlapping between two contiguous stages, if both are going to be fractured.

Finally, number of stages is

$$N = \frac{|8,000 \text{ ft} - 10,000 \text{ ft}|}{200 \text{ ft}} = 10 \text{ stages}$$

Data required for all stages to calculate gas rate production are presented in **Tables 5.1** and **5.2**.

**Table 5.1** Reservoir properties and initial propped pack permeability for stages 1 to 10

Stage	$P_{res}$ (psi)	$T_{res}$ (°F)	$min_{hp}$ (ft)	$ml_{hp}$ (ft)	$max_{hp}$ (ft)	$min_k$ (md)	$ml_k$ (md)	$max_k$ (md)	$P_c$ (psi)	$k_f$ (md)
1	5,842	250	8	9.5	11	0.05	0.083	0.10	7,200	182,000
2	5,950	250	1	3	5	0.01	0.020	0.03	7,300	178,000
3	6,256	250	10	15	18	0.04	0.063	0.90	7,400	174,000
4	7,365	250	10	15	18	0.09	0.123	0.20	8,300	140,250
5	7,480	253	1	2	4	0.01	0.030	0.04	8,600	130,500
6	7,645	256	1	3	5	0.02	0.030	0.04	8,700	133,750
7	7,848	257	30	51	60	0.10	0.200	0.25	8,800	124,000
8	7,935	260	2	3	5	0.01	0.020	0.04	8,900	120,750
9	8,050	264	30	75	80	0.05	0.073	0.10	9,000	117,500
10	8,200	267	1	2	4	0.02	0.040	0.06	9,100	114,250

**Table 5.2** Common data for stages 1 to 10

$r_e$ (ft)	745
$SG_g$	0.664
$N_2$ (%)	0.099
$CO_2$ (%)	0.159
$H_2S$ (%)	0
$p_{wf}$ (psi)	1,400
$SG_p$	2.70
$\phi_p$	0.42

### Decisions

At each stage, decision will be to inject 0 or 60,000 lbm of proppant. Of course, decision set could include more values (i.g. 0, 20,000, 40,000, etc). However, the main purpose of this example is to show the usefulness of DP technique. Therefore, only two values are considered to simplify computations and computer programming. This work can be extended to include more details in both data and formulation of the problem.

### Objective function

It is assumed that total mass of proppant to inject in PS #1 is 300,000 lbm. Then,

$$\text{Max} \sum_{i=1}^{10} q_i(m_i)$$

subject to

$$\sum_{i=1}^{10} m_i = 300,000 \text{ lbm} \quad i = 1, 2, \dots, N \quad \text{and} \quad m_i = \{0, 60,000\}$$

### Recursive relation

$$f_i(s_i) = \begin{cases} q_i(m_i), & \text{if } i = 10 \\ \max \{q_i(m_i) + f_{i+1}(s_i - m_i) : m_i \leq \{s_i\}\}, & \text{if } i = 1 \text{ to } 9 \end{cases}$$

Recursive relation is typically solved in DP using tables such as **Tables 5.3, 5.4** and **5.5**. These are the solution “by hand” of one realization of Montecarlo simulation for stages 1, 9 and 10. The tables for the others stages are presented in Appendix D. Rows shaded in green represent optimal decision for correspondent stage. This process was automated using VB (see code in Appendix D). Optimal policy and consequently final results (**Table 5.6**) were the same from both the tables and VB code which validates the code and simplicity of DP technique to solve such as multistage decision problem.

**Table 5.3** Recursive relation for stage 10

<b>i = 10</b>		
$s_i \setminus m_i$	<b>Opt <math>m_i</math></b>	<b><math>f_i(m_i)</math></b>
<b>0</b>	<b>0</b>	<b>0</b>
<b>60,000</b>	60,000	161
<b>120,000</b>	60,000	161
<b>180,000</b>	60,000	161
<b>240,000</b>	60,000	161
<b>300,000</b>	60,000	161

**Table 5.4** Recursive relation for stage 9

<b>i = 9</b>				
$s_i \setminus m_i$	<b>0</b>	<b>60,000</b>	<b>Opt <math>m_i</math></b>	<b><math>f_i(m_i)</math></b>
<b>0</b>	0	-	0	0
<b>60,000</b>	161	4,957	60,000	4,957
<b>120,000</b>	161	5,118	60,000	5,118
<b>180,000</b>	161	5,118	60,000	5,118
<b>240,000</b>	161	5,118	60,000	5,118
<b>300,000</b>	161	5,118	60,000	5,118

**Table 5.5** Recursive relation for stage 1

<b>i = 1</b>				
$s_i \setminus m_i$	<b>0</b>	<b>60,000</b>	<b>Opt <math>m_i</math></b>	<b><math>f_i(m_i)</math></b>
<b>300,000</b>	17,920	18,444	60,000	18,444



**Table 5.6** Optimal policy for multistage fracturing of PS #1 for one realization of Montecarlo simulation

<b>Stage</b>	<b><math>m_i</math> (lbm)</b>	<b><math>q(m_i)</math> (Mscfd)</b>
<b>1</b>	60,000	685
<b>2</b>	0	0
<b>3</b>	60,000	3,383
<b>4</b>	60,000	1,822
<b>5</b>	0	0
<b>6</b>	0	0
<b>7</b>	60,000	7,597
<b>8</b>	0	0
<b>9</b>	60,000	4,957
<b>10</b>	0	0
<b>Total</b>		<b>18,444</b>

Additional realizations of Montecarlo simulation were evaluated. Optimal policy did not changed but total gas production did.

## CHAPTER VI

### SUMMARY AND CONCLUSIONS

#### 6.1 Summary

This work started with a review of  $\beta$  correlations available in the literature. Three type of correlations were identified: correlations obtained from proppant lab tests, correlations obtained from packed bead and core lab tests, and correlation obtained from analytical studies.

A spreadsheet was developed for optimal fracture designs in natural gas wells considering the effects of closure stress, non-Darcy flow and gel damage. To account the non-Darcy flow and gel damage effects in the design process is optional to the user. This new application is based on H2FD spreadsheet developed by Economides, Oligney and Valko.<sup>12</sup> Effective propped pack permeability and optimal geometry is calculated through and iterative process. A proppant database is included in the spreadsheet to get proppant properties such as specific gravity, porosity and permeability vs. closure stress for each available mesh size, required in the calculations. Moreover, a  $\beta$  factor correlation database is also included to evaluate the impact of correlation selected in optimal fracture geometry and gas deliverability.

The new spreadsheet was used to evaluate all  $\beta$  correlations available, as well all, perform fracture designs and analysis of 11 stages of three wells (i.e. PS #1, PS #2 and PS #3) completed in a natural tight gas reservoir in South Texas. Four types of 20/40 proppants are considered in this work: RCS, LWC LS, SB and LWC HS. In addition to this, Dynamic Programming technique was implemented in the multistage fracture design of PS #1 to maximize total gas production. Monte Carlo simulation was performed to incorporate the stochastic nature of average reservoir permeability and net pay of each stage in the optimization process.

## 6.2 Conclusions

The following conclusions can be derived from the present research:

1.  $\beta$  factor is a property of the porous media and is related the nature of its morphological structure.
2. Pursell *et al* and Martin *et al*  $\beta$  factor equations are recommended as general equations in the design and analysis of fracture treatments considering non-Darcy flow effects if there is no specific  $\beta$  equation available for proppant being used. The Thauvin and Mohanty and Li *et al.* equations could be also used, but, of course, equations developed from proppant lab tests should be considered first.
3. The  $\beta$  factor equation selection should not be influenced by the  $k_g h_p$  product of the formation to be fractured.
4. Shorter and wider fractures are required to compensate the effects of non-Darcy flow for a specified mass of proppant to be injected into the formation. The optimum fracture geometry varies somewhat with pressure drawdown. Therefore, operational  $p_{wf}$  should be estimated as best as possible for an optimal design. Finding the optimum dimensions compensates for a large part of the non-Darcy. This point has been neglected in the previous literature.
5. The higher the  $k_g h_p$  product is, the more important is to implement the non-Darcy flow compensation within the optimization loop.
6. The more factors decreasing propped pack permeability are considered (i.g. gel damage) the wider and shorter the fracture should be to compensate their effects.
7. DP is a powerful and easy to implement optimization technique in multistage fracture design for maximum gas deliverability when total mass of proppant to be injected into the well is a constraint. It is recommended to expand its application, through more application examples, incorporating all the complexities of the process.

## NOMENCLATURE

$a$	=	numerator of $\beta$ equation
$AR$	=	aspect ratio
$b$	=	power of proppant permeability in $\beta$ equation
$B_g$	=	gas formation volumetric factor, rcf/scf
$c$	=	power of proppant porosity in $\beta$ equation
$C_{fD}$	=	dimensionless fracture conductivity,
$C_{fDopt}$	=	optimal dimensionless fracture conductivity
$i$	=	index of number of stage
$h_f$	=	fracture height, ft
$h_p$	=	net pay, ft
$I_x$	=	penetration ratio
$J$	=	well productivity index, Mscfd/psi
$J_D$	=	dimensionless productivity index
$k_g$	=	reservoir gas permeability, md
$k_f$	=	initial or nominal proppant permeability, md
$k_{f-eff}$	=	effective proppant permeability, md or $cm^2$ or $D$
$\Delta L$	=	differential length in pressure drop calculation, ft
$M_{air}$	=	molecular weight of air, lb/lb mole
$M_g$	=	molecular weight of gas mixture, lb/lb mole
$m_i$	=	mass of proppant to inject in stage $I$ , lbm
$M_{total}$	=	total mass of proppant available for one well, lbm
$N$	=	number of stages
$N_{Re}$	=	Reynold number
$N_{Re\ new}$	=	Reynold number calculated at the end of actual iteration
$N_{Re\ old}$	=	Reynold number calculated in previous iteration
$N_{prop}$	=	proppant number
$p$	=	pressure of interest for gas properties calculation, psi
$\Delta P$	=	pressure drop, psi
$P_c$	=	closure pressure, psi
$p_{fracture}$	=	Pressure within the fracture, psi
$p_{pc}$	=	critical pressure, psi
$p_{pr}$	=	pseudo reduced pressure
$p_{res}$	=	reservoir pressure, psi
$p_{wf}$	=	flowing bottomhole pressure, psi
$q_i$	=	gas rate production for stage $i$ , Mscf/day
$q_{gsc}$	=	gas rate production at standard conditions, Mscf/day
$R$	=	universal constant of gas law, $psia.ft^3/lb\ mole^{\circ}R$
$r_e$	=	drainage radius, ft
$r_w$	=	well radius, ft
$s_i$	=	state of the system at stage $i$
$s_f$	=	pseudo fracture skin factor
$SG_{pp}$	=	proppant specific gravity
$SG_g$	=	gas specific gravity

$T$	= temperature of interest for gas properties calculation, °R or °F
$T_{pc}$	= critical temperature
$T_{pr}$	= pseudo reduced temperature
$T_{res}$	= reservoir temperature, °R or °F
$v$	= gas velocity, ft/day
$V_{p-2w}$	= volume of proppant in the net pay, ft <sup>3</sup>
$V_{p-1w}$	= volume of proppant in pay in one wing, ft <sup>3</sup>
$V_{i-2w}$	= total volume of proppant to be injected, ft <sup>3</sup>
$V_{res}$	= reservoir volume, ft <sup>3</sup>
$w_{fp}$	= propped fracture width, ft or in
$X$	= inertial force due to gas flow, gr-cm <sup>2</sup> s/cp
$x_e$	= reservoir length, ft
$x_f$	= fracture half- length, ft
$z$	= gas compressibility factor
$\alpha_1$	= conversion units constant
$\beta$	= non-Darcy flow coefficient, 1/ft or 1/m or 1/cm or atm-sec <sup>2</sup> /gr
$\phi_{pp}$	= proppant porosity
$\mu_g$	= gas viscosity, cp
$\mu_\gamma$	= fluid viscosity in Cooke experiments, cp
$\rho_g$	= gas density, lb/ft <sup>3</sup>
$\rho_{pr}$	= pseudo reduced gas density
$\sigma_{eff}$	= effective in situ stress, psi

## REFERENCES

1. Penny, G.S., and Jin, L.: "The Development of Laboratory Correlations Showing the Impact of Multiphase Flow, Fluid, and Proppant Selection Upon Gas Well Productivity," paper SPE 30494 presented at the 1995 SPE Technical Conference and Exhibition, Dallas, 22-25 October.
2. Guppy, K.H., Cinco-Ley, H., Ramey, H.J. and Samaniego, F.: "Non-Darcy Flow in Wells With Finite-Conductivity Vertical Fractures," *Society of Petroleum Engineers Journal*, (October 1982), 681.
3. Alvarez, C.H., Holditch, S.A., and McVay, D.A.: "Effects on Non-Darcy Flow on Pressure Transient Analysis of Hydraulically Fractured Gas Wells," paper SPE 77468 presented at the 2002 SPE Annual Technical Conference and Exhibition, San Antonio, 29 September – 2 October.
4. Richardson, M.: "A New and Practical Method for Fracture Design and Optimization," paper SPE 59736 presented at the 2000 SPE/CERI Gas Technology Symposium, Calgary, 3-5 April.
5. Barree, R.D., Cox, S.A., Barree, V.L. and Conway, M.W.: "Realistic Assessment of Proppant Pack Conductivity for Material Selection," paper SPE 84306 presented at the 2003 SPE Annual Technical Conference and Exhibition, Colorado, 5–8 October.
6. Vincent, M.C., Pearson, M., and Kullman, J.: "Non-Darcy and Multiphase Flow in Propped Fractures: Case Studies Illustrate the Dramatic Effect on Well Productivity," paper SPE 54630 presented at the 1999 SPE Western Regional Meeting, Anchorage, 26-28 May.
7. Settari, A., Stark, A.J., and Jones, J.R.: "Analysis of Hydraulic Fracturing of High Permeability Gas Wells to Reduce Non-Darcy Skin Effects," *Journal of Canadian Petroleum Technology* (May 2000), **39**, No. 5, 57.
8. Holditch, S.A., and Morse, R.A.: "The Effects of Non-Darcy Flow on the Behaviour Of Hydraulically Fractured Gas Wells," *Journal of Petroleum Technology* (October 1976), 1169.
9. Ubani, E.A. and Evans, R.D.: "Non-Darcy Compressible Flow of Real Gases in Propped Fracture," paper SPE 11101 presented at the 1982 Annual Fall Technical Conference and Exhibition, New Orleans, 26-29 September.
10. Gidley, J.L.: "A Method for Correcting Dimensionless Fracture Conductivity for Non-Darcy Flow Effects," *SPE Production Engineering* (November 1991) 391.
11. Settari, A., Bale, A., Bachman, R.C. and Floisand, V.: "General Correlation for the Effect of Non-Darcy Flow on Productivity of Fractured Wells," paper SPE 75715 presented at the 2002 SPE Gas Technology Symposium, Calgary, 30 April-May.
12. Economides, M.J., Oligney, R.E. and Valko, P.: *Unified Fracture Design*, Orsa Press, Alvin, Texas, 2002.

13. Economides, M.J., Oligney, R.E. and Valko, P.: "Applying unified fracture design to natural gas wells," *World Oil* (October 2002) 50.
14. Geertsma, J.: "Estimating the Coefficient of Inertial Resistance in Fluid Flow Through Porous Media," *Society of Petroleum Engineering Journal* (October 1974) 445.
15. Forchheimer, P.: "Wasserbewegung durch Bode," *ZVDI* (1901) **45**, 1781.
16. Cornell, D. and Katz, D.L.: "Flow of Gases through Consolidated Porous Media," *Industrial and Engineering Chemistry* (1953) **45**, No. 10, 2145.
17. Maloney, D.R., Gall, B.L. and Raible, C.J.: "Non-Darcy Gas Flow Through Propped Fractures: Effects of Partial Saturation, Gel Damage, and Stress," paper SPE 16899 presented at the 1987 Annual Technical Conference and Exhibition of the Society of Petroleum Engineers, Dallas, 27-30 September.
18. Pursell, D.A., Holditch, S.A. and Blakeley, D.M.: "Laboratory Investigation of Inertial Flow in High-Strength Fracture Proppants," paper SPE 18319 presented at the 1988 Annual Technical Conference and Exhibition of the Society of Petroleum Engineers, Houston, 2-5 October.
19. Flowers, J.R., Hupp, M.T. and Ryan, J.D.: "The Results of Increased Fracture Conductivity on Well Performance in a Mature East Texas Gas Field," paper SPE 84307 presented at the 2003 Annual Technical Conference and Exhibition of the Society of Petroleum Engineers, Denver, 5-8 October.
20. Li, D. and Engler, T.W.: "Literature Review on Correlations of the Non-Darcy Coefficient," paper SPE 70015 presented at the 2001 SPE Permian Basin Oil and Gas Recovery Conference, Midland, 15-16 May.
21. Cooke, C.E.: "Conductivity of Fracture Proppants in Multiple Layers," *Journal of Petroleum Technology* (September 1973) 1101.
22. Kutasov, I.M.: "Equation predicts non-Darcy flow coefficient," *Oil & Gas Journal* (15 March 1993) 66.
23. Martins, J.P., Milton-Taylor, D. and Leung, H.K.: "The Effects of Non-Darcy Flow in Propped Hydraulic Fractures," paper SPE 20709 presented at the 1990 Annual Technical Conference and Exhibition of the Society of Petroleum Engineers, New Orleans, 23-26 September.
24. Belhaj, H.A., Agha, K.R., Nouri, A.M., Butt, S.D. and Islam, M.R.: "Numerical and Experimental Modeling of Non-Darcy Flow in Porous Media," paper SPE 81037 presented at the 2003 SPE Latin American and Caribbean Petroleum Engineering Conference, Port-of-Spain, 27-30 April.
25. Coles, M.E. and Hartman, K.J.: "Non-Darcy Measurements in Dry Core and the Effect of Immobile Liquid," paper SPE 39977 presented at the 1998 SPE Gas Technology Symposium, Calgary, 15-18 March.
26. Ergun, S.: "Fluid Flow Through Packed Columns," *Chemical Engineering Progress* (1952) **48**, No. 2, 89.

27. Frederick Jr., D.C. and Graves, R.M.: "New Correlations To Predict Non-Darcy Flow Coefficients at Immobile and Mobile Water Saturation," paper SPE 28451 presented at the 1994 SPE Annual Technical Conference and Exhibition, New Orleans, 25-28 September.
28. Evans, R.D., Hudson, C.S. and Greenlee, G.E.: "The Effect of Liquid Saturation on the Non-Darcy Flow Coefficient in Porous Media," paper SPE 14206 presented at the 1985 SPE Annual Technical Conference, Las Vegas, 22-25 September.
29. Janicek, J.D. and Katz, D.L.: "Applications of Unsteady State Gas Flow Calculations," *Proc.*, U. of Michigan Research Conference, June 20, 1995.
30. Jones, S.C.: "Using the Inertial Coefficient,  $\beta$ , To Characterize Heterogeneity in Reservoir Rock," paper SPE 16949 presented at the 1987 Annual Technical Conference and Exhibition of the Society of Petroleum Engineers, Dallas, 27-30 September.
31. Li, D.: "Analytical Study of the Wafer Non-Darcy Flow Experiments," paper SPE 76778 presented at the 2002 SPE Western Regional/AAPG Pacific Section Joint Meeting, Anchorage, 20-22 May.
32. Macdonald, I.F., El-Sayed, M.S., Mow, K. and Dullen, F.A.L.: "Flow through Porous Media-the Ergun Equation Revisited," *Ind. Eng. Chem. Fundam.* (1979) **18**, No. 3, 199.
33. Tek, M.R., Coats, K.H. and Katz, D.L.: "The Effect of Turbulence on Flow of Natural Gas Through Porous Reservoirs," *Journal of Petroleum Technology* (July 1962) 799.
34. Thauvin, F. and Mohanty, K.K.: "Network Modeling of Non-Darcy Flow Through Porous Media," *Transport in Porous Media* (1998) **31**, 19.
35. Babcock, R. E. and Perry, R.H.: "Non-linear Dynamic programming of Hydraulic fracturing models," paper SPE 2159 presented at the 1968 Annual Fall Meeting of the SPE of AIME, Houston, 29 September-2 October.
36. Rahman, M.M., Rahman, M.K. and Rahman, S.S.: "Multivariate Fracture Treatment Optimization for Enhanced Gas Production From Tight Reservoirs," paper SPE 75702 presented at the 2002 SPE Gas Technology Symposium, Calgary, 30 April-2 May.
37. Meng, H.Z. and Brown, K.E.: "Coupling of Production Forecasting, Fracture Geometry requirements and Treatment Scheduling in the Optimum Hydraulic Fracture Design," paper SPE 16345 presented at the 1987 SPE/DOE Low Permeability Reservoir Symposium, Denver, 18-19 May.
38. Hareland, G. and Rampersand, P.R.: "Hydraulic Fracturing Design Optimization in Low-Permeability Gas Reservoirs," paper SPE 27033 presented at the 1994 SPE Latin American and Caribbean Petroleum Engineering Conference, Buenos Aires, 27-29 April.



39. Huffman, C.H., Harkrider, J.D. and Thompson, R.S.: "Fracture Simulation Treatment Design Optimization: What Can the NPV vs X, Plot Tell Us?," paper SPE 36575 presented at the 1996 SPE Annual Technical Conference and Exhibition, Denver, 6-9 October.
40. Aly, A.M. El-Banbi, A.H., Holditch, S.A., Wahdan, M., Salah, N.M. *et.al.*: "Optimization of Gas Condensate Reservoir Development by Coupling Reservoir Modeling and Hydraulic Fracturing Design," paper SPE 68175 presented at the 2001 SPE Annual Middle East Oil Show and Conference, Bahrain, 17-20 March.
41. Mohaghegh, S., Hefner, M.H. and Ameri, S.: "Fracture Optimization eXpert (FOX) – How Computational Intelligence Helps the Bottom-Line in Gas Storage; A Case Study," paper SPE 37341 presented at the 1996 SPE Eastern Regional Conference, Columbus, 23-25 October.
42. Xiong, H. and Holditch, S.A.: "An Investigation Into the Application of Fuzzy Logic to Well Stimulations Treatment Design," paper SPE 27672 presented at the 1994 SPE Permian Basin Oil and Gas Recovery Conference, Midland, 16-18 March.
43. Mohaghegh, S., Balan, B., Ameri, S. and McVey, D.S.: "A Hybrid, Neuro-Genetic Approach to Hydraulic Fracture Treatment Design and Optimization," paper SPE 36602 presented at the 1996 SPE Annual Technical Conference and Exhibition, Denver, 6-9 October.
44. Butenko, S.: "*Introduction to Dynamic Programming*," Class notes, Non-Linear and Dynamic Programming Course, Department of Industrial Engineering, Texas A&M University, Spring 2004.
45. Gluss, B.: *An Elementary Introduction to Dynamic Programming*, Allyn and Bacon Inc., Boston, Massachusetts, 1972.
46. White, D.J.: *Dynamic Programming*, Oliver & Boyd LTD, Tweeddale, Edinburgh, 1969.
47. Bentsen, R.G. and Donohue, D.A.T.: "A Dynamic Programming Model of the Cyclic Steam Injection Process," *Journal of Petroleum Technology* (December 1969) 1582.
48. Shamir, U.: "Optimal route for Pipelines in Two-Phase Flow," *Society of Petroleum Engineers Journal* (September 1971) 215.
49. Martch, H.B. and Norman, J.M.: "Optimization of the Design and Operation of Natural Gas Pipeline Systems," paper SPE 4006 presented at the 1972 Annual Fall Meeting of the SPE of AIME, San Antonio, 8-11 October.
50. Huppler, J.D.: "Scheduling Gas Field Production for Maximum Profit," paper SPE 4039 presented at the 1974 SPE-AIME Annual Fall Meeting, San Antonio, 8-11 October.
51. Lang, Z.X. and Horne, R.N.: "Optimum Production Scheduling Using Reservoir Simulators: A Comparison of Linear Programming and Dynamic Programming

- Techniques,” paper SPE 12159 presented at the 1983 SPE Annual Technical Conference and Exhibition, San Francisco, 5-8 October.
52. Jegier, J.: “An Application of Dynamic Programming to Casing String Design,” Institute of Mathematics, University of Mining and Metallurgy, Cracow, (June 1983)
  53. Economides, M.J. and Nolte, K.G.: *Reservoir Stimulation*, John Wiley & Sons LTD, Chichester, West Sussex, 2000.
  54. Montgomery, C.T. and Steanson, R.E.: “Proppant Selection: The Key to Successful Fracture Stimulation,” *Journal of Petroleum Technology* (December 1985) 2163.
  55. Parker, M.A. and McDaniel, B.W.: “Fracture Treatment Design Improved by Conductivity Measurements Under In-Situ Conditions,” paper SPE 16901 presented at the 1987 SPE Annual Technical Conference and Exhibition, Dallas, 27-30 September.
  56. Penny, G.S., and Jin, L.: “The Use of Inertial Force and Low Shear Viscosity to Predict Cleanup of Fracturing Fluids within Proppant Packs,” paper SPE 31096 presented at the 1996 SPE Formation Damage Symposium, Lafayette, 22-25 February.
  57. McCain, W.D.: “Reservoir-Fluid Property Correlations-State of the Art,” *SPE Reservoir Engineering* (May 1991) 266.
  58. McCain, W.D.: *The Properties of Petroleum Fluids*, PennWell Publishing Company, Tulsa, Oklahoma, 1990.
  59. Dranchuk, P.M. and Abou-Kassem J.H.: “Calculation of Z Factors for Natural Gases Using Equations of State,” *Journal of Canadian Petroleum Technology* (July-September 1975) 34.
  60. Takacs, G.: “Comparisons made for computer Z-factor calculations,” *The Oil and Gas Journal* (December 1976) 65.
  61. Piper, L.D., McCain Jr., W.D. and Corredor, J.H.: “Compressibility Factors for Naturally Occurring Petroleum Gases,” paper SPE 26668 presented at the 1993 SPE Annual Technical Conference and Exhibition, Houston, 3-6 October.
  62. Lee, A.L., Gonzalez, M.H. and Eakin, B.E.: “The Viscosity of Natural Gases,” *Journal of Petroleum Technology* (August 1966) 997.

## APPENDIX A

### PROPPANT AND BETA EQUATION DATABASE

Specifications for four types of commonly used proppants are provided in the spreadsheet. These were included just as a reference. The same database is used for both Traditional and TSO design. Remember User can input a new proppant if it is going to be used in the field. Proppants included are:

- **Resin Coated Sand (RCS).** It corresponds to Acfrac Excel 20/40. Data was provided by Borden Chemical.
- **Low weight ceramic (LWC) low strenght.** It corresponds to CARBO ECONOPROP<sup>®</sup> 20/40 proppant. Data was provided by Carboceramics.
- **Low weight ceramic (LWC) high strenght.** It corresponds to CARBO LITE<sup>®</sup> 20/40 proppant. Data was provided by Carboceramics.
- **Sintered Bauxite.** It corresponds to CARBO HSP<sup>™</sup> 20/40 proppant. Data was provided by Carboceramics.

#### **How to enter a new proppant?**

Follow the steps presented below to enter a new proppant and its properties in the proppant database. Each step is illustrated in **Fig. A.1**.

	A	B	C	D	E	F	G	H	I	J	K	L	M
	PROPPANT	TYPE	SG	Closure Stress psi	Porosity	Mesh Size Permeability (md)							
1													
2	SAND	Sand	2.65			8/16	12/20	16/30	20/40				
3				500	0.38	3279000	1726000	930000	499000				
4				1000	0.38	2604000	1582000	838000	467000				
5				2000	0.38	1438000	1233000	640000	401000				
6				3000	0.38	728000	866000	433000	327000				
7				4000	0.38	415000	487000	289000	245000				
8	LWC LOW STRENGTH	LWC	2.70			20/40	30/50						
9				2000	0.42	340000	230000						
10				4000	0.42	300000	190000						
11				6000	0.42	230000	150000						
12				8000	0.42	150000	100000						
13				10000	0.42	85000	70000						
14	LWC HIGH STRENGTH	LWC	2.71			12/18	16/20	20/40					
15				2000	0.42	2003000	1286000	570000					
16				4000	0.42	1325000	955000	480000					
17				6000	0.42	570000	510000	340000					
18				8000	0.42	293000	276000	210000					
19				10000	0.42	141000	150000	120000					
20	SINTERED BAUXITE	Bauxite	3.56			12/18	16/30	20/40	30/60				
21				2000	0.45	2742000	1207000	539000	254000				
22				4000	0.45	2395000	939000	440000	224000				
23				6000	0.45	1609000	721000	370000	197000				
24				8000	0.45	894000	515000	302000	167000				
25				10000	0.45	409000	393000	246000	134000				
26				12000	0.45	284000	290000	204000	99000				
27				14000	0.45	194000	230000	166000	73000				
28													
29													
30													
31													
32													

**Fig. A.1** Steps to input a new proppant in the database

1. Select “Proppants” worksheet. **Fig. A.1** shows the window user will see when this worksheet is selected.
2. Enter the name, type of proppant, specific gravity and mesh sizes for new proppant in the first empty row just below the last register. (e.g. Row 28 in **Fig. A.1**)
  - a. Enter in column A the name you want to use to identify the new proppant. It is the name that will appear in the Proppant selection Combo Box of the input windows. It can be a generic name or the commercial name.
  - b. Enter in column B the type of proppant that correspond to new proppant. This register is used to define what  $\beta$  factor equation might be used for proppant selected. Remember that some  $\beta$  equations have been developed for a specific type of proppant. Spreadsheet is case sensitive so use Upper and Lower case appropriately to match Proppant Restriction of  $\beta$  equation database. Possible types of proppant are presented below.

- i.** Sand: Ottawa sand, Brady sand, etc might be considered just Sand for this purpose.
    - ii.** RSC: Resine Coated Sand.
    - iii.** LWC: Low Weight Ceramic.
    - iv.** Bauxite: Sintered Bauxite may be included in this group.
  - c. Enter in column C the specific gravity of the proppant.
  - d. Enter from column F (i.e. column F, column G and so on) the mesh sizes available for this proppant. Use the standard format to specify mesh size (i.g. 12/20). Check that format of the cell is “Text”.
- 3.** Enter from the row just below the row used in step 2 the closure stresses, porosity and permeabilities of the proppants
  - a. Enter in Column D, from this row until the required row, the closure stress manufacturer considered to evaluate proppant permeability and porosity.
  - b. Enter in Column E the porosity that corresponds to each closure pressure. This variable is not usually reported in the Product Datasheet provided by the manufacturer. Therefore, if no information is available, enter for all closure stresses the estimated average porosity of this proppant.
  - c. Enter the permeability that corresponds to a closure stress for each mesh size of the proppant in the respective column (starting from column F). This information is usually provided by the manufacturer in the technical datasheet of the product.
- 4.** Check all data entered is correct. Then click “Update” button to include the new proppant in the Proppant selection combo box list of the INPUT DATA windows.
- 5.** Click “Back to Traditional Design” or “Back to TSO” to return to “TRAD” or “TSO” worksheets respectively.

Any proppant can be removed from the proppant database. For that, just select the rows where information of the proppant is stored and the Delete these rows.

**Check not to leave empty rows between last register of a proppant and the first register of the next one. Finally click on “Update” button.**

Spreadsheet includes all  $\beta$  factor equations presented in Chapter II. These equations are in the Beta factor worksheet which basically consists on name of the correlation and a, b and c parameters of the equation.

### How to enter a new $\beta$ equation ?

Users have the option to include new  $\beta$  equations. Before explaining the steps to do so remember that:

- $\beta$  factor equations included in the spreadsheet follows this general form

$$\beta = \frac{a}{k_f^b \phi_p^c}$$

- $\beta$  must be in 1/ft and  $k_f$  in md.

## TRADITIONAL DESIGN

**PROPPANT PERMEABILITY CORRECTION**

**Effects to be consider** Back Home

Non-Darcy Flow

Gel Damage

**Non-Darcy Flow**

β Equation: Belhaj et al \* Equation for proppant

**Input a new equation**

**Gel Damage**

% of Damage: 50

Apply to:  Proppant Permeability  Beta Factor

STEP 1

**Fig. A.2** Access to  $\beta$  equations database from Proppant Permeability Correction window

1. Access “Beta Equations” worksheet from “Proppant Permeability Correction” window (see **Fig. A.2**) or the traditional way people access a worksheet in an Excel workbook (see **Fig. A.3**)
2. Enter the new  $\beta$  equation information in the row just below the last  $\beta$  equation already existing in the database (i.g. row 26 in **Fig. A.3**).
  - a. Enter in Column A the name of the equation. It is usually the last name(s) of the author(s) of the equation.

For example:

*Lopez* ( 1 author)

*Lopez and Romero* (2 authors)

*Lopez et al* (more than 2 authors)

- If equation was developed for proppant enter a \* right after the last character of the original name of the equation. For example:

*Lopez\** ( 1 author)

*Lopez and Romero\** (2 authors)

*Lopez et al\** (more than 2 authors)

- Sometimes in the same work equations are developed for different type of proppants or mesh. In this case enter the parameter that differentiates the equation developed for the same author(s). For example, if *Lopez et al* developed a equation for 16/30 Bauxite and other for 20/40 Bauxite, then enter these like two different equations with the following name (it is the case of Cooke and Pen and Jin equations in the original database)

*Lopez et al\** 16/30, in one row and

*Lopez et al\** 20/40, in the next row

- b. Enter coefficient  $a$  in Column B. Usually coefficient  $a$  is related to the units of the original equation. Therefore, if  $\beta$  factor and  $k_f$  are in other units different than  $1/\text{ft}$  and  $\text{md}$  respectively in the original equation, convert first the original units to proposed units. Then input the resulting  $a$  value.
- c. Enter coefficient  $b$  in Column C. Although original units of  $\beta$  and  $k_f$  are different than required, parameter  $b$  remain the same.
- d. Enter coefficient  $c$  in Column D. Although original units of  $\beta$  and  $k_f$  are different than required, parameter  $c$  remain the same.
- e. If the new equation is restricted to a type of proppant, specify it in Column E (“Proppant Restriction”). Type of proppant specified here should match with at least one type of proppant of proppant available in the database. Consider the following classification like a reference:
  - i.** Sand. Ottawa sand, Brady sand, etc might be considered just Sand for this purpose.
  - ii.** RSC: Resine Coated Sand.
  - iii.** LWC: Low Weight Ceramic.
  - iv.** Bauxite. Sintered Bauxite may be included in this group.

Note that spreadsheet is case sensitive so use Upper and Lower case appropriately. If a  $\beta$  factor equation was developed for a specific type of proppant and size do a unique reference in TYPE of proppant in proppant database and Proppant Restriction in  $\beta$  equations database. For example is a  $\beta$  equation was developed for CARBO HSP™ 20/40, enter carbohsp2040 in the fields mentioned above.
- f. When new  $\beta$  equation is restricted to a mesh it must be specified in Column F (“Mesh Restriction”). Use the standard format to specify mesh size (i.g. 20/40). Check that format cell is “Text”.



When  $\beta$  equation has been developed from cores or analytical studies leave Column E and F in blank.

6. Check all data entered is correct. Then click “Update” button. It will order equations alphabetically and will include news one it in the  $\beta$  Equation combo box of the “Proppant Permeability Correction” window if this equation is eligible for the actual type of proppant or mesh size. It applies for both Traditional and TSO design
7. Click “Back to Traditional Design” or “Back to TSO” to return to actual design.

A  $\beta$  factor equation can be removed from the database. Eliminate the rows that contain the  $\beta$  equation and then Click on “Update” button.

	A	B	C	D	E	F	G	H	I
	CORRELATION	a	b	c	Proppant Restriction	Mesh Restriction			
1									
2	Belhaj <i>et al</i>	0.115	1.000	1.000					
3	Cole and Hartman	8,170.000	1.790	-0.537					
4	Cooke* 8/12	17,423.608	1.240	0.000	Sand	8/12			
5	Cooke* 10/20	27,539.481	1.340	0.000	Sand	10/20			
6	Cooke* 20/40	110,470.387	1.540	0.000	Sand	20/40			
7	Cooke* 40/60	69,405.308	1.600	0.000	Sand	40/60			
8	Ergun	0.0452	0.500	1.500					
9	Frederick <i>et al</i>	6,496.380	1.640	0.000					
10	Geertsma	0.0015916	0.500	5.500					
11	Janice and Katz	182.000	1.250	0.750					
12	Jones	2,017.800	1.550	0.000					
13	Kutasov*	0.0453	0.500	1.500					
14	Li <i>et al</i>	13.860	0.850	1.150					
15	Mac Donal <i>et al</i>	0.000452	0.500	1.500					
16	Maloney <i>et al</i> *	0.000382	0.500	7.100					
17	Martins <i>et al</i> *	269.290	1.036	0.000					
18	Penny and Jin* Bauxite	87.100	0.980	0.000	Bauxite	20/40			
19	Penny and Jin* LWC	3,936.390	1.250	0.000	LWC	20/40			
20	Penny and Jin* RCS	11,220.180	1.350	0.000	RCS	20/40			
21	Penny and Jin* Sand	16,790.410	1.450	0.000	Sand	20/40			
22	Pursell <i>et al</i> * 12/20	91.923	0.635	0.000		12/20			
23	Pursell <i>et al</i> * 20/40	10.675	0.326	0.000		20/40			
24	Tek <i>et al</i>	0.000000	0.000000	0.000000					
25	Thauvi 2.a ohanty	2.b	2.c	2.d	2.e	2.f			
26									
27									
28									
29									
30									
31									
32									
33									

Update → STEP 3

Back to Traditional Design

Back to TSO Design

STEP 4

STEP 2

STEP 1

Fig. A.3 Steps to input a new  $\beta$  equation in the database

## APPENDIX B

### VB CODE FOR GAS VISCOSITY AND Z FACTOR ESTIMATION

Correlations were codified in VBA as Excel functions. Each function follows the structure of original correlation. Only name of parameters were changed specially those parameters represented with greek letters.

#### Code to calculate critical temperature of the mixture ( $T_{pc}$ )

##### Input

sg: specific gravity of the gas  
 n2: % of nitrogen in the gas mixture  
 co2: % of carbon dioxide in the gas mixture  
 h2s: % of hydrogen sulfide in the gas mixture

Function Tpc(sg As Double, n2 As Double, co2 As Double, h2s As Double) As Double

Dim yn2 As Double; mole fraction of Nitrogen

Dim yco2 As Double; mole fraction of Carbon Dioxide

Dim yh2s As Double; mole fraction of Hydrogen Sulfide

Dim J As Double

Dim K As Double

Const a0 As Double = 0.11582;  $\alpha_0$

Const a1 As Double = -0.4582;  $\alpha_1$

Const a2 As Double = -0.90348;  $\alpha_2$

Const a3 As Double = -0.66026;  $\alpha_3$

Const a4 As Double = 0.70729;  $\alpha_4$

Const a5 As Double = -0.099397;  $\alpha_5$

Const b0 As Double = 3.8216;  $\beta_0$

Const b1 As Double = -0.06534;  $\beta_1$

Const b2 As Double = -0.42113;  $\beta_2$

Const b3 As Double = -0.91249;  $\beta_3$

Const b4 As Double = 17.438;  $\beta_4$

Const b5 As Double = -3.2191;  $\beta_5$

Const Tcn2 As Double = 227.5; Critical temperature of Nitrogen

Const Pcn2 As Double = 493.1; Critical pressure of Nitrogen

Const Tcco2 As Double = 547.9; Critical temperature of Carbon Dioxide

Const Pcco2 As Double = 1071; Critical pressure of Carbon Dioxide

Const Tch2s As Double = 672.4; Critical temperature of Hydrogen Sulfide

Const Pch2s As Double = 1300; Critical pressure of Hydrogen Sulfide

yn2 = n2 / 100

yco2 = co2 / 100

yh2s = h2s / 100

$J = a_0 + a_1 * yh_{2s} * (Tch_{2s} / Pch_{2s}) + a_2 * yco_2 * (Tcco_2 / Pcco_2) + a_3 * yn_2 * (Tcn_2 / Pcn_2) + a_4 * sg + a_5 * (sg^2)$

$K = b_0 + b_1 * yh_{2s} * (Tch_{2s} / Sqr(Pch_{2s})) + b_2 * yco_2 * (Tcco_2 / Sqr(Pcco_2)) + b_3 * yn_2 * (Tcn_2 / Sqr(Pcn_2)) + b_4 * sg + b_5 * (sg^2)$

Tpc = (K ^ 2) / J  
End Function

### Code to calculate critical pressure of the mixture ( $P_{pc}$ )

#### Input

sg: specific gravity of the gas  
n2: % of nitrogen in the gas mixture  
co2: % of carbon dioxide in the gas mixture  
h2s: % of hydrogen sulfide in the gas mixture

Function Ppc(sg As Double, n2 As Double, co2 As Double, h2s As Double) As Double  
Dim yn2 As Double; mole fraction of Nitrogen  
Dim yco2 As Double; mole fraction of Carbon Dioxide  
Dim yh2s As Double; mole fraction of Hydrogen Sulfide  
Dim J As Double  
Dim K As Double  
Const a0 As Double = 0.11582;  $\alpha_0$   
Const a1 As Double = -0.4582;  $\alpha_1$   
Const a2 As Double = -0.90348;  $\alpha_2$   
Const a3 As Double = -0.66026;  $\alpha_3$   
Const a4 As Double = 0.70729;  $\alpha_4$   
Const a5 As Double = -0.099397;  $\alpha_5$   
Const b0 As Double = 3.8216;  $\beta_0$   
Const b1 As Double = -0.06534;  $\beta_1$   
Const b2 As Double = -0.42113;  $\beta_2$   
Const b3 As Double = -0.91249;  $\beta_3$   
Const b4 As Double = 17.438;  $\beta_4$   
Const b5 As Double = -3.2191;  $\beta_5$   
Const Tcn2 As Double = 227.5; Critical temperature of Nitrogen  
Const Pcn2 As Double = 493.1; Critical pressure of Nitrogen  
Const Tcco2 As Double = 547.9; Critical temperature of Carbon Dioxide  
Const Pcco2 As Double = 1071; Critical pressure of Carbon Dioxide  
Const Tch2s As Double = 672.4; Critical temperature of Hydrogen Sulfide  
Const Pch2s As Double = 1300; Critical pressure of Hydrogen Sulfide  
yn2 = n2 / 100  
yco2 = co2 / 100  
yh2s = h2s / 100  
J = a0 + a1 \* yh2s \* (Tch2s / Pch2s) + a2 \* yco2 \* (Tcco2 / Pcco2) + a3 \* yn2 \* (Tcn2 / Pcn2) + a4 \* sg + a5 \* (sg ^ 2)  
K = b0 + b1 \* yh2s \* (Tch2s / Sqr(Pch2s)) + b2 \* yco2 \* (Tcco2 / Sqr(Pcco2)) + b3 \* yn2 \* (Tcn2 / Sqr(Pcn2)) + b4 \* sg + b5 \* (sg ^ 2)  
Ppc = (K / J) ^ 2  
End Function

## Code to calculate z-Factor

Because z-Factor is an implicit correlation, it was solved using Newton-Raphson method. Initially the correlations was solved for  $\rho_{pr}$ . Then z-factor was calculated for solution of  $\rho_{pr}$ .

$$x^{k+1} = x^k - \frac{f(x^k)}{f'(x^k)}$$

### Input

p: pressure of interest  
 t: temperature of interest  
 sg: specific gravity of the gas  
 n2: % of nitrogen in the gas mixture  
 co2: % of carbon dioxide in the gas mixture  
 h2s: % of hydrogen sulfide in the gas mixture

```
Function z(p As Double, t As Double, sg As Double, n2 As Double, co2 As Double, h2s As Double) As
Double
Dim Tc As Double; Critical temperature of the gas mixture
Dim Tpr As Double; Pseudo reduce temperature of the gas mixture
Dim Pc As Double; Critical pressure of the gas mixture
Dim Ppr As Double; Pseudo reduced pressure of the gas mixture
Dim deviation As Double
Dim rho1 As Double; new value of  $\rho_{pr}$ 
Dim rho0 As Double; old value of  $\rho_{pr}$ 
Dim frho0 As Double;  $f(\rho_{pr})$ 
Dim Dfrho0 As Double;  $f'(\rho_{pr})$ 
Const a1 As Double = 0.3265
Const a2 As Double = -1.07
Const a3 As Double = -0.5339
Const a4 As Double = 0.01569
Const a5 As Double = -0.05165
Const a6 As Double = 0.5475
Const a7 As Double = -0.7361
Const a8 As Double = 0.1844
Const a9 As Double = 0.1056
Const a10 As Double = 0.6134
Const a11 As Double = 0.721
Tc = Tpc(sg, n2, co2, h2s)
Tpr = t / Tc
Pc = Ppc(sg, n2, co2, h2s)
Ppr = p / Pc
deviation = 100
rho1 = 0.27 * Ppr / Tpr
Do
rho0 = rho1
frho0 = 1 - 0.27 * Ppr / (rho0 * Tpr) + (a1 + a2 / Tpr + a3 / Tpr ^ 3 + a4 / Tpr ^ 4 + a5 / Tpr ^ 5) * rho0 +
(a6 + a7 / Tpr + a8 / Tpr ^ 2) * rho0 ^ 2 - a9 * (a7 / Tpr + a8 / Tpr ^ 2) * rho0 ^ 5 + a10 * (1 + a11 * rho0 ^
2) * (rho0 ^ 2 / Tpr ^ 3) * Exp(-a11 * rho0 ^ 2)
```

```

Dfrho0 = 0.27 * Ppr / (rho0 ^ 2 * Tpr) + a1 + a2 / Tpr + a3 / Tpr ^ 3 + a4 / Tpr ^ 4 + a5 / Tpr ^ 5 + (a6 + a7
/ Tpr + a8 / Tpr ^ 2) * 2 * rho0 - a9 * (a7 / Tpr + a8 / Tpr ^ 2) * 5 * rho0 ^ 4 + (2 * a10 * rho0 / Tpr ^ 3) *
(1 + a11 * rho0 ^ 2 - a11 ^ 2 * rho0 ^ 4) * Exp(-a11 * rho0 ^ 2)
rho1 = rho0 - frho0 / Dfrho0
deviation = 100 * Abs(rho1 - rho0) / rho0
Loop Until deviation < 0.01
z = 0.27 * Ppr / (rho1 * Tpr)
End Function

```

## Code to calculate gas viscosity ( $\mu_g$ )

### Input

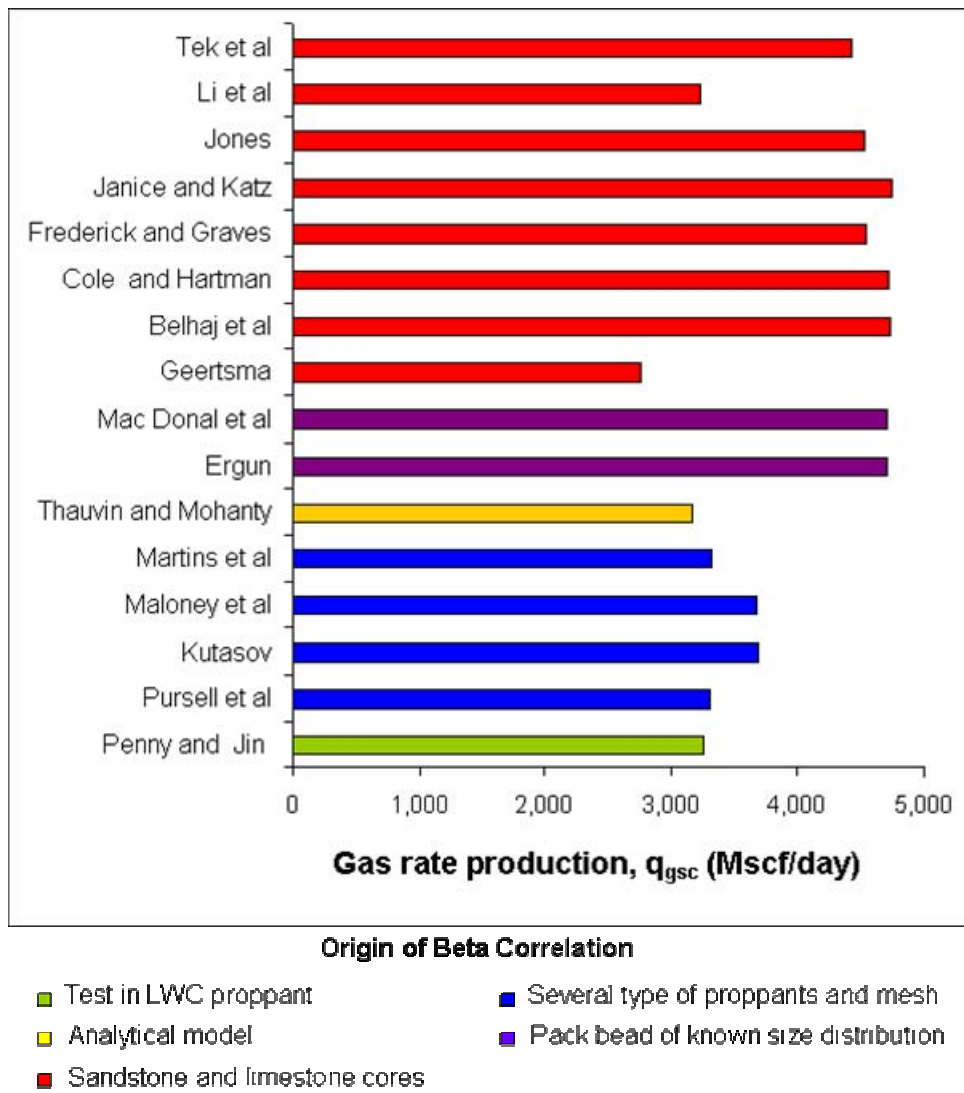
p: pressure of interest  
 t: temperature of interest  
 sg: specific gravity of the gas  
 n2: % of nitrogen in the gas mixture  
 co2: % of carbon dioxide in the gas mixture  
 h2s: % of hydrogen sulfide in the gas mixture

```

Function ug(p As Double, t As Double, sg As Double, n2 As Double, co2 As Double, h2s As Double) As
Double
Dim zug As Double; z-factor
Dim mw As Double; Molecular weight of the gas mixture
Dim a As Double
Dim b As Double
Dim c As Double
Dim rho As Double; density of the gas mixture
zug = z(p, t, sg, n2, co2, h2s)
mw = 28.97 * sg
a = (9.379 + 0.01607 * mw) * t ^ 1.5 / (209.2 + 19.26 * mw + t)
b = 3.448 + 986.4 / t + 0.01009 * mw
c = 2.447 - 0.2224 * b
rho = p * mw / zug / 669.8 / t
ug = a * Exp(b * rho ^ c) * 0.0001
End Function

```

## APPENDIX C

 **$\beta$  CORRELATIONS EVALUATION AND EFFECTIVE PROPPANT PERMEABILITY**

**Fig. C.1** Comparison of optimal design results in terms of gas rate production for 20/40 LWC\_LS proppant (PS #1\_Stage3)

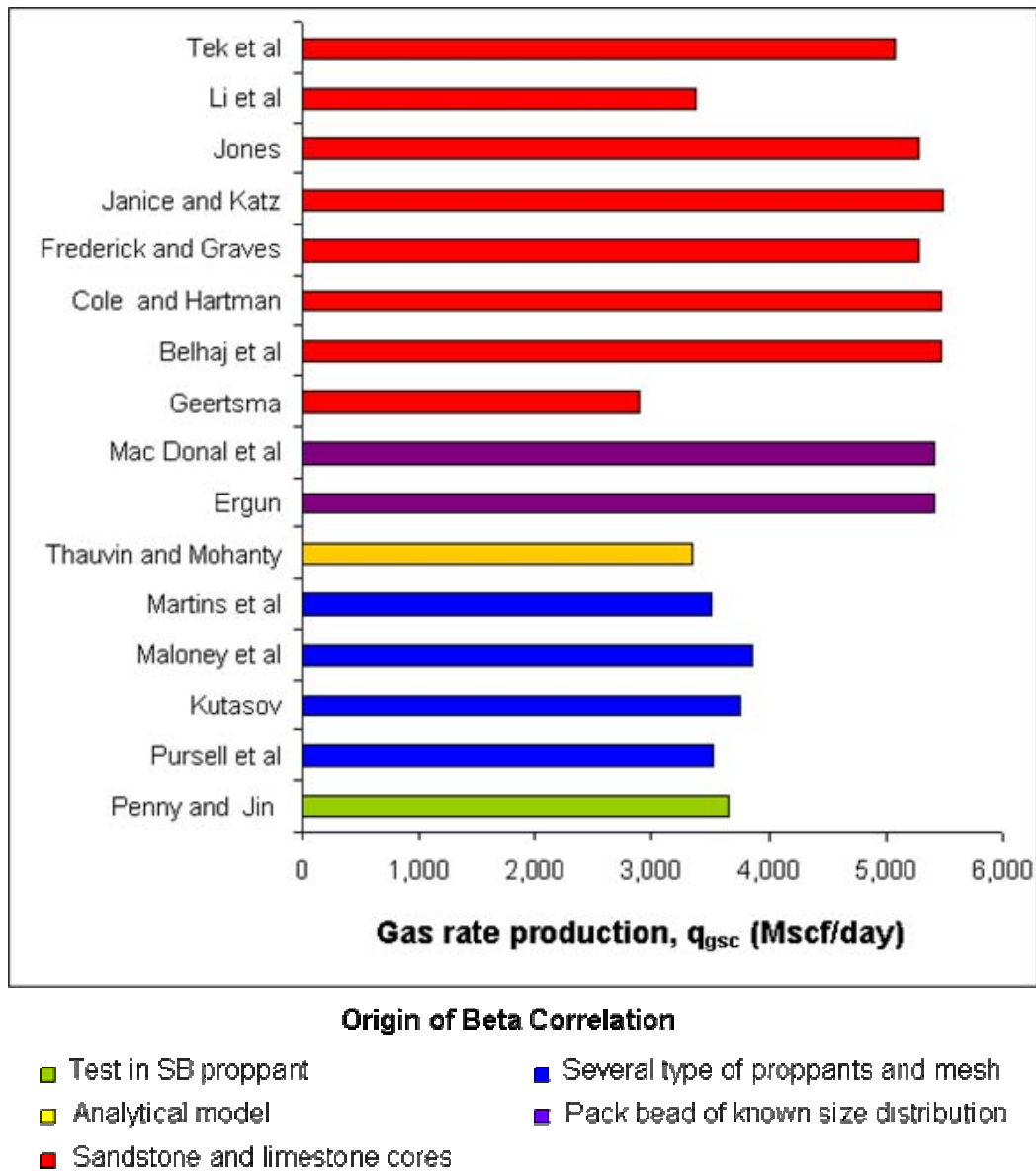


**Fig. C.2** Comparison of optimal design results in terms of gas rate production for 20/40 SB proppant (PS #1\_Stage3)

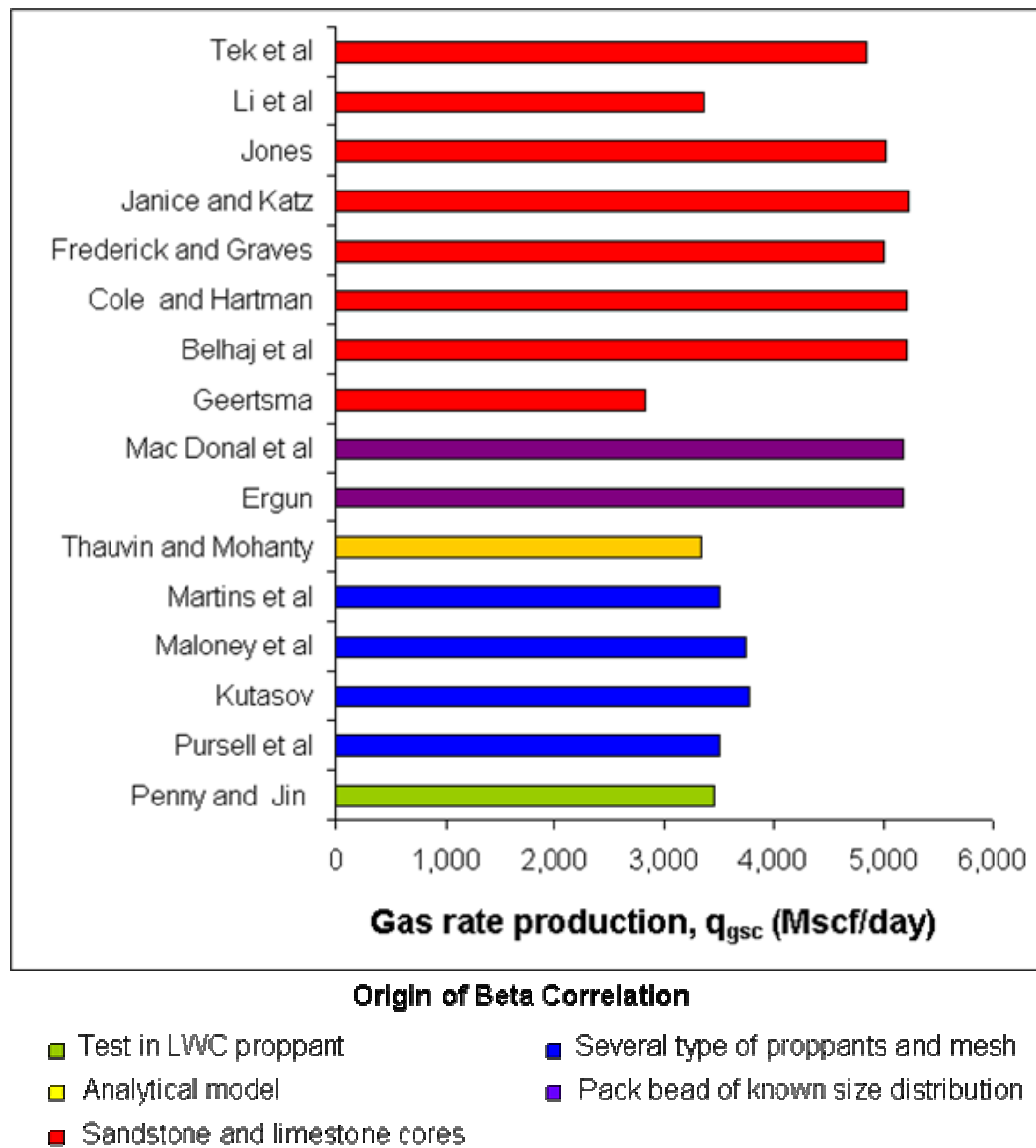


**Fig. C.3** Comparison of optimal design results in terms of gas rate production for 20/40 LWC\_HS proppant (PS #1\_Stage3)



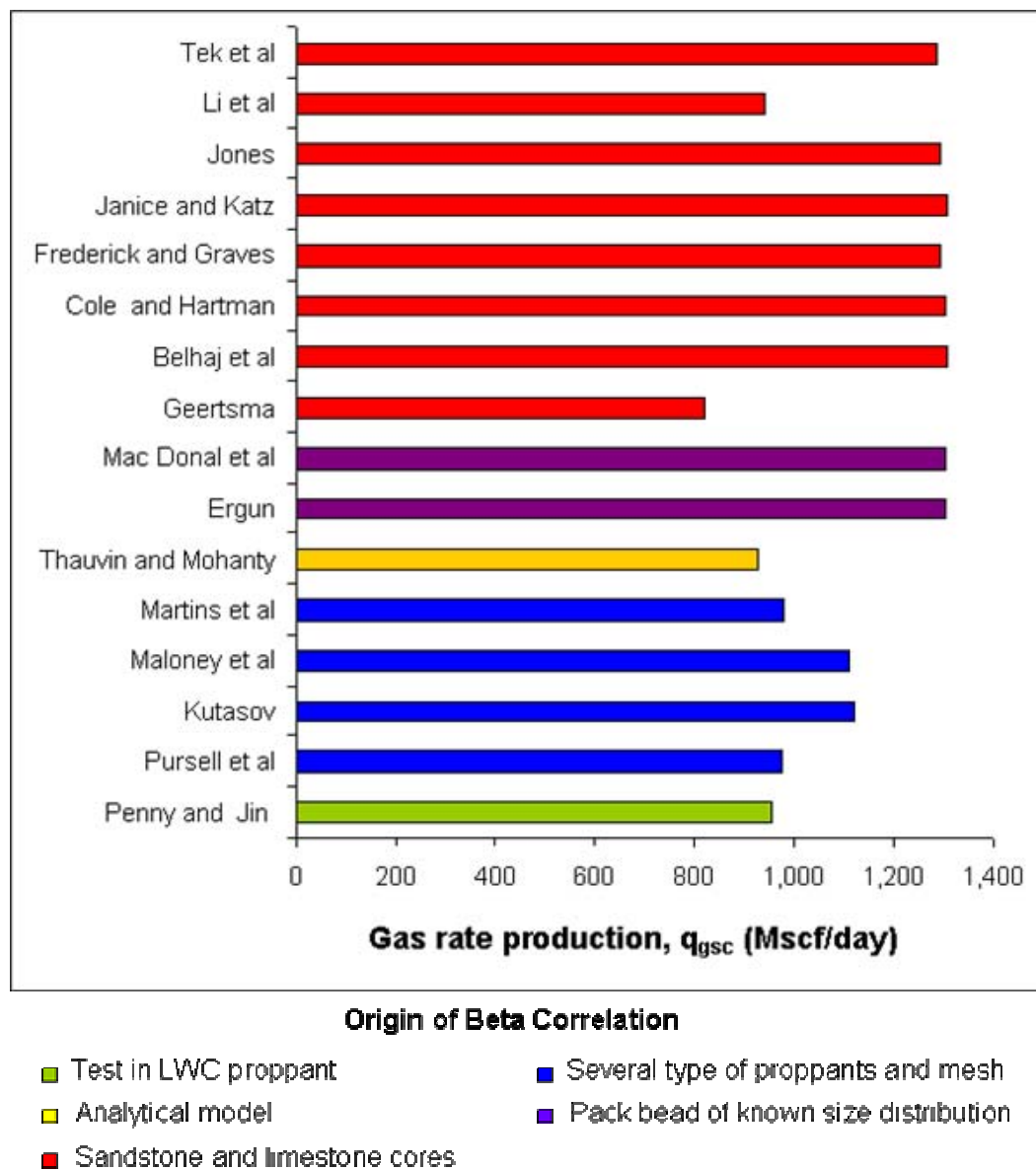


**Fig. C.4** Comparison of optimal design results in terms of gas rate production for 20/40 LWC\_LS proppant (PS #2\_Stage1)

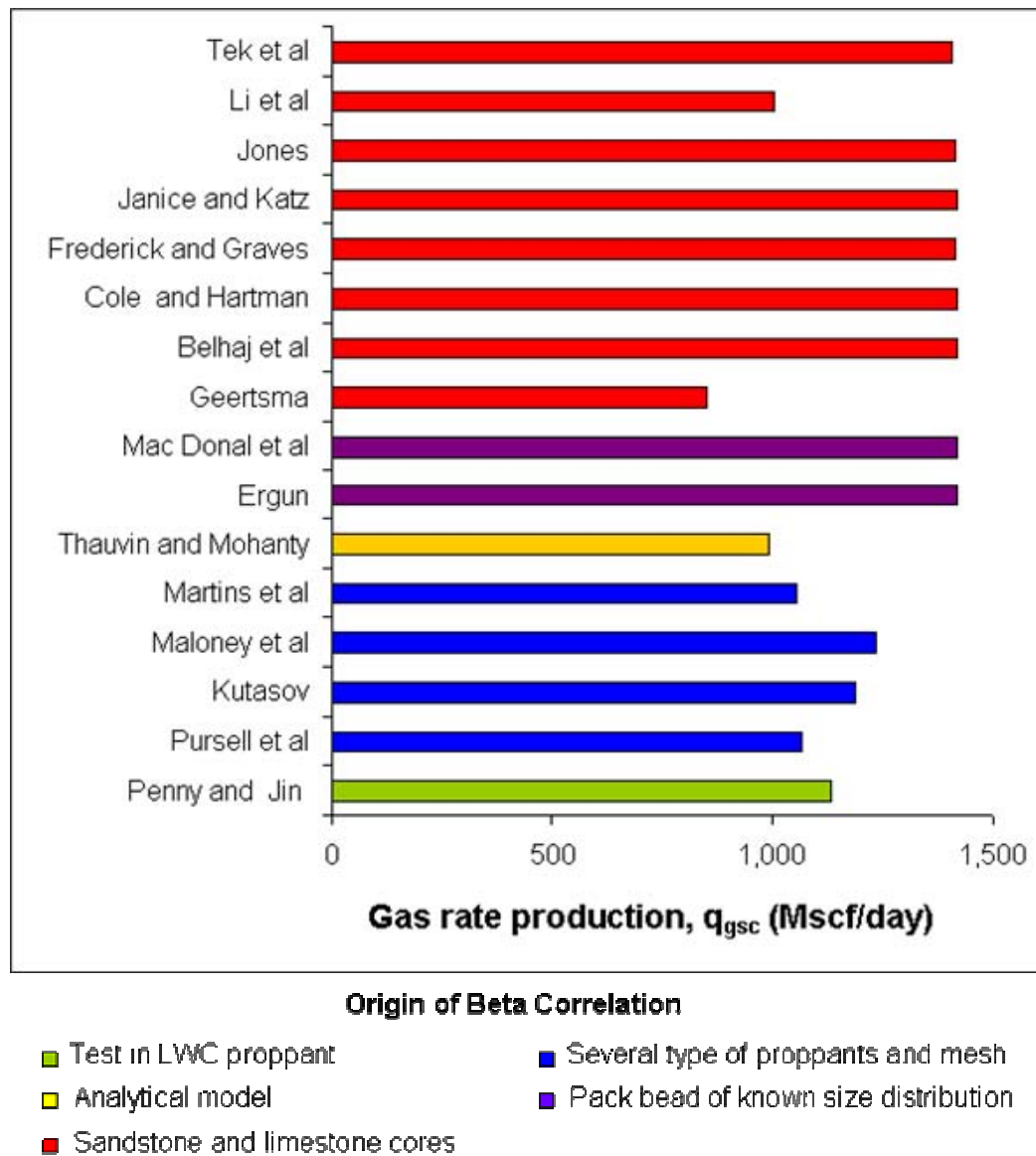


**Fig. C.5** Comparison of optimal design results in terms of gas rate production for 20/40 SB proppant (PS #2\_Stage1)

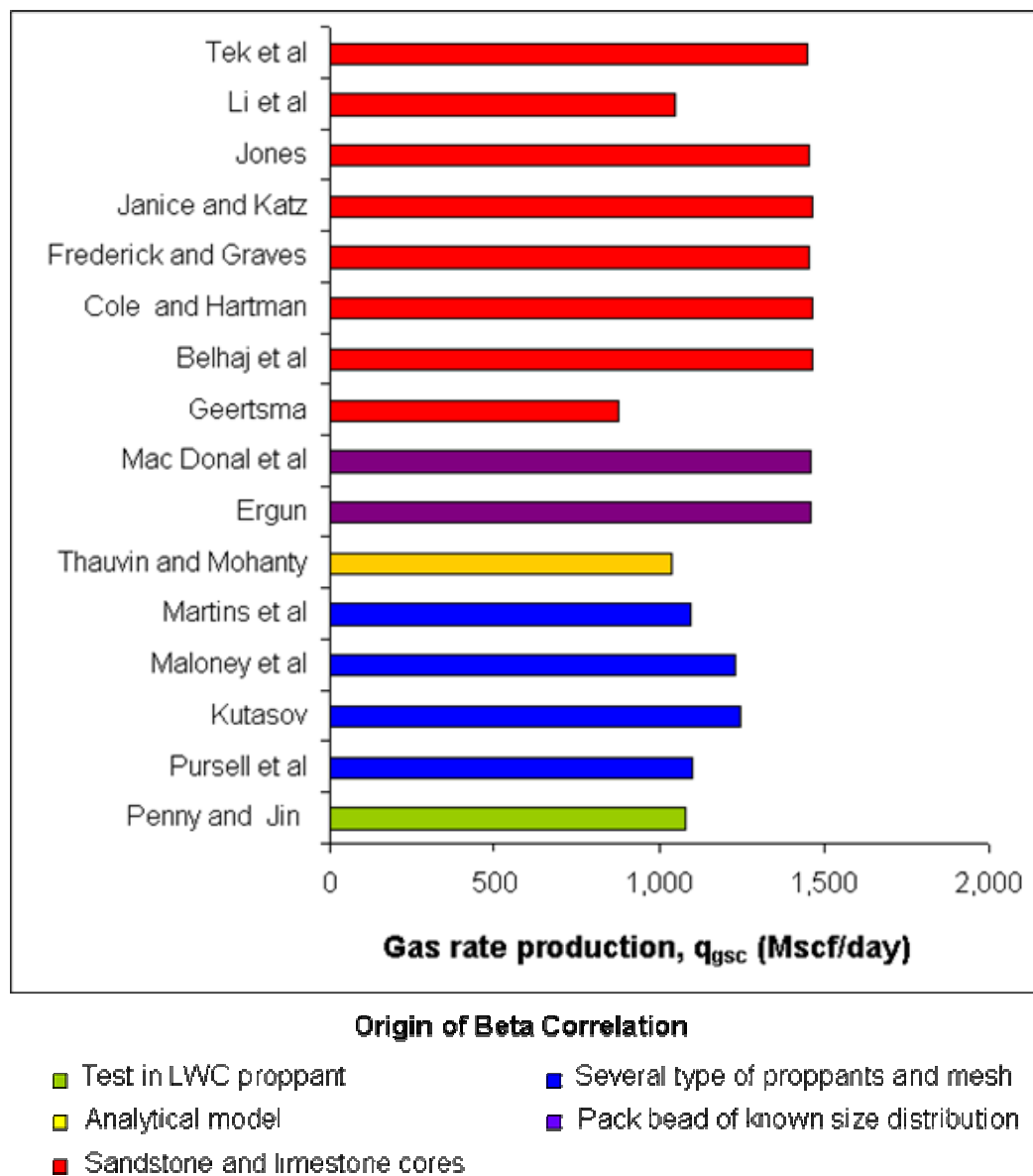


**Fig. C.6** Comparison of optimal design results in terms of gas rate production for 20/40 LWC\_HS proppant (PS #2\_Stage1)

**Table C.1** Effects of closure stress, non-Darcy flow and gel damage upon propped pack effective permeability

<b>Effective propped pack permeability, <math>k_{f\text{-eff}}</math> (md)</b>					
<b>Well</b>	<b>Stage</b>	<b>Closure stress</b>	<b>Non-Darcy Flow</b>	<b>Non-Darcy Flow + GD applied to permeability</b>	<b>Non-Darcy Flow + GD applied to <math>\beta</math> factor</b>
<b>PS #1</b>	<b>1</b>	117,500	8,389	4,682	4,016
	<b>2</b>	124,000	8,230	4,549	3,874
	<b>3</b>	140,250	23,447	12,859	11,492
	<b>4</b>	174,000	37,839	20,925	19,326
	<b>5</b>	182,000	48,826	27,077	25,612
<b>PS #2</b>	<b>1</b>	144,800	44,253	24,172	23,262
	<b>2</b>	154,000	34,264	18,912	17,526
	<b>3</b>	163,440	35,842	19,916	18,430
	<b>4</b>	163,200	41,660	22,820	21,434
<b>PS #3</b>	<b>1</b>	231,120	65,115	35,293	33,666
	<b>2</b>	231,120	21,539	12,012	10,243

## APPENDIX D

### VB CODE FOR OPTIMAL MULTISTAGE HYDRAULIC FRACTURING DESIGN USING DYNAMIC PROGRAMMING

#### VB code of inversion function of triangular probability distribution

```

Function trianinv(min As Double, ml As Double, max As Double, u As Double) As Double
Dim h, AT1, a1, b1, c1, AT2, a2, b2, c2 As Double
h = 2 / (max - min)
AT1 = (ml - min) * h / 2
If u < AT1 Then
    a1 = 1
    b1 = -2 * min
    c1 = min ^ 2 - 2 * u * (ml - min) / h
    trianinv = (-b1 + (b1 ^ 2 - 4 * a1 * c1) ^ 0.5) / (2 * a1)
Else
    AT2 = (max - ml) * h / 2
    a2 = 1
    b2 = -2 * max
    c2 = max ^ 2 - 2 * (max - ml) * (AT1 + AT2 - u) / h
    trianinv = (-b2 - (b2 ^ 2 - 4 * a2 * c2) ^ 0.5) / (2 * a2)
End If
End Function

```

#### VB code to calculate gas rate from an optimal fracture design as an Excel function

```

Function qgas(pr As Double, tr As Double, k As Double, hp As Double, re As Double, sg As Double, n2
As Double, co2 As Double, h2s As Double, bhp As Double, m As Double, kf As Double, phip As Double,
sgp As Double, a As Double, b As Double, c As Double, geldam As Double) As Double
' Units conversion constants
Const acre As Double = 4046.9
Const bbl As Double = 0.1589873
Const gallon As Double = 0.00378541
Const inch As Double = 0.0254
Const ft As Double = 0.3048
Const lbm As Double = 0.4535924
Const lbf As Double = 4.448222
Const psi As Double = 6894.757
Const cp As Double = 0.001
Const md As Double = 9.869233E-16
Const Pi As Double = 3.14159265358979
' Fix variables
Dim vres As Double 'Reservoir volume, ft3
Dim pave As Double 'Average pressure, psi
Dim ugave As Double 'Gas viscosity at reservoir temperature and average pressure
Dim zgave As Double 'Z-factor at reservoir temperature and average pressure
Dim ugwf As Double 'Gas viscosity at wellbore flowing conditions
Dim zgwf As Double 'Z-factor at at wellbore flowing conditions
Dim bg As Double 'Gas formation volume factor, rcf/scf

```

```

Dim gasden As Double 'Gas density, kg/m3
Dim beta As Double 'Beta factor, 1/m
'Dynamic variables
Dim nreold As Double 'Reynold number for dynamic calculation
Dim nrenew As Double 'Reynold number for dynamic calculation
Dim error As Double 'Error between old and new Reynold number
Dim kfeff As Double 'Effective permeability, md
Dim vprop As Double 'Propped pack volume, ft3
Dim nprop As Double 'Proppant number
Dim jd As Double 'Dimensionless productivity index
Dim cfd As Double 'Dimensionless productivity index
Dim ix As Double 'Penetration ratio
Dim xf As Double 'Fracture lenght, ft
Dim wf As Double 'Propped width, in
Dim hf As Double 'Fracture height, ft
Dim v As Double 'gas velocity within the fracture
Dim qg As Double 'gas rate production, mscfd
'FIXED CALCULATIONS
vres = 3.14159265358979 * re ^ 2 * hp
pave = (pr + bhp) / 2
ugave = ug(pave, tr + 460, sg, n2, co2, h2s)
zgave = z(pave, tr + 460, sg, n2, co2, h2s)
ugwf = ug(bhp, tr + 460, sg, n2, co2, h2s)
zgwf = z(bhp, tr + 460, sg, n2, co2, h2s)
bg = 0.0283 * zgwf * (tr + 460) / bhp
gasden = sg * 1.22 / bg
kf = kf * (1 - geldam / 100)
beta = a / ((kf ^ b) * (phip ^ c))
'INITIAL VALUES BEFORE ITERATION
nreold = 9
hf = 200
error = 100
'ITERATIONS
Do Until error < 0.01
    kfeff = kf / (1 + nreold)
    vprop = 0.016 * (m / 2) / ((1 - phip) * sgp) * (hp / hf)
    nprop = (4 * vprop * kfeff) / (k * vres)
    Call FracOpt(nprop, jd, cfd, ix)
    xf = ((vprop * kfeff) / (cfd * hp * k)) ^ 0.5
    hf = xf / 2
    wf = 12 * ((cfd * vprop * k) / (hp * kfeff)) ^ 0.5
    qg = k * hp * (pr ^ 2 - bhp ^ 2) * jd / (1424 * ugave * zgave * (tr + 460))
    v = 0.021159 * bg * qg / (hf * wf) 'units
    nrenew = beta * (kf * 9.869233E-16) * v * gasden / (ugwf * 0.001)
    error = 100 * Abs(nrenew - nreold) / nreold
    nreold = nrenew
Loop
qgas = qg
End Function

```

## VB code to calculate average gas rate from Montecarlo simulation

```

Option Explicit
Sub qgrandom()
'This soubroutine is to generate averaged random gas production
'VARIABLES DECLARATION
'Input
Dim pres(1 To 10) As Double
Dim tres(1 To 10) As Double
Dim minhp(1 To 10) As Double
Dim mlhp(1 To 10) As Double
Dim maxhp(1 To 10) As Double
Dim mink(1 To 10) As Double
Dim mlk(1 To 10) As Double
Dim maxk(1 To 10) As Double
Dim re(1 To 10) As Double
Dim sgg(1 To 10) As Double
Dim n2(1 To 10) As Double
Dim co2(1 To 10) As Double
Dim h2s(1 To 10) As Double
Dim bhp(1 To 10) As Double
Dim kf(1 To 10) As Double
Dim pf(1 To 10) As Double
Dim sgf(1 To 10) As Double
Dim a(1 To 10) As Double
Dim b(1 To 10) As Double
Dim c(1 To 10) As Double
Dim pgd(1 To 10) As Double
'Mass of proppant
Dim m As Double
'Auxiliar variables for random process
Dim uhp As Double
Dim hpa As Double
Dim uk As Double
Dim ka As Double
Dim qga As Double
Dim cumm As Double
'Counters
Dim i As Integer
Dim j As Integer
'Ultimate production
Dim qgave As Double
'
'CALCULATIONS
m = 60000
With ThisWorkbook.Worksheets("random")
For i = 1 To 10
pres(i) = .Cells(1 + i, 2).Value
tres(i) = .Cells(1 + i, 3).Value
minhp(i) = .Cells(1 + i, 4).Value
mlhp(i) = .Cells(1 + i, 5).Value
maxhp(i) = .Cells(1 + i, 6).Value
mink(i) = .Cells(1 + i, 7).Value
mlk(i) = .Cells(1 + i, 8).Value
maxk(i) = .Cells(1 + i, 9).Value

```

```

re(i) = .Cells(1 + i, 10).Value
sgg(i) = .Cells(1 + i, 11).Value
n2(i) = .Cells(1 + i, 12).Value
co2(i) = .Cells(1 + i, 13).Value
h2s(i) = .Cells(1 + i, 14).Value
bhp(i) = .Cells(1 + i, 15).Value
kf(i) = .Cells(1 + i, 16).Value
pf(i) = .Cells(1 + i, 17).Value
sgf(i) = .Cells(1 + i, 18).Value
a(i) = .Cells(1 + i, 19).Value
b(i) = .Cells(1 + i, 20).Value
c(i) = .Cells(1 + i, 21).Value
pgd(i) = .Cells(1 + i, 22).Value
Cells(1 + i, 23).Value = ""
Next i
End With
For i = 1 To 10
cumm = 0
For j = 1 To 100
uhp = staticrand()
hpa = trianinv(minhp(i), mlhp(i), maxhp(i), uhp)
uk = staticrand()
ka = trianinv(mink(i), mlk(i), maxk(i), uk)
qga = qgas(pres(i), tres(i), ka, hpa, re(i), sgg(i), n2(i), co2(i), h2s(i), bhp(i), m, kf(i), pf(i), sgf(i), a(i), b(i),
c(i), pgd(i))
cumm = cumm + qga
Next j
qgave = cumm / 100
With ThisWorkbook.Worksheets("random")
Cells(1 + i, 23).Value = qgave
End With
Next i
Call dpopt
End Sub

```

### **VB code to solve the recursive relation function**

```

Sub dpopt()
Dim n As Integer
Dim totalm As Integer
Dim i As Integer
Dim qgr() As Double
Dim r As Integer
Dim f() As Double
Dim m As Integer
Dim xi() As Double
Dim optm() As Integer
Dim j As Integer
Dim k As Integer
Dim totalgas As Double
Dim remain As Integer
Dim x As Double
Dim interval() As Integer
Dim qginterval() As Double

```



```

Dim c As Integer
With ThisWorkbook.Worksheets("random")
  For c = 1 To 5
    Cells(1 + c, 25).Value = ""
    Cells(1 + c, 26).Value = ""
  Next c
Cells(7, 26).Value = ""
End With
n = 10
totalm = 300
ReDim qgr(1 To n, 0 To 60)
ReDim f(1 To n + 1, 0 To totalm)
ReDim xi(1 To n, 0 To totalm, 0 To 60)
ReDim optm(1 To n, 0 To totalm)
ReDim interval(1 To 5)
ReDim qginterval(1 To 5)
With ThisWorkbook.Worksheets("random")
  For i = 1 To n
    qgr(i, 0) = 0
    qgr(i, 60) = .Cells(1 + i, 23).Value
  Next i
End With
For r = 0 To totalm Step 60
  f(n + 1, r) = 0
Next r
For i = n To 1 Step -1
  For r = 0 To totalm Step 60
    For m = 0 To 60 Step 60
      If r >= m Then
        xi(i, r, m) = qgr(i, m) + f(i + 1, r - m)
      Else
        xi(i, r, m) = 0
      End If
    Next m
    If xi(i, r, 0) >= xi(i, r, 60) Then
      optm(i, r) = 0
      f(i, r) = xi(i, r, 0)
    Else
      optm(i, r) = 60
      f(i, r) = xi(i, r, 60)
    End If
  Next r
Next i
j = 0
k = 0
totalgas = 0
remain = totalm
Do
  Do
    j = j + 1
    x = optm(j, remain)
  Loop Until x = 60
  k = k + 1
  interval(k) = j
  qginterval(k) = qgr(j, 60)
  totalgas = totalgas + qgr(j, 60)

```

```

remain = remain - 60
Loop Until remain = 0
With ThisWorkbook.Worksheets("random")
  For c = 1 To k
    Cells(1 + c, 25).Value = interval(c)
    Cells(1 + c, 26).Value = qginterval(c)
  Next c
Cells(2 + k, 26).Value = totalgas
End With
End Sub

```

**Table D.1** Recursive relation for stage 8

<b>i = 8</b>				
<b><math>s_i \setminus m_i</math></b>	<b>0</b>	<b>60,000</b>	<b>Opt <math>m_i</math></b>	<b><math>f_i(m_i)</math></b>
<b>0</b>	0	-	0	0
<b>60,000</b>	4,957	127	0	4,957
<b>120,000</b>	5,118	5,084	0	5,118
<b>180,000</b>	5,118	5,245	60,000	5,245
<b>240,000</b>	5,118	5,245	60,000	5,245
<b>300,000</b>	5,118	5,245	60,000	5,245

**Table D.2** Recursive relation for stage 7

<b>i = 7</b>				
<b><math>s_i \setminus m_i</math></b>	<b>0</b>	<b>60,000</b>	<b>Opt <math>m_i</math></b>	<b><math>f_i(m_i)</math></b>
<b>0</b>	0	-	0	0
<b>60,000</b>	4,957	7,597	60,000	7,597
<b>120,000</b>	5,118	12,554	60,000	12,554
<b>180,000</b>	5,245	12,715	60,000	12,715
<b>240,000</b>	5,245	12,842	60,000	12,842
<b>300,000</b>	5,245	12,842	60,000	12,842

**Table D.3** Recursive relation for stage 6

<b>i = 6</b>				
<b><math>s_i \setminus m_i</math></b>	<b>0</b>	<b>60,000</b>	<b>Opt <math>m_i</math></b>	<b><math>f_i(m_i)</math></b>
<b>0</b>	0	-	0	0
<b>60,000</b>	7,597	108	0	7,597
<b>120,000</b>	12,554	7,705	0	12,554
<b>180,000</b>	12,715	12,662	0	12,715
<b>240,000</b>	12,842	12,823	0	12,842
<b>300,000</b>	12,842	12,950	60,000	12,950

**Table D.4** Recursive relation for stage 5

<b>i = 5</b>				
<b><math>s_i \setminus m_i</math></b>	<b>0</b>	<b>60,000</b>	<b>Opt <math>m_i</math></b>	<b><math>f_i(m_i)</math></b>
<b>0</b>	0	-	0	0
<b>60,000</b>	7,597	84	0	7,597
<b>120,000</b>	12,554	7,681	0	12,554
<b>180,000</b>	12,715	12,638	0	12,715
<b>240,000</b>	12,842	12,799	0	12,842
<b>300,000</b>	12,950	12,926	0	12,950

**Table D.5** Recursive relation for stage 4

<b>i = 4</b>				
<b><math>s_i \setminus m_i</math></b>	<b>0</b>	<b>60,000</b>	<b>Opt <math>m_i</math></b>	<b><math>f_i(m_i)</math></b>
<b>0</b>	0	-	0	0
<b>60,000</b>	7,597	1,822	0	7,597
<b>120,000</b>	12,554	9,419	0	12,554
<b>180,000</b>	12,715	14,376	60,000	14,376
<b>240,000</b>	12,842	14,537	60,000	14,537
<b>300,000</b>	12,950	14,664	60,000	14,664

**Table D.6** Recursive relation for stage 3

<b>i = 3</b>				
<b><math>s_i \setminus m_i</math></b>	<b>0</b>	<b>60,000</b>	<b>Opt <math>m_i</math></b>	<b><math>f_i(m_i)</math></b>
<b>0</b>	0	-	0	0
<b>60,000</b>	7,597	3,383	0	7,597
<b>120,000</b>	12,554	10,980	0	12,554
<b>180,000</b>	14,376	15,937	60,000	15,937
<b>240,000</b>	14,537	17,759	60,000	17,759
<b>300,000</b>	14,664	17,920	60,000	17,920

**Table D.7** Recursive relation for stage 2

<b>i = 2</b>				
<b><math>s_i \setminus m_i</math></b>	<b>0</b>	<b>60,000</b>	<b>Opt <math>m_i</math></b>	<b><math>f_i(m_i)</math></b>
<b>0</b>	0	-	0	0
<b>60,000</b>	7,597	72	0	7,597
<b>120,000</b>	12,554	7,669	0	12,554
<b>180,000</b>	15,937	12,626	0	15,937
<b>240,000</b>	17,759	16,009	0	17,759
<b>300,000</b>	17,920	17,831	0	17,920

**VITA**

Name: **Henry De Jesus Lopez Hernandez**

Date of Birth: March 15, 1974

Place of Birth: Merida, Merida, Venezuela

Permanent Address: Calle 18 # 4-46  
Merida, Edo. Merida  
5101, Venezuela  
Phone: 58-274-2522680

E-mail: [hjlh74@hotmail.com](mailto:hjlh74@hotmail.com)

Education: B.S., Mechanical Engineering (Nov. 1997)  
Universidad de Los Andes  
Merida, Edo. Merida, Venezuela

M.S., Petroleum Engineering (Aug. 2004)  
Texas A&M University  
College Station, Texas 77840

Prof. Aff.: Society of Petroleum Engineers, Member